Deutsches Zentrum
für Luft- und Raumfahrt e.V.
in der Helmholtz-Gemeinschaft

EnMAP Ground Segment

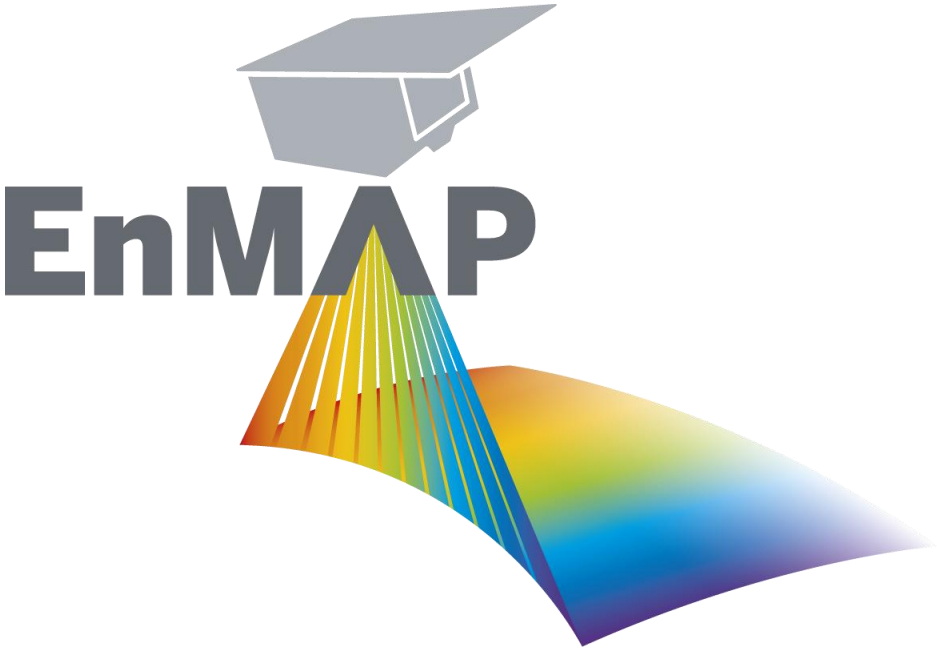
Mission Quarterly Report #16

01.04.2026 to 30.06.2026

Public

Doc. ID	EN-GS-RPT-1116
Issue	1.0
Date	20.10.2026

Configuration Controlled: Yes



German Remote Sensing Data Center (DFD)
Remote Sensing Technology Institute (IMF)
German Space Operations Center (GSOC)
Helmholtz Centre for Geosciences (GFZ)
German Space Agency at DLR

TABLE OF SIGNATURES

Prepared

Emiliano Carmona Flores

Digitally signed by Emiliano Carmona Flores
DN: C=DE, CN=Emiliano Carmona Flores, GN=Emiliano, L=Koeln, O=Deutsches Zentrum fuer Luft- und Raumfahrt e. V., SN=Carmona Flores, ST=Nordrhein-Westfalen, E=emiliano.carmona@dlr.de, organizationIdentifier=VATDE-121965658
Reason: Prepared
Location:
Date: 2026.10.29 10:15:10+01'00'
Foxit PDF Reader Version: 2026.2.1

Date — Emiliano Carmona, (DLR MF-ASP, EnMAP OMM)

Sabine Chabrillat

Digital unterschrieben von Sabine Chabrillat
Datum: 2026.10.29 21:28:28 +01'00'

Date — Sabine Chabrillat, (GFZ, EnMAP SciLead)

Reviewed

Daniel Schulze

Digital signiert von Daniel Schulze
DN: C=DE, CN=Daniel Schulze, GN=Daniel, L=Koeln, O=Deutsches Zentrum fuer Luft- und Raumfahrt e. V., SN=Schulze, ST=Nordrhein-Westfalen, E=d.schulze@dlr.de, organizationIdentifier=VATDE-121965658
Grund: Ich bin der Verfasser dieses Dokuments
Ort:
Datum: 2026.10.30 14:17:08+01'00'
Foxit PDF Reader Version: 2026.2.1

Date — Daniel Schulze, (DLR RB-MIB, dep. EnMAP OMM)

Sabine Engelbrecht

Digital signiert von Sabine Engelbrecht
DN: C=DE, CN=Sabine Engelbrecht, GN=Sabine, L=Koeln, O=Deutsches Zentrum fuer Luft- und Raumfahrt e. V., SN=Engelbrecht, ST=Nordrhein-Westfalen, E=sabine.engelbrecht@dlr.de, organizationIdentifier=VATDE-121965658
Grund: Ich habe dieses Dokument geprüft
Ort: Oberpfaffenhofen
Datum: 2026.10.30 13:55:50+01'00'
Foxit PDF Editor Version: 14.0.8

Date — Sabine Engelbrecht, (DLR DFD-INF, EOC PAD)

Robert Groessel

Digital signiert von Robert Groessel
DN: C=DE, CN=Robert Groessel, GN=Robert, L=Koeln, O=Deutsches Zentrum fuer Luft- und Raumfahrt e. V., SN=Groessel, ST=Nordrhein-Westfalen, E=robert.groessel@dlr.de, organizationIdentifier=VATDE-121965658
Grund: Ich bin der Verfasser dieses Dokuments
Ort:
Datum: 2026.10.30 12:35:01+01'00'
Foxit PDF Reader Version: 2026.2.1

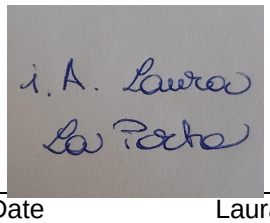
Date — Robert Größel, (DLR RB-CTA, GSOC PAD)

Karl Segl

Digital unterschrieben von Karl Segl
Datum: 2026.10.29 16:55:32 +01'00'

Date — Karl Segl, (GFZ, dep. EnMAP SciLead)

Approved & Released



2026.11.02
11:03:23+01'00'
14.0.8

Date — Laura La Porta, (DLR AR-AO, EnMAP MM)

DISTRIBUTION LIST

The document is publicly available via www.enmap.org.

CHANGE RECORD

Version	Date	Chapter	Comment
1.0	20.10.2026	All	First issue of Mission Quarterly Report #16 corresponding to 01.04.2026 to 30.06.2026.

Custodian of this document is Carmona, Emiliano.

CONTENTS

Table of Signatures **2**
Distribution List **3**
Change Record **3**
Contents **4**
List of Figures **5**
List of Tables **8**
1 Introduction **9**
1.1 Purpose 9
1.2 Scope 9
2 References **10**
3 Terms, Definitions and Abbreviations **11**
4 Mission **12**
4.1 Mission Objectives 12
4.2 Mission Description 12
4.3 Mission Status Summary 13
5 Users and Announcements-of-Opportunities **15**
5.1 Users 15
6 Archived and Delivered Observations **18**
6.1 Archived Acquisitions 18
6.2 Delivered Observations 22
6.2.1 Delivered L2A products from the Download service (EOC Geoservice) 23
7 Detailed Status **25**
7.1 Satellite 25
7.1.1 Orbit and Attitude Maneuvers 25
7.1.2 Life Limited Items 26
7.1.3 Redundancies 27
7.2 Ground Stations 27
7.2.1 S-Band 27
7.2.2 X-Band 27
7.3 User Interfaces 27
7.4 Processors 28
7.5 Calibrations 29
7.5.1 Dead Pixels 31
7.5.2 Spectral Calibration 31
7.5.3 Radiometric Calibration 35
7.5.4 Geometric Calibration 48
7.6 Internal Quality Control 48
7.6.1 Archive 48
7.6.2 Level 1B 50
7.6.3 Level 1C 55
7.6.4 Level 2A 60
8 External Product Validation **76**
8.1 Level 1B 76
8.2 Level 1C 78
8.3 Level 2A 79
8.4 Summary of External Product Monitoring 80
9 Others **81**

LIST OF FIGURES

Figure 5-1 Number of registered users (with at least one active user role) per country 16
Figure 6-1 Geographic location of all Earth observation tiles archived, World 19
Figure 6-2 Geographic location of all Earth observation tiles archived, Europe 20
Figure 6-3 Cloud coverage in [%] of archived Earth observation tiles 21
Figure 6-4 Observation angle of archived Earth observation tiles 21
Figure 6-5 Levels of delivered Earth observation tiles from acquisition orders 22
Figure 6-6 Levels of delivered Earth observation tiles from catalog orders 22
Figure 6-7 Downloads in Geoservice per month 24
Figure 7-1 Number of ACS Precise Modes per day during Q2 2026 26
Figure 7-2 Decay per day from Lamp (RAD), Linearity (LIN) and Spectral (SPC) measurements for low gain (top) and high gain (bottom) 29
Figure 7-3 Change in percentage for individual pixels based on OBCA-Lamp measurements given for 5 bands and 5 cross track elements (coloured lines). 30
Figure 7-4 Average percentage change in the VNIR radiometric coefficients for five selected bands since launch 30
Figure 7-5 VNIR Dead Pixel Mask 31
Figure 7-6 SWIR Dead Pixel Mask 31
Figure 7-7 VNIR (top) and SWIR (bottom) center wavelength in nm 33
Figure 7-8 Change in center wavelength per spectral pixel for VNIR (top) and SWIR (bottom). Left panels show the changes with respect to current spectral calibration table in use and right panels with respect to the previous measurements. 33
Figure 7-9 Long-term VNIR (top) and SWIR (bottom) spectral shifts since the beginning of the mission for VNIR band 45 at 654 nm and SWIR band 105 at 2042 nm. 34
Figure 7-10 VNIR (top) and SWIR (bottom) FWHM in nm 35
Figure 7-11 VNIR (top) and SWIR (bottom) calibration coefficient in mW/cm^2/sr/µm 37
Figure 7-12 Percentage change in VNIR Calibration Coefficients (top) and SWIR Calibration Coefficients (bottom) 38
Figure 7-13 VNIR (top) and SWIR (bottom) gain matching calibration coefficients 38
Figure 7-14 VNIR (top) and SWIR (bottom) response non-uniformity coefficients 39
Figure 7-15 SNR contour map for VNIR high gain from the LED linearity observations observed on 14.06.2026. The reference radiance is shown with a blue line and after bandwidth normalization to a 10 nm pixel (dotted). Contour lines with SNR values of 150 and 500 are also shown in black. 40
Figure 7-16 SNR contour map for VNIR low gain from the LED linearity observations observed on 14.06.2026. The reference radiance is shown with a blue line and after bandwidth normalization to a 10 nm pixel (dotted). Contour lines with SNR values of 150 and 500 are also shown in black. The mission requirement is evaluated at 495 nm for a radiance value of 36 mW/cm^2/µm/sr (marked with a black cross) and is expected to be greater than 500. 40
Figure 7-17 SNR contour map for SWIR high gain from the LED linearity observations observed on 14.06.2026. The reference radiance is shown with a blue line and after bandwidth normalization to a 10 nm pixel (dotted). Contour lines with SNR values of 150 and 500 are also shown in black. The mission requirement is evaluated at 2200 nm for a radiance value of 0.5 mW/cm^2/µm/sr (marked with a black cross) and is expected to be greater than 150. 41

Figure 7-18 SNR contour map for SWIR low gain from the LED linearity observations observed on 14.06.2026. The reference radiance is shown with a blue line and after bandwidth normalization to a 10 nm pixel (dotted). Contour lines with SNR values of 150 and 500 are also shown in black. 41
Figure 7-19 VNIR estimated spectral shift at 760 nm w.r.t the valid spectral calibration table (CTB_SPC), and relative spectral stability expressed at 1 sigma (Q2 2026, 14104 tiles) 53
Figure 7-20 Center wavelengths per cross-track pixel based on the spectral calibration table (VNIR band 62) in the calibration table (CTB_SPC) 54
Figure 7-21 SWIR estimated spectral shift at 2050 nm w.r.t the valid spectral calibration table (CTB_SPC, shown below), and relative spectral stability expressed at 1 sigma (Q2 2026, 14104 tiles) 54
Figure 7-22 Center wavelengths per cross-track pixel based on the spectral calibration table (SWIR band 86). 55
Figure 7-23 Assessment of RMSE X values (top) and RMSE Y values (bottom), calculated based on found ICPs, for all datatakes where ICP could be found 56
Figure 7-24 Mean deviation of EnMAP L1C products in pixel (left). RMSE value for EnMAP L1C products in pixel (right) 57
Figure 7-25 Mean deviation in pixel between VNIR and SWIR data of EnMAP L1C products (left). RMSE in pixel between VNIR and SWIR data of EnMAP L1C Products (right) 58
Figure 7-26 Development of co-registration accuracy based on the previous geometric QC reports. The values with re-processed L0 data and archived version ≥V01.03.00 are also shown59
Figure 7-27 Scene-ID 200437; RGB-Quicklook with Bands 611.02nm – 550.69nm – 463.73nm 61
Figure 7-28 Scene-ID 200437; Geo Mask with Blue – Water, Green – Land, Light Blue - Shadows, Orange – Clouds, White – NA 61
Figure 7-29 Scene-ID 200437; At-sensor-radiance sampled at location AC 1; red: measured, blue: adjacency corrected 62
Figure 7-30 ID 200437; At-sensor-radiance sampled at location AC 2; red: measured, blue: adjacency corrected 62
Figure 7-31 Normalized Water Leaving Reflectance of scene-ID 200437; Wavelengths for RGB: 611.02nm – 550.69nm – 463.73nm 63
Figure 7-32 Scene-ID 200437; nWLR sampled at location nWLR 1 63
Figure 7-33 Scene-ID 200437; nWLR sampled at location nWLR 2 64
Figure 7-34 DT187507, TrueColorComposite (left) and QualityClasses (right; blue: water, brown: land, white: other). 65
Figure 7-35 DT187507, from left to right: TrueColorComposite; Snow Mask, Cloud Mask, Haze Mask, Cloud Shadow Mask; all other masks are correctly empty. 65
Figure 7-36 DT187507, as before now zoomed in. 66
Figure 7-37 DT187507, left to right: TrueColor, linear stretch; TrueColor, nonlinear stretch; CIR nonlinear stretch 66
Figure 7-38 DT187507, single pixel spectra of various surfaces 67
Figure 7-39 DT187507, single pixel spectra of snow & ice areas surfaces 67
Figure 7-40 DT191634, T03, TrueColorComposite (left) and CIR (right) 68
Figure 7-41 DT191634, T03, from left to right: CIR; Cirrus Classes (grey: clear; blue: thin cirrus; green: medium cirrus; red: thick cirrus); QualityClasses (blue: water, brown: land, white: other); Cloud Mask; Cloud Shadow Mask; Haze Mask; all other masks are correctly empty 68
Figure 7-42 DT191634, T03, zoom in. From left to right: TrueColorComposite; Cirrus Classes (grey: clear; blue: thin cirrus; green: medium cirrus; red: thick cirrus); Cloud Mask; Haze Mask.69
Figure 7-43 DT191634, T03, single pixel spectra of various surfaces. 69
Figure 7-44 DT191634, T04, TrueColorComposite (left) and CIR (right) 70

Figure 7-45 DT191634, T04, from left to right: CIR; Cirrus Classes (grey: clear; blue: thin cirrus; green: medium cirrus; red: thick cirrus); QualityClasses (blue: water, brown: land, white: other); Cloud Mask; Cloud Shadow Mask; Haze Mask; all other masks are correctly empty.....70
Figure 7-46 DT191634, T04, zoom in: CIR image (left) and QualityClasses (blue: water, brown: land, white: other) 71
Figure 7-47 DT191634, T04, single pixel spectra of various surfaces. 71
Figure 7-48 DT191634; top-left: T03 in TrueColourComposite; bottom-left: T04 in TrueColorComposite; center: mosaicked TrueColorComposite; right: mosaicked CIR. ...72
Figure 7-49 DT202075, T010, TrueColorComposite.....73
Figure 7-50 DT202075, T010, from left to right: CIR; QualityClasses (blue: water, brown: land, white: other); cloud mask; haze mask; all other masks are correctly empty. 73
Figure 7-51 DT202075, T010, zoom in area on plateau: CIR (left); QualityClasses (right; blue: water, brown: land, white: other).....74
Figure 7-52 DT202075, T010, single pixel spectra of various surfaces. 75
Figure 8-1: Errors between EnMAP TOA radiance and propagated TOA radiance from in situ measurements against wavelength for all arid validation sites based on 47 match-up 76
Figure 8-2 Errors between EnMAP TOA radiance and propagated TOA radiance from in situ measurements against radiance level for all arid validation sites based on 47 match-ups. 77
Figure 8-3 Previously used reference radiance curve (orange) and updated reference radiance curve (blue) as a function of wavelength. 78
Figure 8-4 Errors between EnMAP and in situ BOA reflectance against wavelength for all validation sites based on 66 match-ups. 79
Figure 8-5 Errors between EnMAP and in situ BOA reflectance against reflectance level for all validation sites based on 66 match-ups. 80

LIST OF TABLES

Table 2-1 References 10
Table 5-1 Number of registered users per continent with **at least one active user role** (number of user countries during reporting period) 15
Table 5-2 Number of registered users and number of released user roles per category (Cat-1 Science, Cat-2 Commercial and Cat-1 Distributor) 16
Table 5-3 Number of released science proposals per Announcement-of-Opportunity (AOs#) and total number of granted tiles per AO#. 17
Table 5-4 Number of accepted science proposals and total number of granted tiles per topic 17
Table 6-1 Number and size of archived and not archived products (more than one version of the same image can be archived) 18
Table 6-2 Number and size of delivered products 18
Table 6-3 Processing parameters used for the L2A ARD products in Geoservice / EOLab 23
Table 6-4 Absolut amount of downloads in Geoservice 23
Table 7-1 Status of life-limited items 26
Table 7-2 S-Band Ground Station Passes 27
Table 7-3 X-Band Ground Station Passes 27
Table 7-4 Number and size of archived radiometric and spectral calibration observations 29
Table 7-5 Number and percent of dead pixels 31
Table 7-6 Number and size of archived spectral calibration observations 31
Table 7-7 Generated spectral calibration tables 35
Table 7-8 Number and size of archived radiometric calibration observations 36
Table 7-9 SNR values per wavelength for VNIR and SWIR low and high gains 47
Table 7-10 Generated radiometric calibration tables 48
Table 7-11 Generated new geometric calibration tables 48
Table 7-12 Overall quality rating statistics 49
Table 7-13 Overall quality rating in relation to Sun Zenith Angle (SZA) 49
Table 7-14 Reduced and low quality rating statistics 49
Table 7-15 QualityAtmosphere rating statistics 49
Table 7-16 QualityAtmosphere rating in realtion to Sun Zenith Angle (SZA) 49
Table 7-17 QualityAtmosphere rating in relation to Cloud Cover and DDV availability 50
Table 7-18 Dead pixel statistics, VNIR 51
Table 7-19 Dead pixel statistics, SWIR 51
Table 7-20 Saturation statistics, VNIR 52
Table 7-21 Saturation statistics, SWIR 52
Table 7-22 Artifacts statistics (without striping), VNIR 52
Table 7-23 Artifact statistics (without striping), SWIR 53
Table 7-24 Improvement of geometric performance 58
Table 7-25 Datatake IDs of analyzed water products 60
Table 7-26 Datatake IDs of analyzed land products 64

1 Introduction

1.1 Purpose

This mission quarterly report (MQR) states information on the EnMAP mission status with regard to the registered user community, announcements-of-opportunities and observations as well as the status of the user interfaces, satellite (platform and payload), ground stations (S-band and X-band), processor (Archive, Level 1B, Level 1C, Level 2A (land and water)), calibration (spectral, radiometric, geometric), data quality control and validation of EnMAP.

Please visit www.enmap.org for further information on EnMAP.

1.2 Scope

This 16th Mission Quarterly Report (MQR) applies to the operations of EnMAP in the reporting period of Routine Phase (RP) from **01.04.2026 to 30.06.2026 (Q2 2026)**.

2 References

Reference Identifier	Document Identifier and Title
[1]	L. Guanter et al. (2015) The EnMAP Spaceborne Imaging Spectroscopy Mission for Earth Observation. Remote Sensing, Issue 7, pp. 8830-8857.
[2]	EN-GS-UM-6020 Portals User Manual, Version 1.4
[3]	EN-PCV-ICD-2009-2 Product Specification, Version 1.9
[4]	EN-PCV-TN-4006 Level 1B ATBD, Version 1.10
[5]	EN-PCV-TN-5006 Level 1C ATBD, Version 1.7
[6]	EN-PCV-TN-6007 Level 2A (land) ATBD, Version 2.4
[7]	EN-PCV-TN-6008 Level 2A (water) ATBD, Version 3.1
[8]	Chabrillat, S. et al. (2022) EnMAP Science Plan. EnMAP Technical Report, DOI: 10.48440/enmap.2022.001
[9]	Storch, T.; Honold, H.-P.; Chabrillat S., et al. The EnMAP imaging spectroscopy mission towards operations. Remote Sens. Environ. 2023, 294, 113632. DOI: 10.1016/j.rse.2023.113632
[10]	Brell, M.; Reiners, P.; Guanter, L.; et al. Assessment of EnMAP data quality through global product validation activities. Remote Sensing of Environment 342 (2026) 115459. https://doi.org/10.1016/j.rse.2026.115459

Table 2-1 References

3 Terms, Definitions and Abbreviations

Terms, definitions and abbreviations for EnMAP are collected in a database which is publicly accessible via Internet on www.enmap.org.

An Earth observation of swath length *n* × 30 km (and swath width 30 km) is separated into *n* tiles of size 30 km × 30 km.

4 Mission

4.1 Mission Objectives

The primary goal of EnMAP (Environmental Mapping and Analysis Program) is to measure, derive and analyze quantitative diagnostic parameters describing key processes on the Earth's surface [1].

During the mission operations, with the successful launch on 1st of April 2022 and an expected operational mission lifetime of at least 5 years, EnMAP will provide valuable information for various application fields comprising soil and geology, agriculture, forestry, urban areas, aquatic systems, ecosystem transitions.

4.2 Mission Description

The major elements of the EnMAP mission are the EnMAP Space Segment, built by OHB System AG and owned by the German Space Agency at DLR, the EnMAP Ground Segment built and operated by DLR institutes DFD, MF, RB, and the EnMAP User and Science Segment represented by GFZ. The project management of the EnMAP mission is responsibility of the German Space Agency at DLR.

The EnMAP Space Segment is composed of

- the platform providing power and thermal stability, orbit and attitude control, memory, S-band uplink/downlink for TM/TC data transmission/reception, X-band downlink for payload data transmission, and

- the payload realized as a pushbroom imaging dual-spectrometer covering the wavelength range between 420 nm and 2450 nm with a nominal spectral resolution ≤ 10 nm and allows in combination with a high radiometric resolution and stability to measure subtle reflectance changes.

The EnMAP satellite is operated on a sun-synchronous repeat orbit to observe any location on the globe with comparable illumination conditions. This allows a maximum reflected solar input radiance at the sensor with an acceptable risk for cloud coverage.

The EnMAP Ground Segment is the interface between Space Segment and User and Science Segment. It comprises functionalities to

  - perform planning of imaging, communication and orbit maneuver operations, provision of orbit and attitude data, command and control of the satellite, ground station networks (in particular: Weilheim, Germany, for S-band and Neustrelitz, Germany, for X-Band), receive satellite data, perform long-term archiving and delivery of products, and

  - perform processing chain (for systematic and radiometric correction, orthorectification, atmospheric compensation), instrument calibration operations, and the data quality control of the products.

The EnMAP mission interfaces to the international science and user community through the EnMAP Portal www.enmap.org with official information related to EnMAP by DLR and GFZ-Potsdam (as the document in hand) and links for ordering observations and products.

The EnMAP Science Segment is represented by the EnMAP Science Advisory Group chaired by the mission principal investigator at the GFZ-Potsdam. The Science Segment addresses aspects such as

- supporting and performing validation activities to improve sensor performance and product quality

- developing scientific and application research to fully exploit the scientific potential of EnMAP [8] including provision of software tools for EnMAP data processing and analyses (EnMAP-Box) and provision of teaching and education materials (HYPERedu)

- Organizing workshops, summer schools and in general information, training and networking activities for the user community

The EnMAP User Segment is the community of German and international users ordering acquisitions and accessing products of EnMAP.

4.3 Mission Status Summary

The mission successfully finished the commissioning phase (CP) on 01.11.2022 and entered its routine phase (RP) on 02.11.2022. For an overview of the EnMAP mission and the activities and results of the Launch and Early Orbit and Commissioning Phases, check [9]. For an overview of the EnMAP product validation activities during the commissioning phase and the first two years of the operational phase check [10].

In the reporting period, from 01.04.2026 to 30.06.2026, there have been no major issues affecting the instrument or the satellite, only some minor issues have caused the loss of observation time. The Ground Segment services have been operating normally.

During the period 01.04.2026 to 30.06.2026 (91 days in total), one issue resulted in an extended loss of acquisitions for 5 consecutive days, due to a problem in the attitude control data caused by faulty information from one startracker. During normal operations, the mission is acquiring data at around the maximum acquisition capacity of 5000 km / day. Nevertheless, the average number of acquisitions during this quarter has reduced compared to previous quarters as a result of the introduction of the new cloud strategy to reduce the presence of clouds in the EnMAP imagery.

In this period, 1303 Earth observations of 30 km swath width and up to 990 km swath length were successfully performed which resulted in 14192 archived Earth observation tiles of 30 km × 30 km and 24 calibration acquisitions. In addition, 19418 products were delivered from catalog orders. In total, 24173 Earth observations were performed until 30.06.2026 by the EnMAP team and the 5763 registered users with at least one active user role. This results in 223650 archived Earth observation images (267536 products including the different versions of the re-processed products) and 436234 Earth products delivered from observations requests (232164) and catalogue orders (204070) since the start of the mission. More details are presented in sections 5 and 6.

The mission acquisition process was updated at the end of November 2025 to improve cloud forecast handling during planning. The forecast request window to obtain cloudiness predictions from the German Meteorological Service (DWD) has been reduced to ensure EnMAP acquisitions are planned with the most up-to-date information. Additionally, acquisitions with negative forecasts (predicted cloudiness exceeding the threshold specified in the request) are now excluded from planning, whereas previously they could still be considered and scheduled if no better alternative was available. As a result, the total number of acquisitions has decreased, but the quality of acquisitions has improved significantly thanks to a reduced cloud presence in the EnMAP products. Data shows that user requests in the period 01.04.2025 – 30.06.2025 had a cloudiness median of 18% (18% clouds or less in 50% of the user tasked scenes), while in the same period of 2026 (01.04.2026 – 30.06.2026) the cloudiness median is 2%.

No major limitations are applicable at 30.06.2026. For minor limitations affecting data processing, check section 7.4. Other effects observed in the data by our Quality Control team are reported in section 7.6 where they are investigated in more detail.

Activities within the EnMAP Mission and in particular the Ground Segment are periodically reported in conferences and workshops. More details are available in Section 9.

The following changes were implemented in the reporting period:

- A campaign support webpage is available to register campaigns and get support from the Foreground Mission program for these campaigns. Users are encouraged to make use of this tool and register their campaigns in this tool available at:

https://survey.hifis.dkfz.de/371151?lang=en

More details available at Section 7.3.

- Reprocessing of L0 products to L2A Analysis Ready Data (**ARD**) products with processor version **V01.05.02** in progress. All L2A ARD products at EOC-Geoservice have been updated to a version **≥ V01.05.02** by the end of July 2027. During this re-processing, L1B and L1C ARD products for the complete EnMAP archive will also be generated and made available for download in the next quarters.

The list of changes introduced in this and previous processor updates is available at:

https://www.enmap.org/data/doc/EnMAP_processor_changelog.pdf

Since August 2024, EnMAP L2A ARD products have been available for download through the EOC Geoservice (https://geoservice.dlr.de/) and the EO-Lab platform (https://eo-lab.org/). These possibilities allow the direct download of EnMAP L2A products generated by the EnMAP Ground Segment with a standard set of parameters. Since these L2A products are already processed, users can directly download these products without waiting times, allowing a fast way to get large amounts of EnMAP products from the mission archive. Notice that both EOC Geoservice and EO-Lab are not part of the standard services offered by the EnMAP mission but are accessible with the GS/IPS EnMAP account. More information on the number of products downloaded through Geoservice can be found in section 6.2.1.

The following changes are expected to be performed in the next quarters:

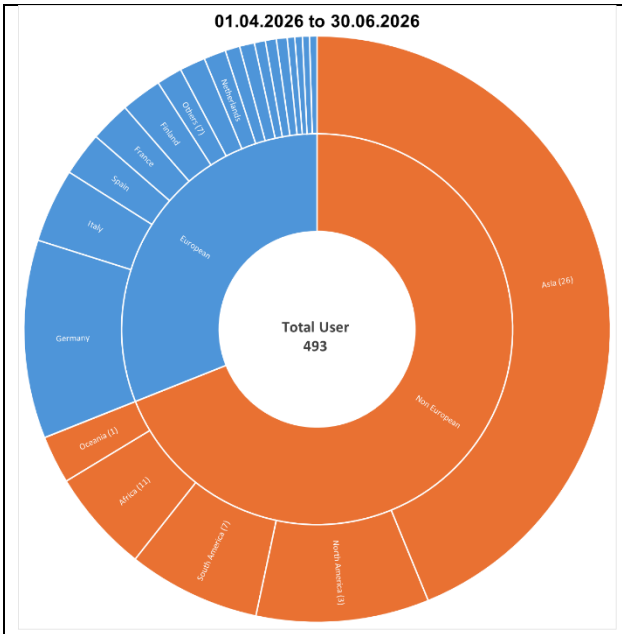
- Implementation of new linearity calibration (and updated calibration) to improve the VNIR-SWIR matching between spectrometers, specially at low radiances.
- Availability of L1B ARD and L1C ARD products at the EOC-Geoservice
- Start processing of L2A-Water ARD products for availability at the EOC-Geoservice

5 Users and Announcements-of-Opportunities

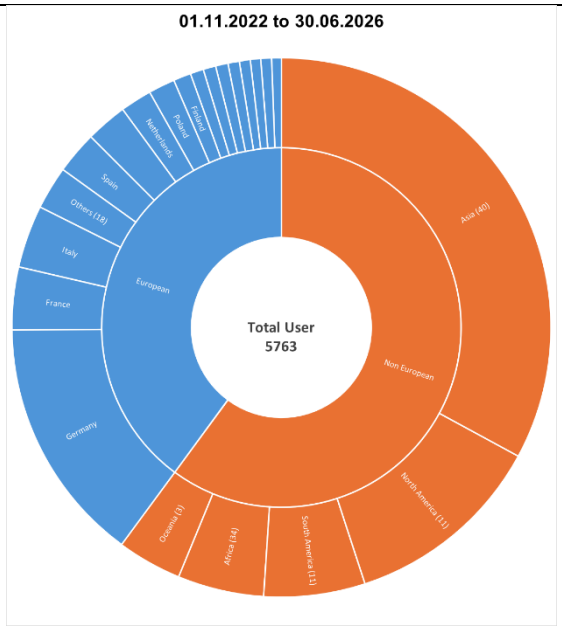
5.1 Users

	Country/Continent (No of Countries) *(of reporting period)*	Reporting Period 01.04.2026 to 30.06.2026		Country/Continent (No of Countries) *(since beginning of routine phase)*	Since beginning of routine phase until 30.06.2026 (end of reporting period)
Total European Users	**Europe (23)**	**153**		**Europe** *(34)*	*2299*
European Countries	• *Germany*	*54*		• *Germany*	*849*
	• *Italy*	*20*		• *France*	*217*
	• *Spain*	*12*		• *Italy*	*216*
	• *Finland*	*11*		• *Spain*	*146*
	• *France*	*11*		• *Great Britain*	*143*
	• *Great Britain*	*7*		• *Netherlands*	*109*
	• *Netherlands*	*6*		• *Poland*	*91*
	• *Austria*	*4*		• *Finland*	*62*
	• *Norway*	*4*		• *Greece*	*46*
	• *Ireland*	*3*		• *Belgium*	*43*
	• *Luxembourg*	*3*		• *Switzerland*	*42*
	• *Sweden*	*3*		• *Austria*	*40*
	• *Belgium*	*2*		• *Norway*	*38*
	• *Czechia*	*2*		• *Czechia*	*36*
	• *Hungary*	*2*		• *Sweden*	*36*
	• *Switzerland*	*2*		• *Hungary*	*34*
	• *Others (7)*	*7*		• *Others (18)*	*151*
Non European	**North America (3)**	**47**		**North America (11)**	**695**
	South America (7)	**36**		**South America (11)**	**350**
	Asia (26)	**216**		**Asia (40)**	**1897**
	Africa (11)	**28**		**Africa (34)**	**298**
	Oceania (1)	**13**		**Oceania (3)**	**224**
	Total (71)	**493**		**Total(133)**	**5763**

Table 5-1 Number of registered users per continent with **at least one active user role** (number of user countries during reporting period)



Reporting Period 01.04.2026 to 30.06.2026 with a total of 493 Users of 71 different countries.



Since beginning of operational phase until 30.06.2026 (end of reporting period) with total of 5763 Users of 133 different countries.

Figure 5-1 Number of registered users (with at least one active user role) per country

User per Category		New within reporting period 01.04.2026 to 30.06.2026	Since beginning of routine phase start until 30.06.2026 (end of reporting period)
Registered users	Total*	826	8273
	with active role assignment**	493	5763
Cat-1 Science	Total	439	5585
	AO Process 00001**	439	4718
	AO Process 00002**	0	641
	AO Process 00003**	0	225
Cat-2 Commercial	Total	29	102
Cat-1 Distributor***	Total	307	4247

Table 5-2 Number of registered users and number of released user roles per category (Cat-1 Science, Cat-2 Commercial and Cat-1 Distributor)

* Registered users inhibited user accounts excluded

**Registered users with at least one active user role

***Catalogue User, ordering EnMAP data from archive

Notice that registered users belong to different categories, therefore the sum of Cat-1 Science and Cat-1 Distributors or other categories does not correspond to the total registered users.

5.2 Announcements-of-Opportunities

Announcement-of-Opportunity	New within reporting period 01.04.2026 to 30.06.2026		Since beginning of routine Phase until 30.06.2026 (end of reporting period)	
	Proposals	Total tiles granted	Proposals	Total tiles granted
A00001	109	4973	1105	51678
A00002	0	0	126	10395
A00003	0	0	4	127
Total	109	4973	1235	62200

Table 5-3 Number of released science proposals per Announcement-of-Opportunity (AOs#) and total number of granted tiles per AO#.

Icon	Topic	New within reporting period 01.04.2026 to 30.06.2026		Since beginning of routine Phase until 30.06.2026 (end of reporting period)	
		Proposal	Total tiles granted	Proposal	Total tiles granted
	ATMOSPHERE	5	252	67	4 797
	CAL/VAL	4	468	45	6 143
	GEO/SOIL	22	655	391	11 621
	HAZARD/RISK	4	36	30	1 152
	METHODS	4	98	32	2 410
	SNOW/ICE	2	160	27	1 749
	URBAN	6	120	24	829
	VEGETATION	46	2 663	477	27 255
	WATER	16	521	142	6 244
	Total	**109**	**4 973**	**1 235**	**62 200**

Table 5-4 Number of accepted science proposals and total number of granted tiles per topic

6 Archived and Delivered Observations

The following table shows the number of archived Earth Observation and Calibration products and their sizes within the specified time frames.

Acquisition Type	Archived	Reporting Period 01.04.2026 to 30.06.2026		Since beginning of Commissioning Phase until 30.06.2026 (end of reporting period)	
		Number Tiles / Observations	Size (in GB)	Number Tiles / Observations	Size (in GB)
Earth Observation (EO)	Total	14192 / 1303	6915.31	263988 / 24167	128632.90
	Average / Day	155.96 / 14.32	75.99	170.10 / 15.57	82.88
Calibration (CAL)	Total	24	100.22	531	2117.31
	Average / Day	0.26	1.10	0.34	1.43

Table 6-1 Number and size of archived (more than one version of the same image can be archived)

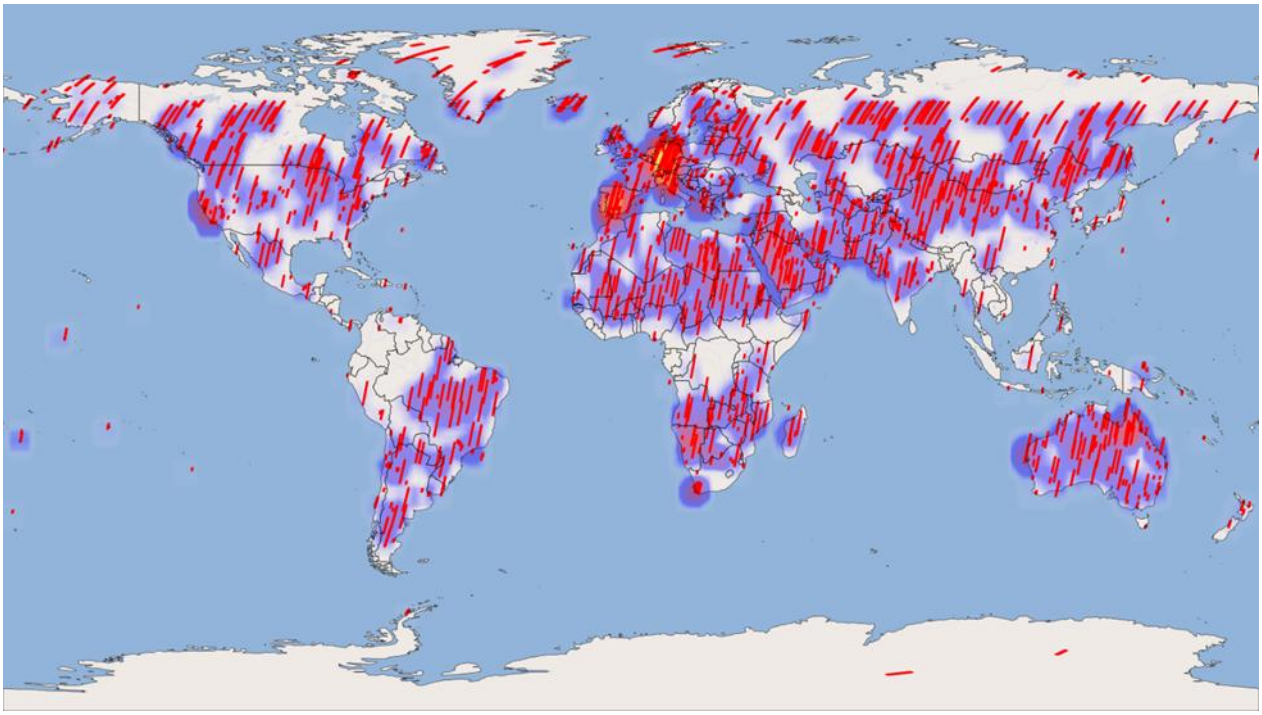
The following table shows the number of delivered products and their sizes within the specified time frames. Product deliveries result either directly from acquisition orders (“Acquisition”) or catalog orders (“Archive”).

Acquisition Type	Order Type		Reporting Period 01.04.2026 to 30.06.2026		Since beginning of Commissioning Phase until 30.06.2026 (end of reporting period)	
			Number Tiles / Observations	Size (in GB)	Number Tiles / Observations	Size (in GB)
Earth Observation (EO)	Acquisition	Total	15143 / 1313	6840.70	232164 / 21129	103275.52
		Average / Day	166.41 / 14.43	75.16	149.59 / 13.61	66.54
	Catalogue	Total	19418	7244.42	204070	75565.29
		Average / Day	213.38	79.60	131.49	48.69
Calibration (CAL)	Acquisition	Total	24	97.43	363	1534.08
		Average / Day	0.26	1.07	0.23	0.99
	Catalogue	Total	0	0.00	77	394.94
		Average / Day	0.00	0.00	0.050	0.25

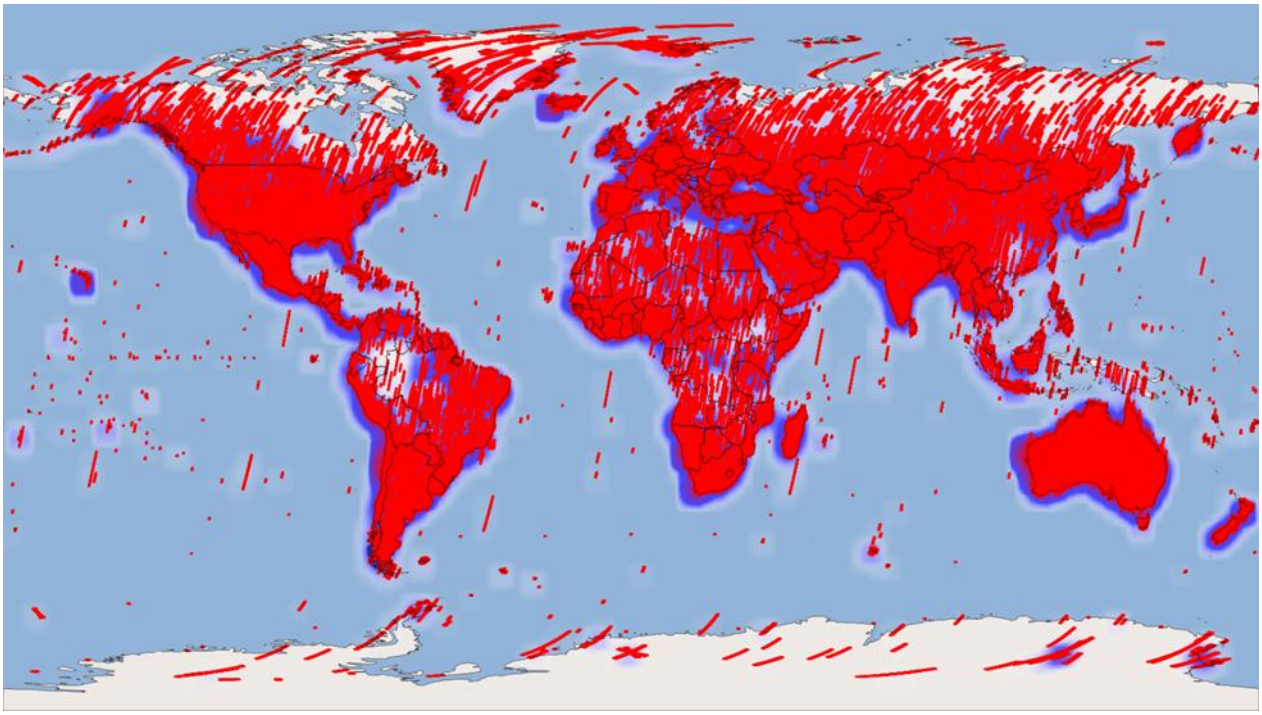
Table 6-2 Number and size of delivered products

6.1 Archived Acquisitions

The following figures show the heatmaps for the whole world and for Europe within the specified time frames. The heatmaps represent the frequencies of products at a geographic location, where the number of products increases from blue over red to yellow.

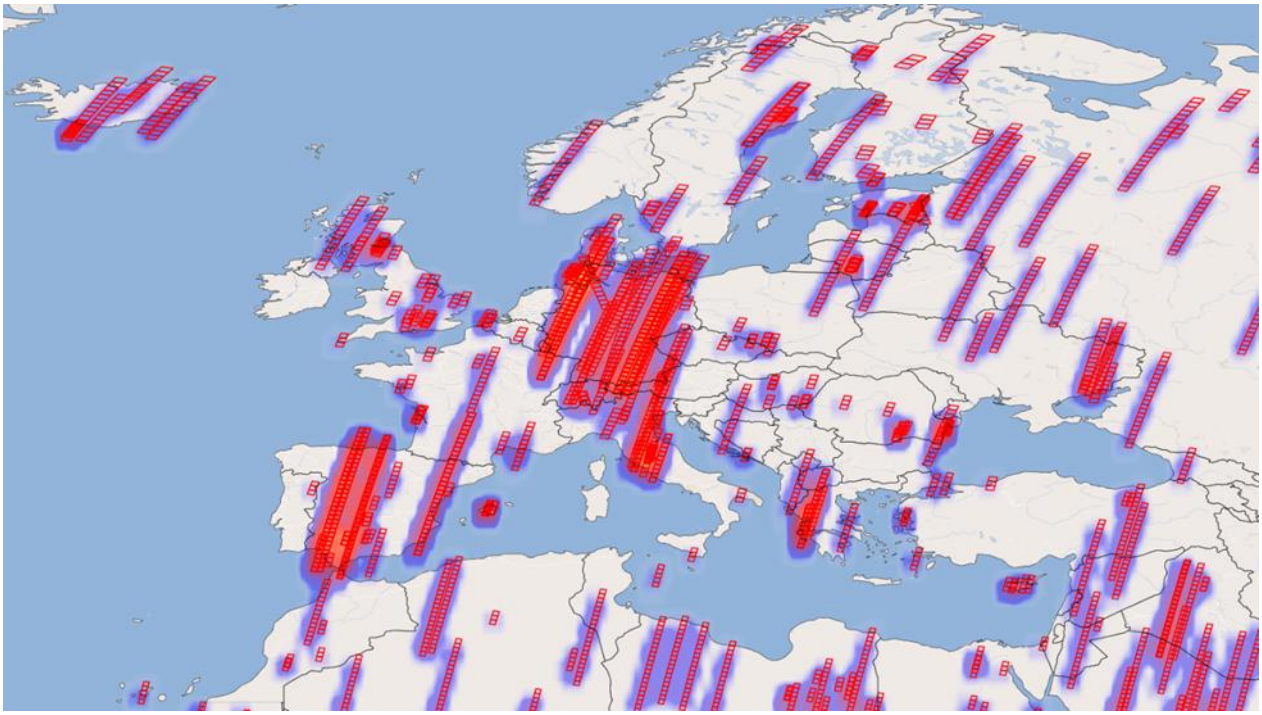


reporting period 01.04.2026 to 30.06.2026

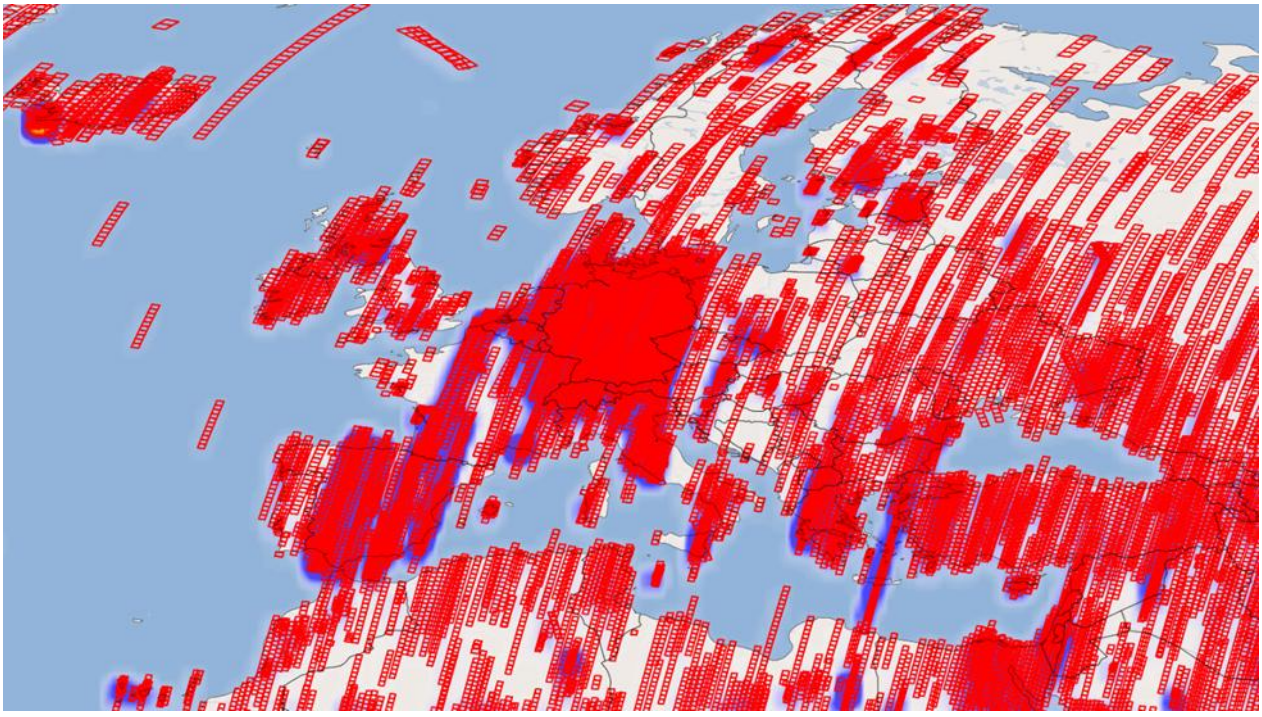


reporting period 2022-04-01 to 30.06.2026 includes commissioning phase acquisitions and different versions of the same tiles)

Figure 6-1 Geographic location of all Earth observation tiles archived, World



reporting period 01.04.2026 to 30.06.2026 Europe



reporting period 2022-04-01 to 30.06.2026 Europe (includes commissioning phase acquisitions)

Figure 6-2 Geographic location of all Earth observation tiles archived, Europe

The following figures show the distribution of cloud coverage for the archived products.

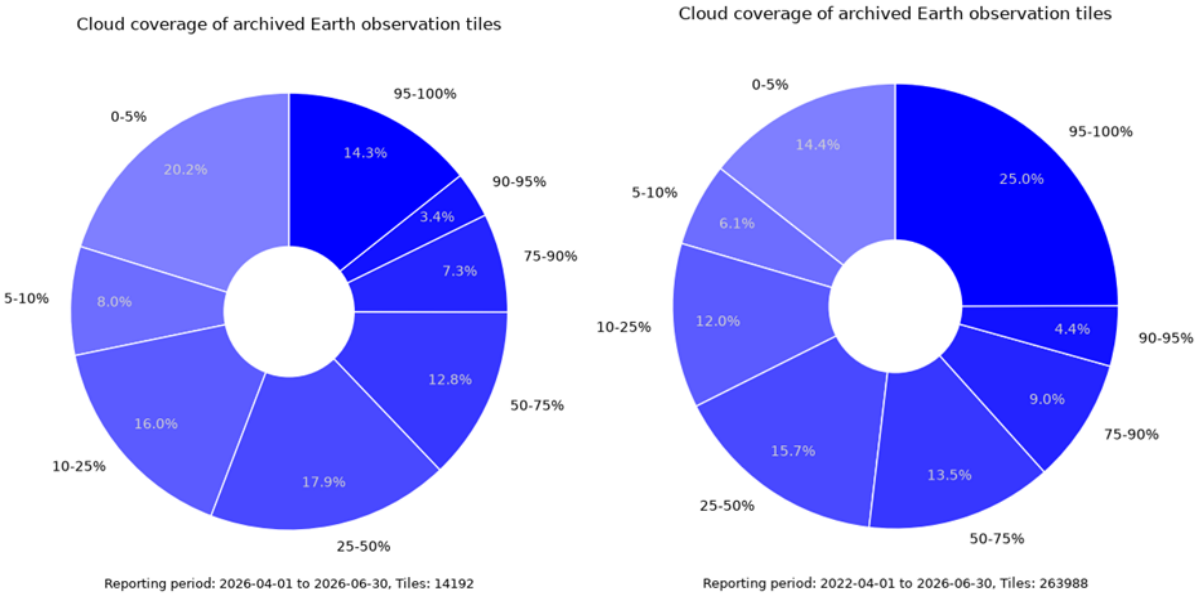


Figure 6-3 Cloud coverage in [%] of archived Earth observation tiles

The following figures show the distribution of observation angles for the archived products.

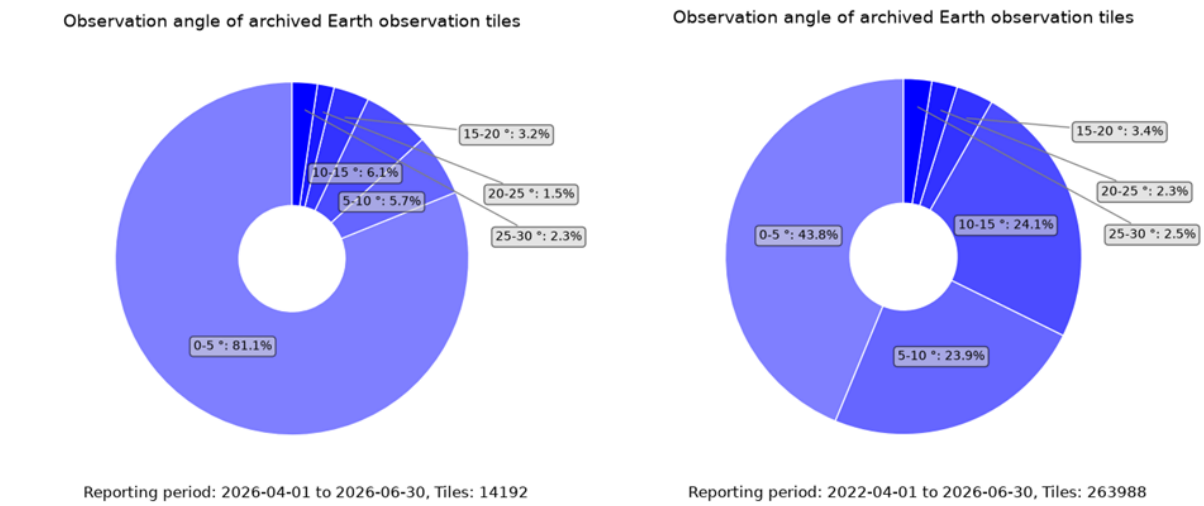


Figure 6-4 Observation angle of archived Earth observation tiles

6.2 Delivered Observations

The following figures show the distribution of processing level of the delivered products from acquisition orders.

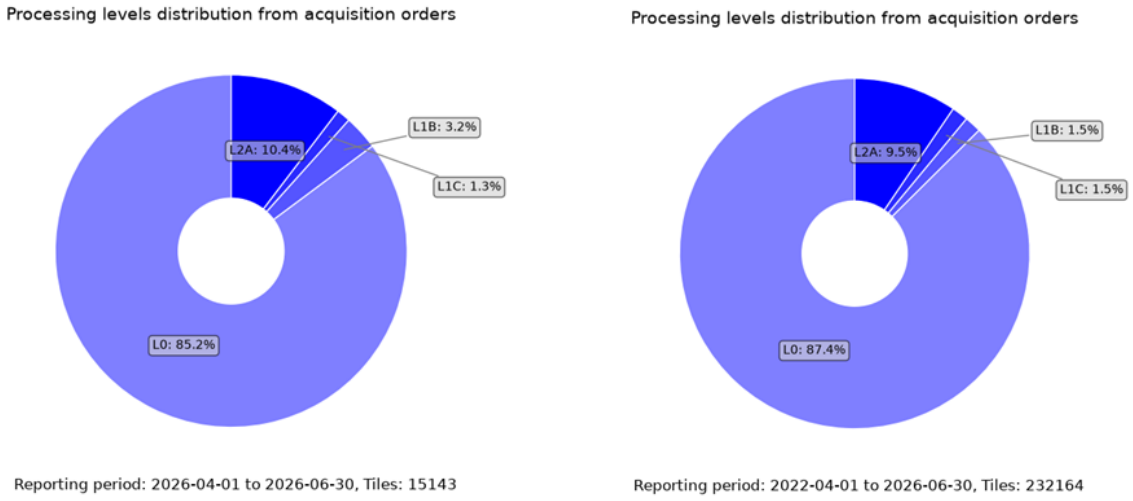


Figure 6-5 Levels of delivered Earth observation tiles from acquisition orders

The following figures show the distribution of processing level and correction type (for L2A) of the delivered products from catalog orders.

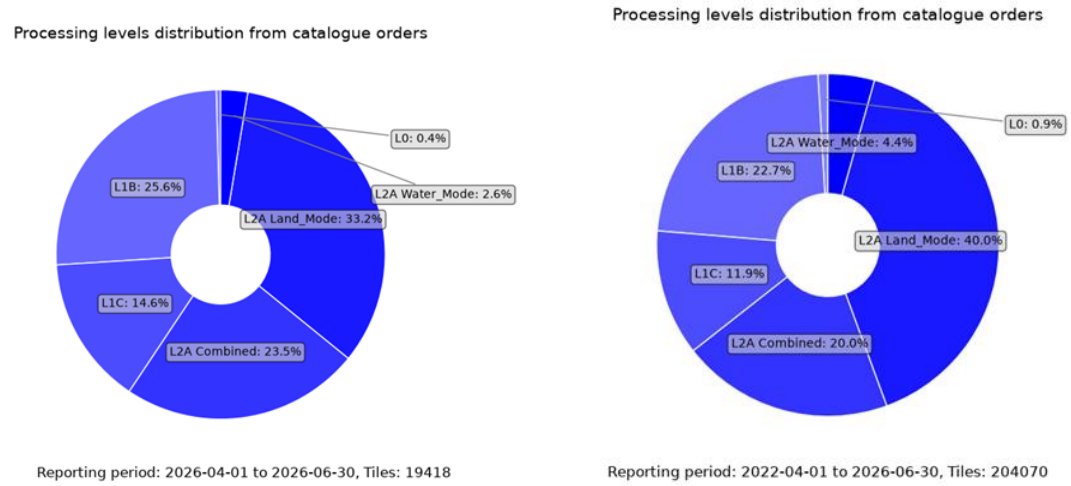


Figure 6-6 Levels of delivered Earth observation tiles from catalog orders

6.2.1 Delivered L2A products from the Download service (EOC Geoservice)

The Ground Segment also produces products already processed with standard parameters. CEOS certified L2A ARD products are available for direct download using the EOC Geoservice and the EOLab platforms. Since July 2025, the IPP account credentials also grant access to the EOC Geoservice to download EnMAP products.

EnMAP's Ground Segment processes all recorded data to L2A ARD format, saving computational and processing time. The default processing parameters of the L2A ARD are the following:

Product_Format = **GeoTIFF+Metadata**
Map Projection = **UTM_Zone_of_Scene_Center**
Image Resampling = **Bilinear_Interpolation**
Correction Type = **Land_Mode**
Cirrus Haze Removal = **No**
Band Interpolation = **No**
Terrain Correction = **Automatic**
Season = **Automatic**
Ozone column = **Automatic**

Table 6-3 Processing parameters used for the L2A ARD products in Geoservice / EOLab

In addition, take into account that:

- the versions of the L2A ARD products may differ depending on their generation time. The processor changelog (https://www.enmap.org/data/doc/EnMAP_processor_changelog.pdf) provides an overview of the software changes. During re-processing of the L2A ARD products, new versions of the products will replace older versions of the products. Currently a re-processing is in progress that shall bring all L2A products to at least version **V01.05.02**.

- No L2A-water products are available as L2A ARD products in Geoservice. For the moment water processing is only available using the on-demand processing options in EOWeb.

- The L2A ARD archive is now complete. All EnMAP products available in the Mission archive are also available as L2A ARD products at Geoservice / EOLab.

The total number of downloads* using the EOC Geoservice is **2176679** for this reporting period (01.04.2026 to 30.06.2026). Number of monthly downloads for this quarter are given in Table 6-4 and the graph with their evolution since the start of the service is shown in Figure 6-7.

Product	Month	# Downloads
ENMAP-L2A	2026-04	238862
ENMAP-L2A	2026-05	891365
ENMAP-L2A	2026-06	1046452
Total in period		2176679

Table 6-4 Absolut amount of downloads in Geoservice.

*Downloads count the download of a file from the EOC Geoservice. A EnMAP L2A product consists of 13 different files

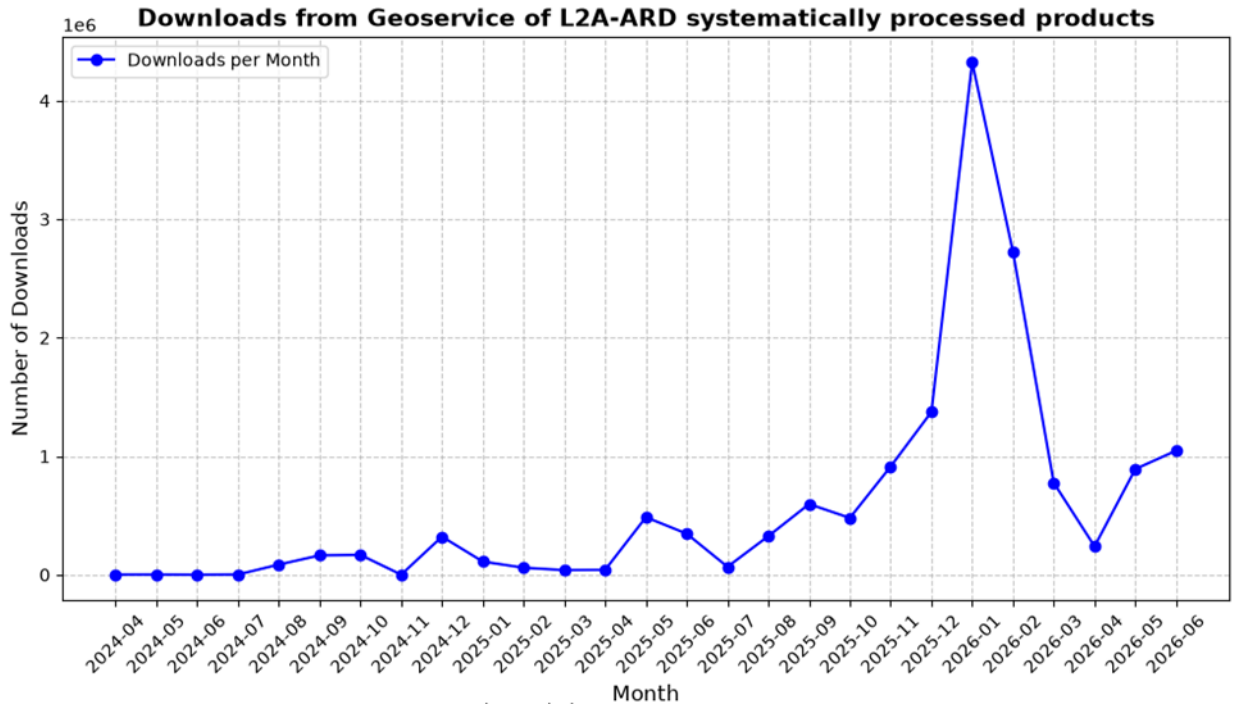


Figure 6-7 Downloads in Geoservice per month

In the current period, there is a remarkable increase in the download numbers as CloudFerro (EOlab) currently downloads all data for CodeDE3.

7 Detailed Status

7.1 Satellite

During the reporting period the mission has experienced different issues that resulted in 5 full days of no data acquisition and some other days with partial loss of acquisitions. The mission experienced a HSI SAFE_POWEROFF on 15.04.2026, and two HSI SAFE_ERRORs on 27.305.2026 and 18.06.2026. Nevertheless, the problem that caused the 5 days outage was an ACS EMERGENCY Mode on 08.05.2026 that was caused by faulty information by star tracker 2 when the field of view was oriented towards the Earth. As reported in all the previous events of these types, no consequences on the image or data quality are observed as a result of these events. For more details on data quality see sections 7.6 and 8.

The sporadic cancellation of acquisitions when the satellite is coming from the eclipse phase (known as “3-minute events”), has not been observed during the reporting period, as it was expected given the seasonal variability of this phenomenon. Changes in the configuration have been introduced in the reporting quarter and are expected to produce a notable reduction of these events. Typically, by end of August and during September the first cancellations start to happen. The Ground Segment will monitor the situation during Q3 and Q4 2026 to confirm if a reduction of these events is achieved.

More details about different satellite aspects are reported in the following subsections.

7.1.1 Orbit and Attitude Maneuvers

The reference orbit is a Sun-synchronous polar orbit with a mean local time of descending node of 11:00 hrs and a repeat cycle of 398 revolutions in 27 days at an altitude of 643 km.

The satellite orbit is controlled with respect to an Earth-fixed reference track over the entire orbit, analogous to a rim, with a control box of +/- 6 km in radial direction and +/- 22 km in normal direction.

During Q2 2026, a total of 1335 ACS Precise Modes were executed onBoard, compared to 1433 during the previous quarter. Due to the implementation of Back-to-Back Image Acquisitions, the number of ACS Precise Modes does not represent the number of performed activities. By executing two or three Images as one sequence, the total number of ACS Precise Modes decreases whereas the number of Image Acquisitions remains stable or increases. Over the whole mission, a total of 25822 ACS Precise Modes have been successfully executed.

During Q2 2026, two in-plane and one out-of-plane maneuvers were executed. No collision avoidance maneuvers were required. The resulting performance error off all maneuvers was estimated by FDS to range between +0.51% and +1.51%. No actuations of the Ball Latch Valve or other OCS configuration changes were performed during Q2 2026**.**

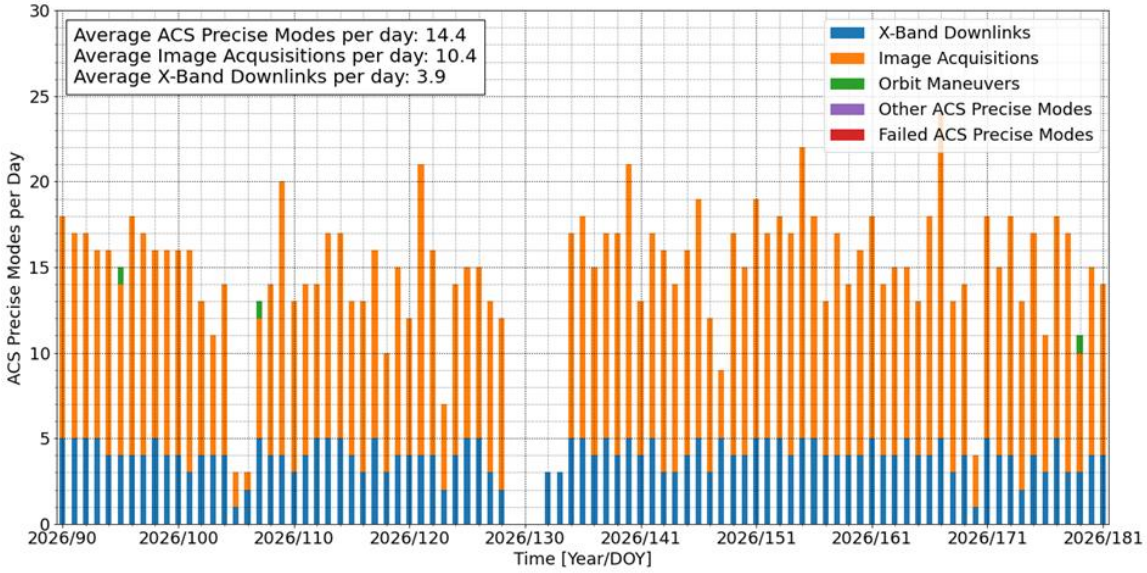


Figure 7-1 Number of ACS Precise Modes per day during Q2 2026

7.1.2 Life Limited Items

The life cycle of the life limited items is evaluated depending on their use. The life-limited items include the following optical and mechanical components:

Life-Limited Item	01.04.2026 to 30.06.2026	until 30.06.2026	Estimated minimum total lifetime / health of the system
Fuel(*)	+0.27 kg	10.3 kg	16.9 years
Battery and Solar Cells(**)	nominal	nominal	Nominal
Thruster thermal cycles	+3	95	333 qualifies cycels
Shutter Usage	+1.52%	28.18%	15.1 years (@ daily use)
FAD movements	+2.00%	35%	15.1 years (@ bimonthly use)
Diffuser exposure time based on sole measurement time(***)	+3.33%	58.33%	8.4 years (@ bimonthly use to reach 100% originally planned used)
Diffuser exposure time based on real cyclogram duration(***)	+3.60%	69.56%	7.3 years (@ bimonthly use to reach 100% originally planned used)
On-Board Calibration Equipment Usage	On-board calibration equipment:		
- OBCA SPC lamp 1	+1.41%	20.88%	19.4 years (@ biweekly use)
- OBCA RAD lamp 1/LED 1	+2.35%	40.96%	12.9 years (@ biweekly use)
- FPA LEDs 1	+0.56%	9.55%	44.5 years (@ monthly use)

Table 7-1 Status of life-limited items

(*) During periods with higher temperature and pressure fluctuations due to e.g., an Instrument shutdown and startup, the calculation of the propellant mass via the Pressure-Volume-Temperature method contains a relatively large margin of errors.

(**) The Power Subsystem is working nominally and as expected. Voltage stays above any critical level.

(***) A 100% Sun diffuser exposure time corresponds to a total planned exposure of 2 hours after 5 years when performing monthly Solar calibrations. The contribution of the diffuser to the total radiometric uncertainty after reaching the reference 100% value is estimated to be **0.6%** according to the instrument manufacturer. This value is significantly below the 5% total radiometric uncertainty requirement, which indicates that the diffuser will not be a relevant contributor to the total radiometric uncertainty of the

instrument even if the diffuser were to be used significantly above the originally allocated 2 hours of exposure time (reference 100% value). Nevertheless, the use of the diffuser is continuously monitored and accounted for in the Life-Limited Item list and thanks to the instrument stability the Sun calibration frequency is adjusted to reduce the number of necessary Solar calibrations.

The consumed resources (except fuel) are calculated based on the processed L0 product metadata, i.e. only successfully processed calibrations can be considered.

7.1.3 Redundancies

To date, the SWIR wavelength range is covered by SWIR-A (SWIR-B can be activated using a one-time switch mechanism).

All satellite subsystems are using nominal configurations.

7.2 Ground Stations

7.2.1 S-Band

S-Band Ground Stations	01.04.2026 to 30.06.2026		
	Total Passes	Non-Routine Passes (e.g. Anomaly Handling/SW Updates)	Failed Passes
All stations (Weilheim-Germany, Neustrelitz-Germany, Inuvik-Canada, O'Higgins-Antarctica, Svalbard-Norway)	567 (192 WHM, 212 NSG, 152 INU)	11	18

Table 7-2 S-Band Ground Station Passes

7.2.2 X-Band

X-Band Ground Stations	01.04.2026 to 30.06.2026	
	Executed Passes	Successful Passes
All stations (Neustrelitz-Germany, Inuvik-Canada)	354 (253 NSG, 101 INU)	354 (253 NSG, 101 INU)

Table 7-3 X-Band Ground Station Passes

Inuvik (Canada) station was integrated in Q4 2023 into the regular operations of the EnMAP Ground Segment for X-Band and S-Band downlinks. After integration, more data and more flexibility in S-band and X-band data reception is achieved, especially concerning image acquisitions over Europe.

7.3 User Interfaces

Further improvements to the user interfaces are continuously on-going and will be reported in this section.

During the reporting period the Ground Segment of EnMAP continues to update the information on future high priority observations of the EnMAP mission (*Foreground Mission*). The tool displaying this information is available at the EnMAP web site (under https://www.enmap.org/data_tools/foreground_mission/).

With this tool the users can get informed weeks in advance about future priority observations with EnMAP. Initially, a set of long flight-lines (990km) over Germany and other European countries have been identified together with the user community and will be regularly scheduled. Since July 2024, the Foreground mission has expanded to include additional European regions. The foreground mission continued in Q2 2026 to

focus on Europe, using the new configuration of monthly and bi-monthly regular flightlines that was the result of the Foreground Mission Survey that took place at the start of 2026.

In addition to the regular flightlines, since May 2026 campaign support with EnMAP's Foreground Mission can be requested in cases where:

- Campaigns are performed in Europe during the Foreground Mission season (March–September)
- Concordant airborne campaigns are performed, or
- Exceptionally large-scale field campaigns involving coordinated satellite and in situ measurements

Support can be requested for campaigns fulfilling these criteria by following these steps:

1. 6 weeks before the start of the campaign, filling the questionnaire that can be found at https://survey.hifis.dkfz.de/371151?lang=en
2. **2 weeks** before the campaign start, Contacting DLR EnMAP Application Support (ENMAP_APPLICATION_SP@dlr.de) to confirm and fine-tune the acquisition

7.4 Processors

Reference [3] provides the product specification and [4], [5], [6], [7] the algorithm theoretical basis for Level 1B, Level 1C and Level 2A (land / water).

In the reporting period (01.04.2026 to 30.06.2026) there has been no update in the EnMAP processing chain. The latest version of the EnMAP processing software, **V01.05.06**, was first made available to the users **06.02.2026**.

The changelog document was not updated during Q2 2026. The document contains the history of EnMAP processor updates and shows the updates performed in the processing software. The document can be downloaded from the EnMAP website:

https://www.enmap.org/data/doc/EnMAP_processor_changelog.pdf

The following changes are expected to be performed in the future quarters:

- Update of the linearity calibration and other adjustments to improve the matching between VNIR and SWIR spectrometers.
- Small update of the spectral calibration
- Optimizations for the processing of Moon Calibration data

7.5 Calibrations

Table 7-4 summarizes the radiometric calibration observations acquired in this quarter and which will be described in the rest of this section. The calibration acquisitions were generally acquired according to the routine operations plan.

Category	01.04.2026 to 30.06.2026	
	Number of Archived Observations	Size (in GB)
Total	24	98.9
Deep Space	3	3.9
Rel. Radiometric	9	35.1
Abs. Radiometric	2	2.6
Linearity	3	51
Spectral Calibration	7	6.3

Table 7-4 Number and size of archived radiometric and spectral calibration observations

The continuous degradation of the VNIR sensor was monitored and quantified. The rate of degradation is constantly decreasing as illustrated in Figure 7-2 and by the end of March 2023 it has reached the point where it is practically negligible and has been kept that way during the reporting period. It shall be noted, though, that this average trend is different at different parts of the detector as illustrated for individual pixels in Figure 7-3. The effect on the radiometric calibration coefficients of a few selected bands is shown in Figure 7-4.

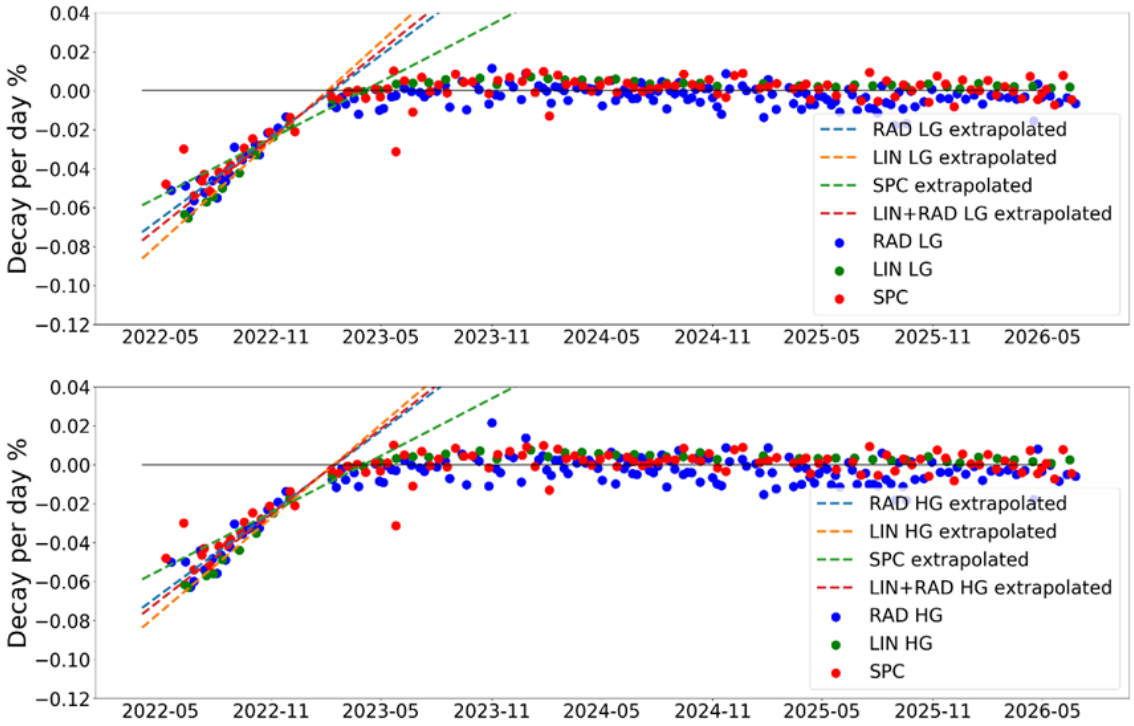


Figure 7-2 Decay per day from Lamp (RAD), Linearity (LIN) and Spectral (SPC) measurements for low gain (top) and high gain (bottom)

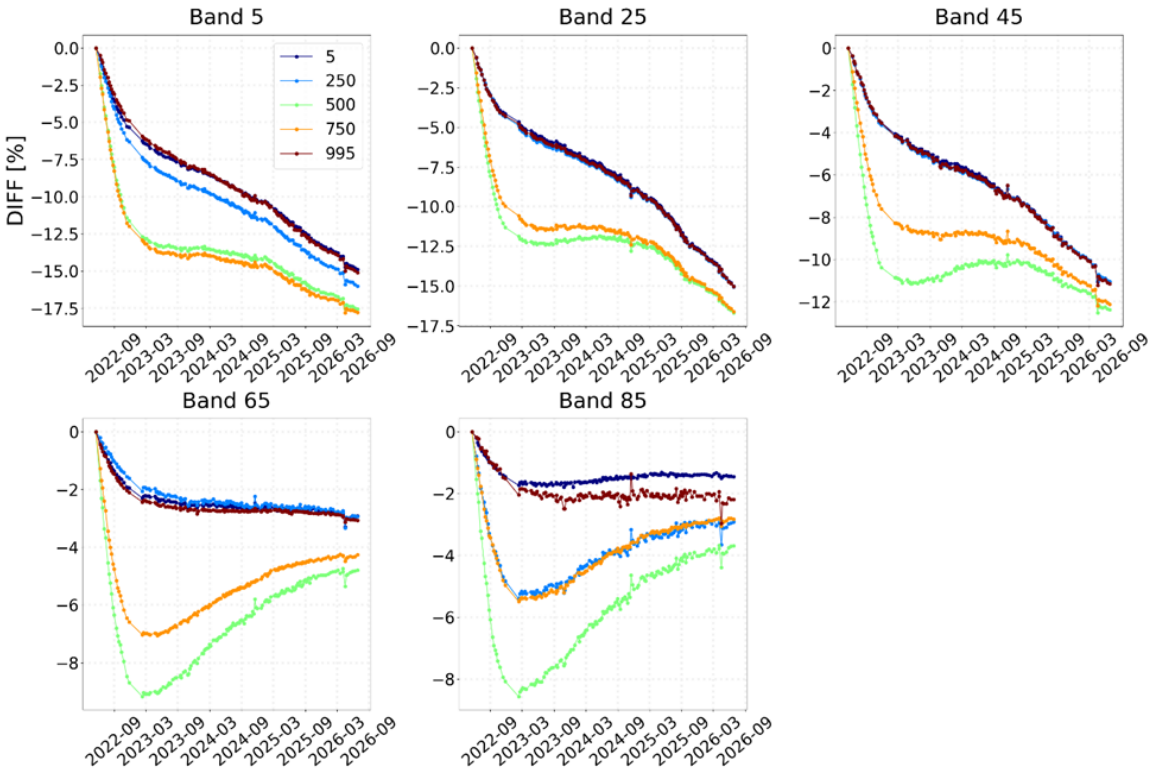


Figure 7-3 Change in percentage for individual pixels based on OBCA-Lamp measurements given for 5 bands and 5 cross track elements (coloured lines).

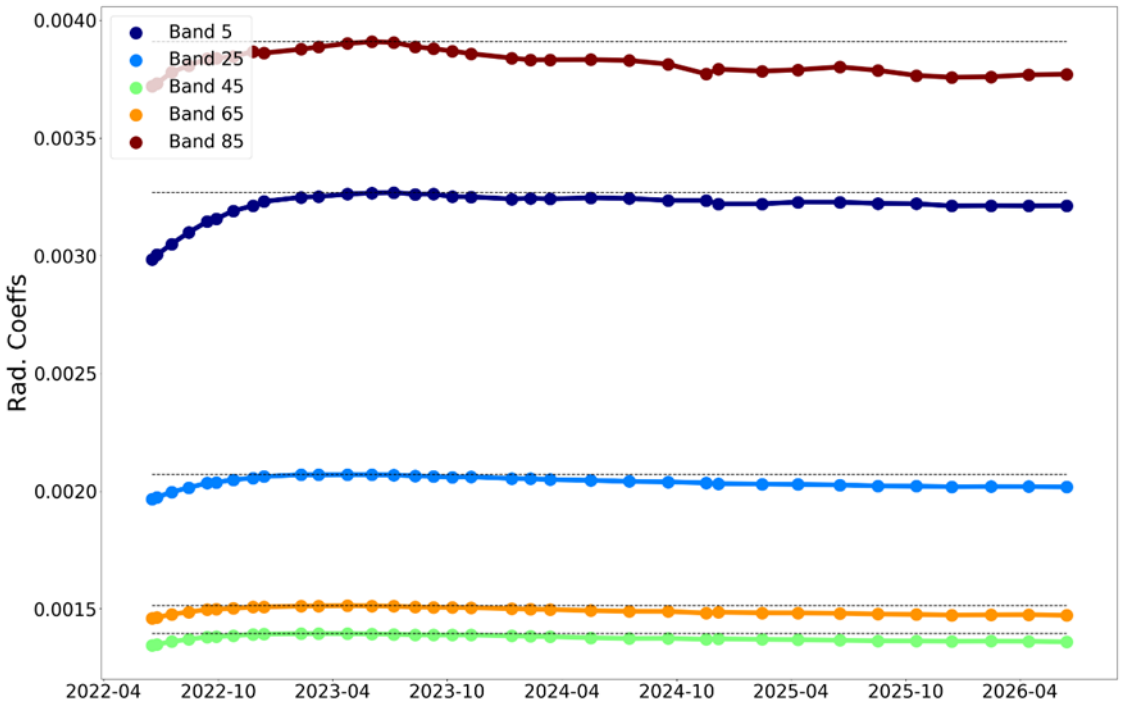


Figure 7-4 Average percentage change in the VNIR radiometric coefficients for five selected bands since launch

7.5.1 Dead Pixels

The following table shows the number and percentage of dead pixels. Figure 7-5 and Figure 7-6 show the position of the dead pixels in the focal plane of VNIR and SWIR sensors respectively. There have been no updates since 31.08.2022.

Defect Pixels	01.04.2026 to 30.06.2026	
	Number of Pixels	Percent
Total	1921	0.8
VNIR	137	0.2
SWIR	1784	1.2

Table 7-5 Number and percent of dead pixels

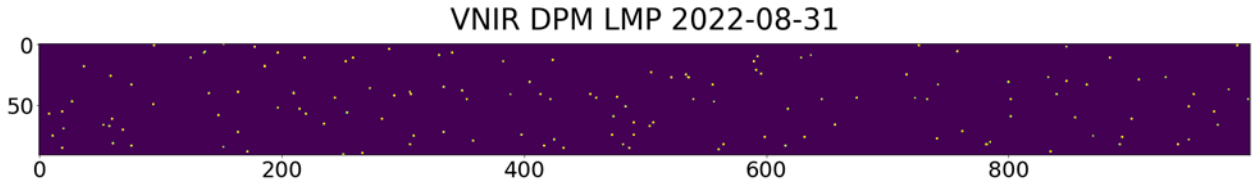


Figure 7-5 VNIR Dead Pixel Mask

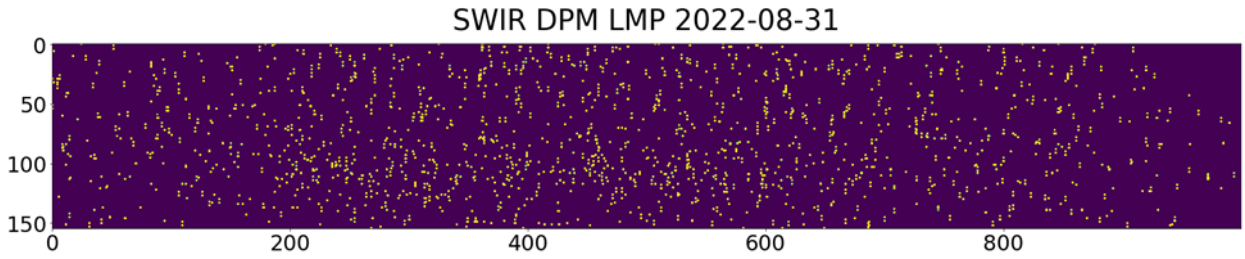


Figure 7-6 SWIR Dead Pixel Mask

There are no clusters of more than three spectrally or spatially adjacent dead pixels.

7.5.2 Spectral Calibration

Remark: In the following figures, OBCA is abbreviation for On-Board Calibration Assembly for spectral and radiometric calibrations.

Category	01.04.2026 to 30.06.2026	
	Number of Archived Observations	Size (in GB)
Total	7	6.3
Spectral Calibration	7	6.3

Table 7-6 Number and size of archived spectral calibration observations

The spectral properties – in particular center wavelength (CW) (see Figure 7-7 and Figure 7-8) and full width at half maximum (FWHM) (see Figure 7-10) for each band (spectral coordinate) and pixel (spatial coordinate) – have been characterized, considering all bands and pixels provided in Level 1B, Level 1C and Level 2A products.

The major conclusions of the monitoring of the spectral performance are summarized as follows:

- During the reporting period, 7 spectral calibration measurements were made which took place on: 10.04.2026, 23.04.2026, 30.04.2026, 06.05.2026, 20.05.2026, 03.06.2026 and 17.06.2026.

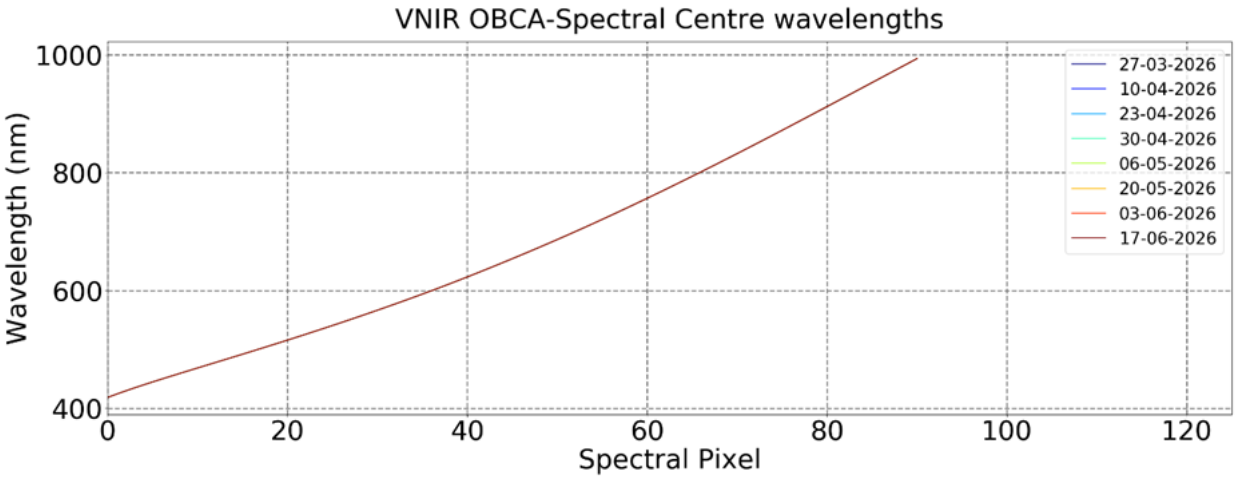
- The VNIR spectral range in this reporting period was found to be 418.5 – 993.4 nm over 91 bands (Figure 7-7). The average spectral sampling distance was 6.4 nm with a total range of 4.7 – 8.2 nm. This meets the requirement for overall wavelength coverage [HSI-POSS-0210], average spectral sampling distance [HSI-POSS-0310] and spectral sampling distance range [HSI-POSS-0320].

- The SWIR spectral range in this reporting period was found to be 902.0 – 2445.3 nm over 155 bands (Figure 7-7). The average spectral sampling distance was 10.0 nm with a total range of 7.5 – 12.0 nm. This meets the requirement for overall wavelength coverage [HSI-POSS-0210], average spectral sampling distance [HSI-POSS-0310] and spectral sampling distance range [HSI-POSS-0320].

- The spectral calibration measurements from this quarter show good temporal stability – measurements showed an absolute <0.14 nm change from the VNIR sensor and <0.25 nm change in SWIR (Figure 7-8) with respect to current spectral calibration table. All changes were below 0.5 nm between measurements for VNIR and below 0.5 nm SWIR. Long-term VNIR and SWIR spectral shifts are reported in Figure 7-9. This meets the requirement for consecutive spectral stability [HSI-POSS-0510] and overall spectral stability [HSI-POSS-0520].

- FWHM for VNIR and SWIR (Figure 7-10) are shown below but are not recalculated inflight.

- A VNIR degradation pattern is not clearly visible between consecutive spectral reference measurements acquired in this period, but there are positive and negative changes across the detector and on average the signal appears to have changed by -0.02% across all pixels from 27.03.2026 to 17.06.2026. A comparable change was reported in the previous quarter (0.01%). Although now very small, the monitoring of this behavior will continue in the next reporting period.



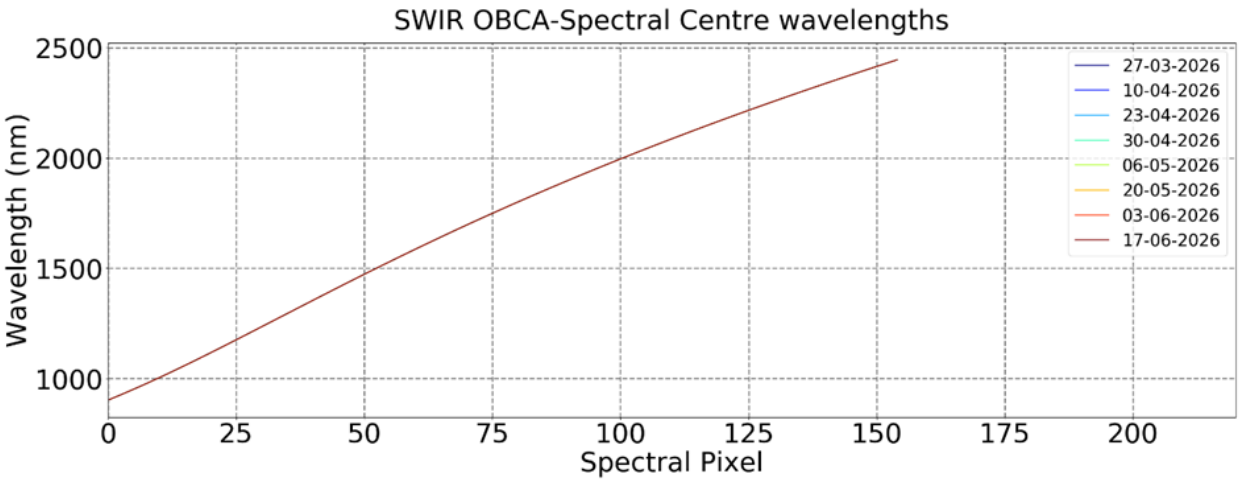


Figure 7-7 VNIR (top) and SWIR (bottom) center wavelength in nm

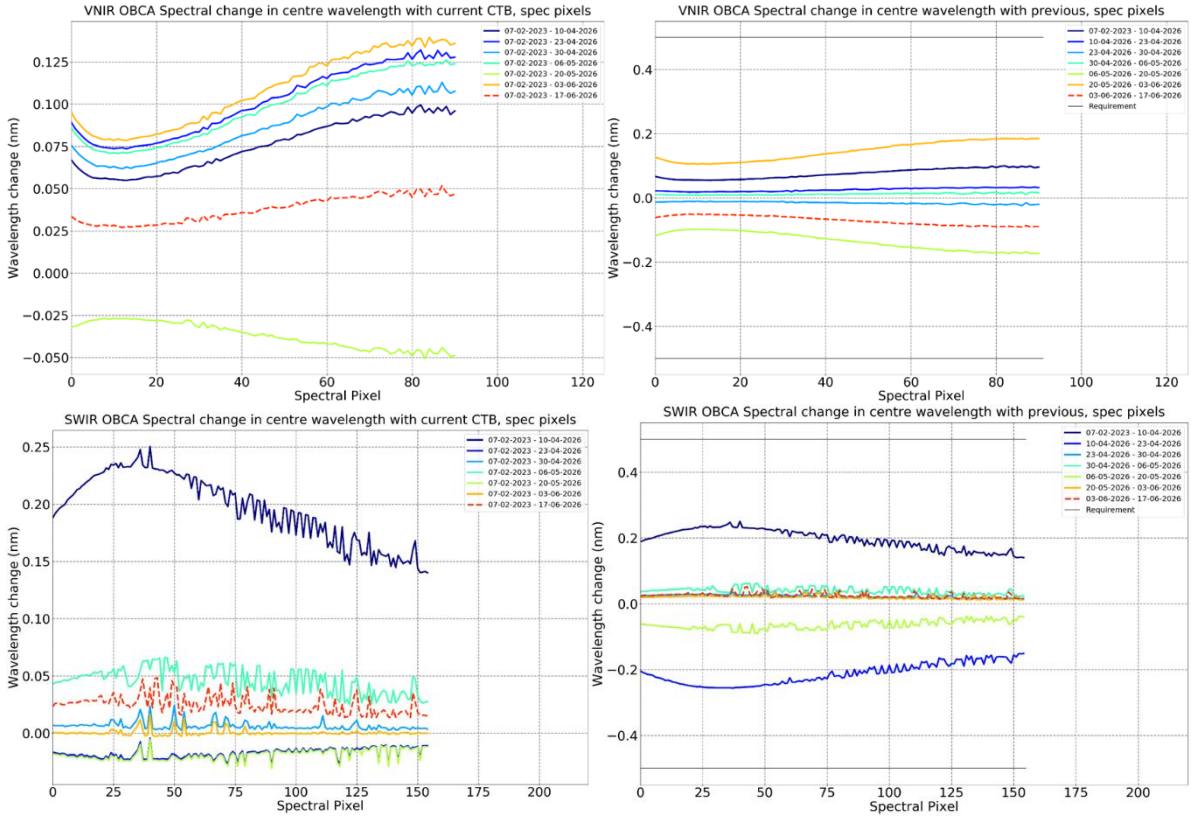


Figure 7-8 Change in center wavelength per spectral pixel for VNIR (top) and SWIR (bottom). Left panels show the changes with respect to current spectral calibration table in use and right panels with respect to the previous measurements.

A long-term shift of approximately 0.2 nm towards longer wavelengths in the SWIR sensor can be seen since the last spectral update in February 2023. This represents a small shift and so had not previously been corrected for. However, due to its persistent nature throughout the operational phase, an investigation is underway to assess the impact of correcting for this shift by backdating a recent spectral calibration table. If successfully validated by Quality Control, a new spectral calibration table will be created from February

2023 which accounts for this 0.2 nm shift in SWIR (with little to no change in VNIR). All subsequent radiometric calibration tables will also be updated.

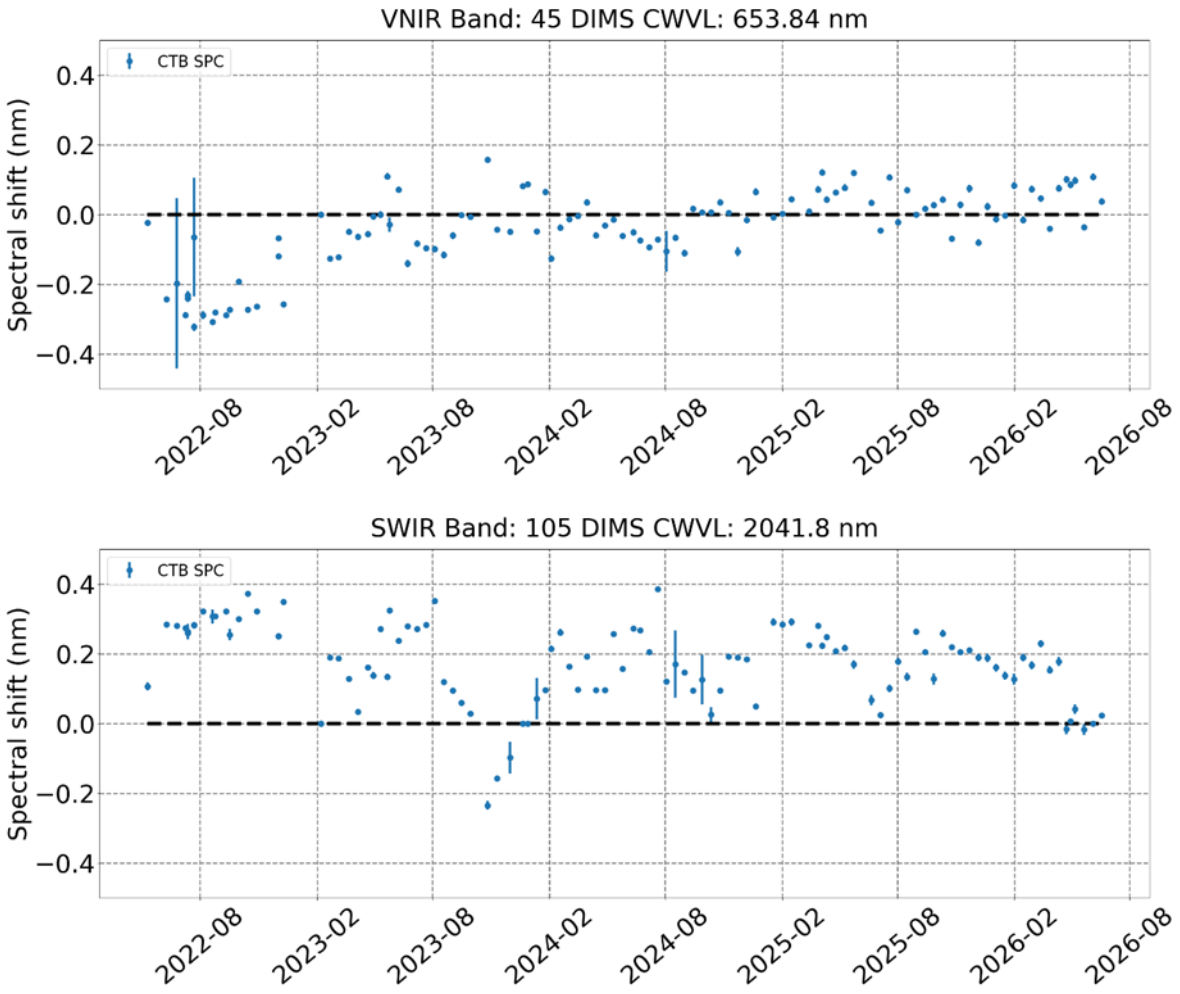


Figure 7-9 Long-term VNIR (top) and SWIR (bottom) spectral shifts since the beginning of the mission for VNIR band 45 at 654 nm and SWIR band 105 at 2042 nm.

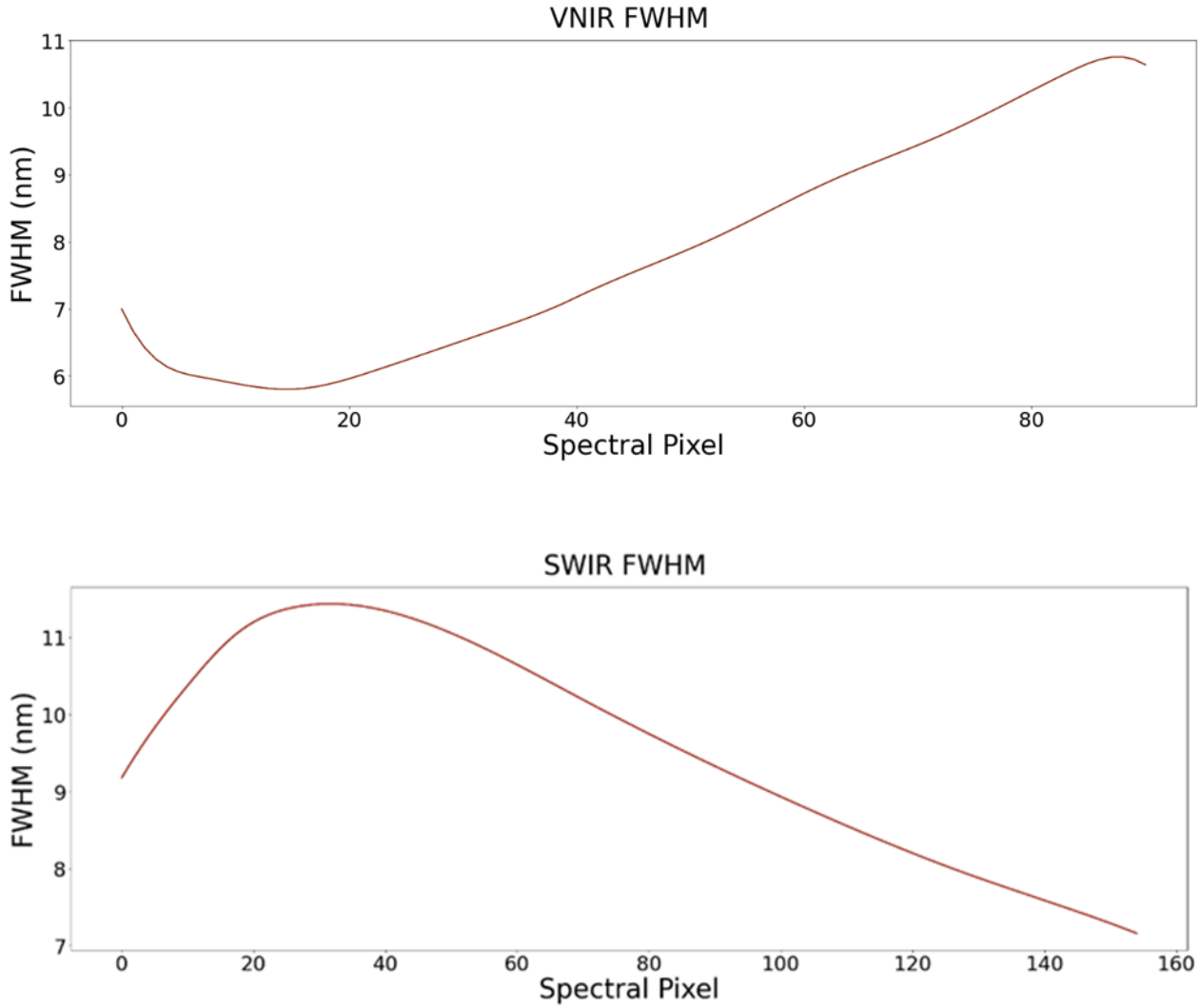


Figure 7-10 VNIR (top) and SWIR (bottom) FWHM in nm

CW and FWHM are available in the spectral calibration tables (see Table 7-7) and System Response Functions (SRF) per band are modelled by a Gaussian shape using those parameters.

Spectral calibration updates

No new calibration products were generated and delivered during the reporting period.

Product	Type	Date of Generation	Date of Validity Start	Date of Validity End	Delivered to
none					

Table 7-7 Generated spectral calibration tables

7.5.3 Radiometric Calibration

Category	01.04.2026 to 30.06.2026	
	Number of Archived Observations	Size (in GB)
Total	17	92.6
Deep Space	3	3.9
Rel. Radiometric	9	35.1

Abs. Radiometric	2	2.6
Linearity	3	51

Table 7-8 Number and size of archived radiometric calibration observations

The radiometric properties – characterized in particular by the calibration coefficient for each band (spectral coordinate) and pixel (spatial coordinate) and radiance – during this reporting period are investigated, considering all bands and pixels and radiances provided in Level 1B, Level 1C and Level 2A products.

Radiometric calibration coefficients (see Figure 7-11, Figure 7-12 and Table 7-10) and VNIR RNU (response non-uniformity, see Figure 7-14) were affected by the degradation of the VNIR sensor during commissioning but have stabilized from Q1 2023. In-flight, the gain matching coefficients (see Figure 7-13), the SWIR calibration coefficients, and the SWIR RNU (response non-uniformity, see Figure 7-14) have been stable.

During the reporting period, two Absolute Radiometric Calibration measurements were obtained. These took place on: 15.04.2026 and 15.06.2026.

Albeit now relatively small in magnitude, changes in the VNIR sensor have led to the creation of new calibration and reference tables for the new absolute radiometric measurement.

Although the VNIR degradation has almost stopped, the overall effects are visible in the reference measurements of the sun. However geometric conditions (sun-earth distance, pointing angle) also play a role in the absolute magnitude so the degradation cannot be quantified with these reference measurements.

The major conclusions of the monitoring of the absolute performance are summarized as follows:

- Changes in the VNIR sensor have affected the absolute Radiometric calibration coefficients: the increasing signal in the VNIR sensor, although not homogeneous, has resulted in decreasing radiometric coefficients. In this reporting period, the calibration coefficients increased by only -0.11% to offset the increase in absolute (Figure 7-11 and Figure 7-12). Regarding RNU, the degradation features are still visible in the focal plane (Figure 7-14). Lastly, the Gain Matching correction has been relatively stable during this reporting period (Figure 7-13).

- The SWIR sensor has shown good stability during this reporting period, with no significant changes in the gain matching, RNU or radiometric calibration coefficients (Figure 7-11 and Figure 7-12).

- Regarding the total change in calibration corrections as a result of the VNIR degradation, almost all pixels experienced a change of less than 2.5% between consecutive measurements as set in requirement [HSI-POSR-0410]. The only pixels which exceeded this value were already marked as dead during inflight assessment. No SWIR pixels experienced a change of more than 2.5% between consecutive absolute calibration measurements.

- New VNIR and SWIR calibration and reference tables were created for the absolute radiometric measurements from 15.04.2026 and 15.06.2026, despite the small changes seen in the calibration coefficients. The VNIR radiometric calibration coefficients have decreased in this reporting period to offset the increasing VNIR signal. If the VNIR (and SWIR) calibration continues to behave in a stable manner, it will not be necessary to create new calibration tables for every Absolute Radiometric calibration measurement.

- Since April 2024, Absolute Radiometric Calibration measurements are planned at intervals of two months, following the stable performance of both sensors, and to allow for the extension of the lifetime of the solar diffuser.

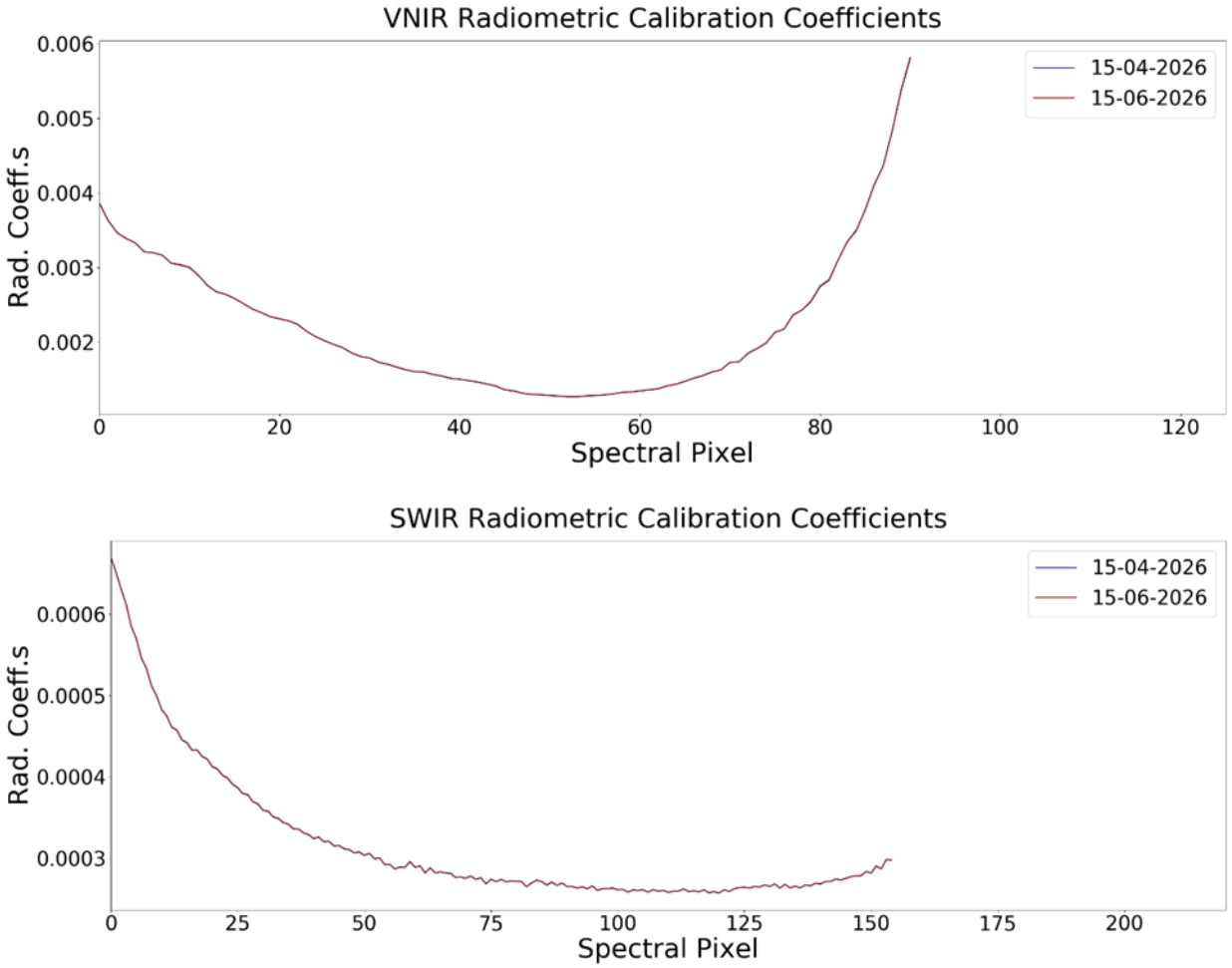


Figure 7-11 VNIR (top) and SWIR (bottom) calibration coefficient in mW/cm²/sr/µm

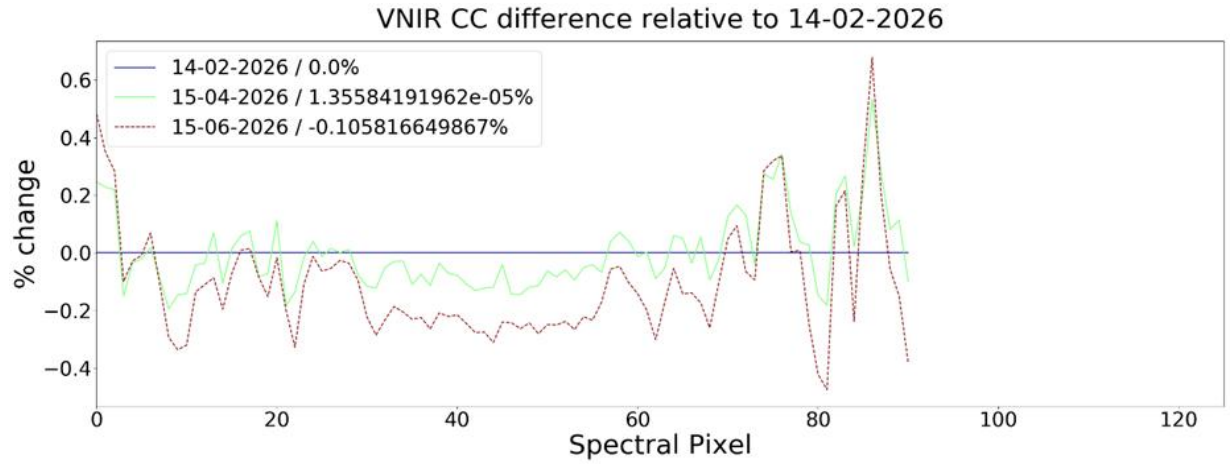




Figure 7-12 Percentage change in VNIR Calibration Coefficients (top) and SWIR Calibration Coefficients (bottom)

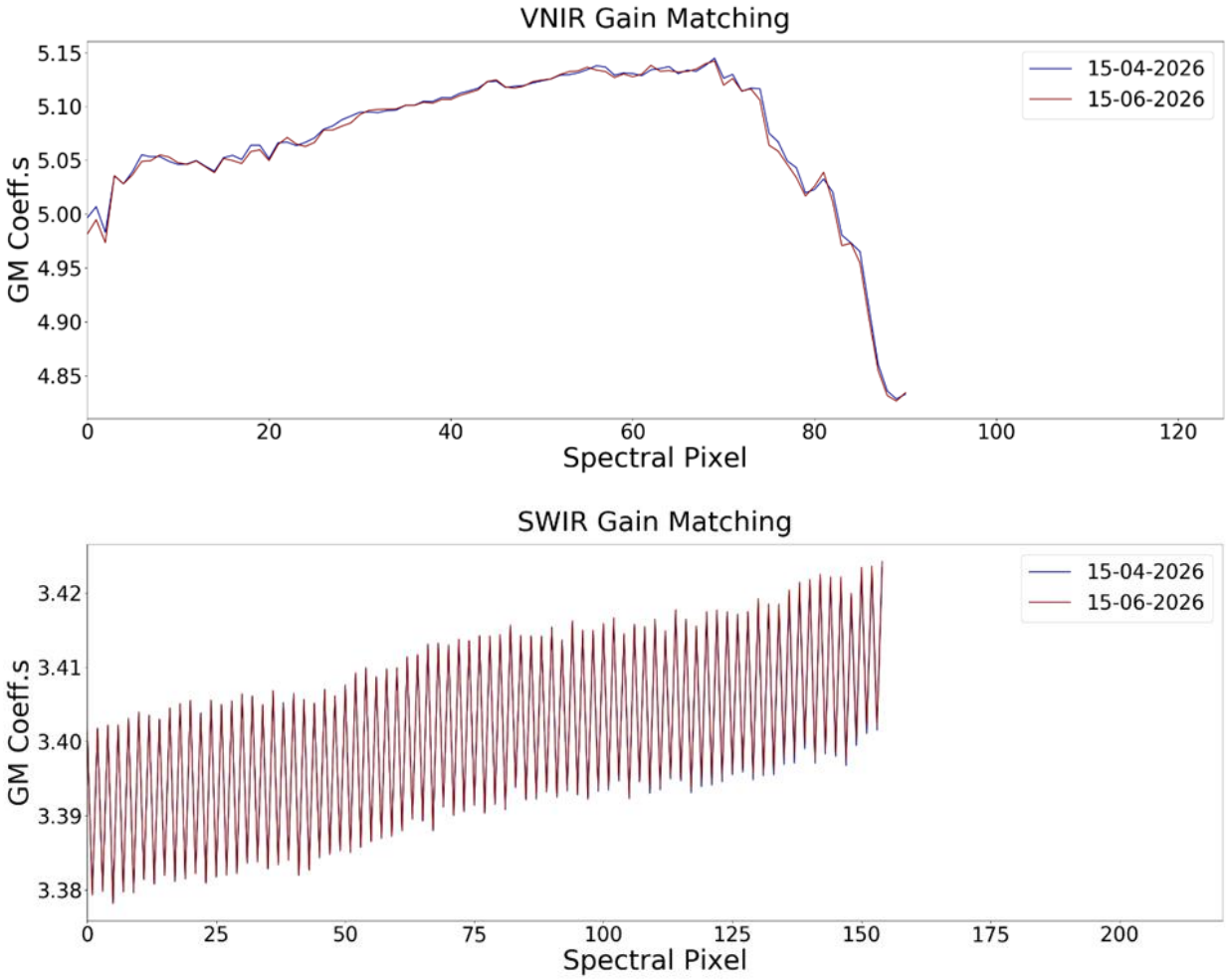


Figure 7-13 VNIR (top) and SWIR (bottom) gain matching calibration coefficients

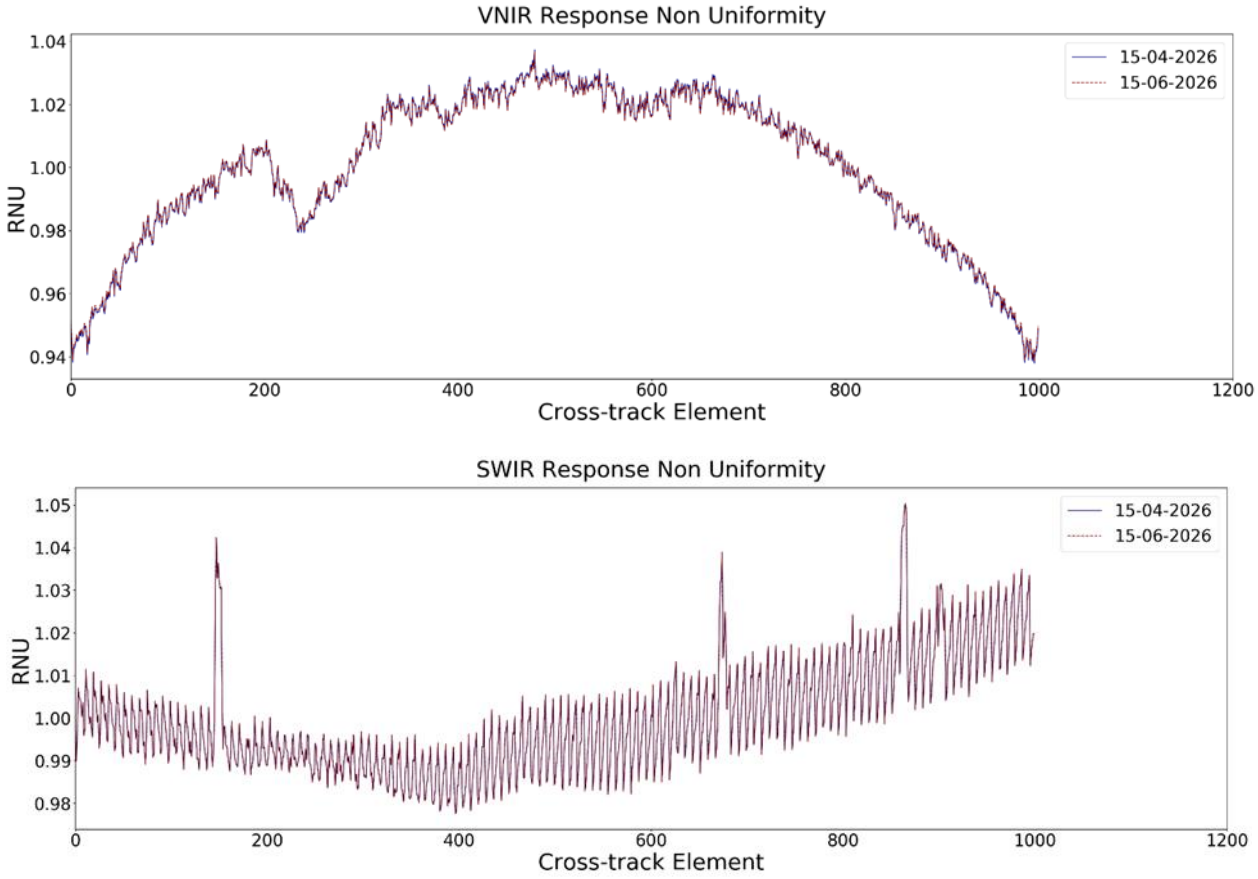


Figure 7-14 VNIR (top) and SWIR (bottom) response non-uniformity coefficients

Signal-to-Noise Ratio

The Signal-to-Noise Ratio (SNR) is derived from the Linearity reference measurements. This is not a perfect set-up for the assessment of the SNR as the linearity measurements only cover a single wavelength and light level at increasing integration times. However, it is well constrained, covering a wide range of radiances including the levels of the reference radiance spectrum that is used to evaluate the requirements (30% reflectance, 30° sun incidence angle, 21 km visibility, target 500 m above sea level). The lamp reference measurements are not used, as the reference spectrum is not well covered at the radiances of the lamp and extrapolation would be required to test the performance at the SNR requirements. Those requirements are: SNR greater than 500 at 495 nm in VNIR for the reference spectrum value given a 10 nm pixel; and SNR greater than 150 at 2200 nm in SWIR for the reference spectrum given a 10 nm pixel.

For the VNIR sensor, SNR is computed from the linearity calibration measurement. SNR values are shown as a contour map with the reference radiance spectrum as a blue line. Contour lines with SNR values of 150 and 500 are also shown in black. The plot in low gain mode includes the mission requirement which is evaluated at 495 nm for a radiance value of 36 mW/cm^2/μm/sr and is expected to be greater than 500: the calculated value here is **592**. The radiance value used here for the evaluation is the value at 495 nm of the reference radiance spectrum after bandwidth normalization to a 10 nm pixel (see Figure 7-16).

For the SWIR sensor, SNR is also computed from the linearity calibration measurement. SNR values for the high gain mode are shown as a contour map with the reference radiance spectrum as a blue line. Contour lines with SNR values of 150 and 500 are also shown in black. The plot in high gain mode includes the mission requirement which is evaluated at 2200 nm for a radiance value of 0.5 mW/cm^2/μm/sr and is expected to be greater than 150: the calculated value here is **249**. The radiance value used here for the evaluation is the value at 2200 nm of the reference radiance spectrum after bandwidth normalization to a 10 nm pixel (see Figure 7-17).

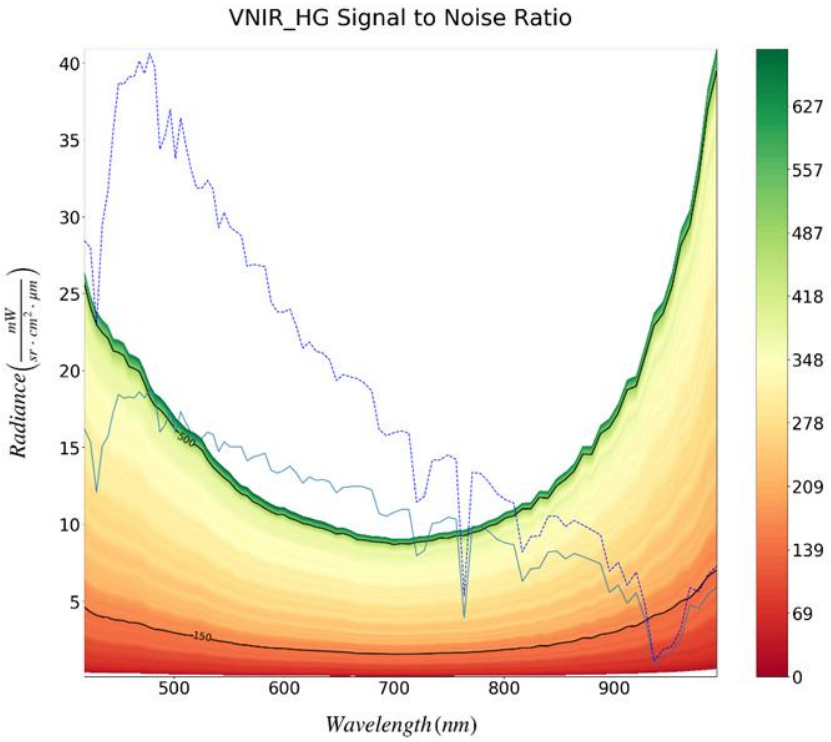


Figure 7-15 SNR contour map for VNIR high gain from the LED linearity observations observed on 14.06.2026. The reference radiance is shown with a blue line and after bandwidth normalization to a 10 nm pixel (dotted). Contour lines with SNR values of 150 and 500 are also shown in black.

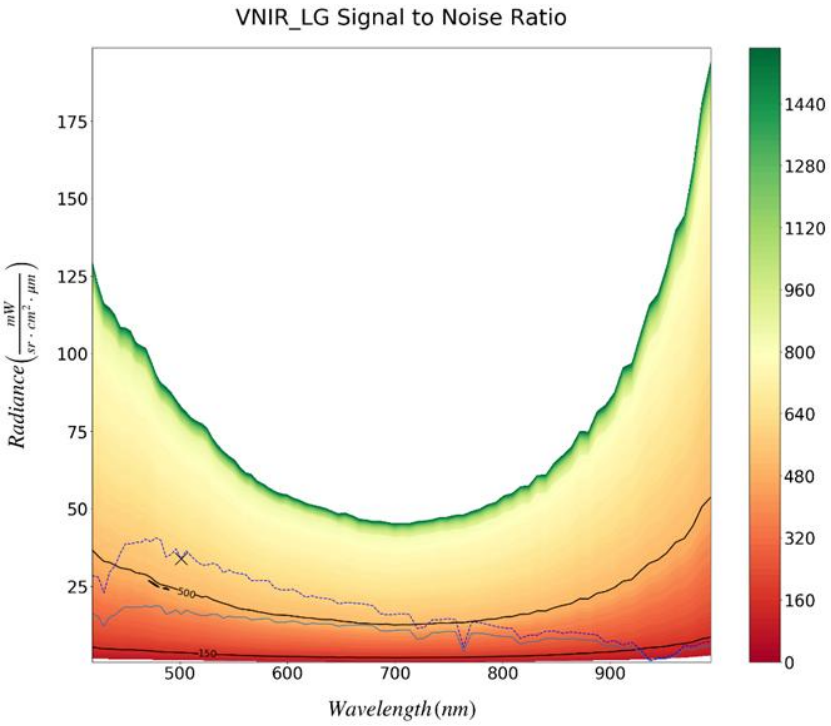


Figure 7-16 SNR contour map for VNIR low gain from the LED linearity observations observed on 14.06.2026. The reference radiance is shown with a blue line and after bandwidth normalization to a 10 nm pixel (dotted). Contour lines with SNR values of 150 and 500 are also shown in black. The mission requirement is evaluated at 495 nm for a radiance value of 36 mW/cm^2/µm/sr (marked with a black cross) and is expected to be greater than 500.

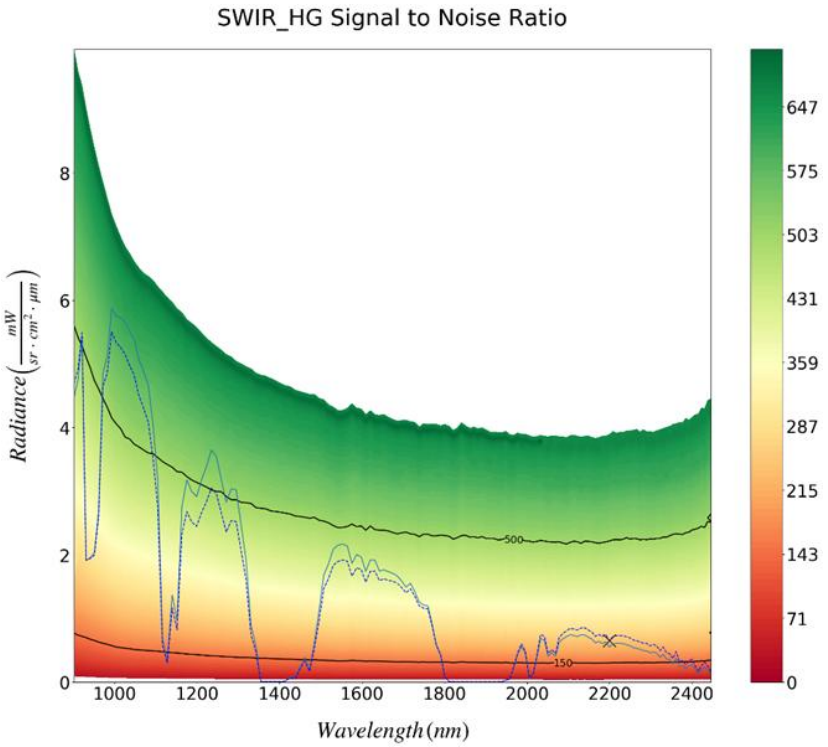


Figure 7-17 SNR contour map for SWIR high gain from the LED linearity observations observed on 14.06.2026. The reference radiance is shown with a blue line and after bandwidth normalization to a 10 nm pixel (dotted). Contour lines with SNR values of 150 and 500 are also shown in black. The mission requirement is evaluated at 2200 nm for a radiance value of 0.5 mW/cm^2/µm/sr (marked with a black cross) and is expected to be greater than 150.

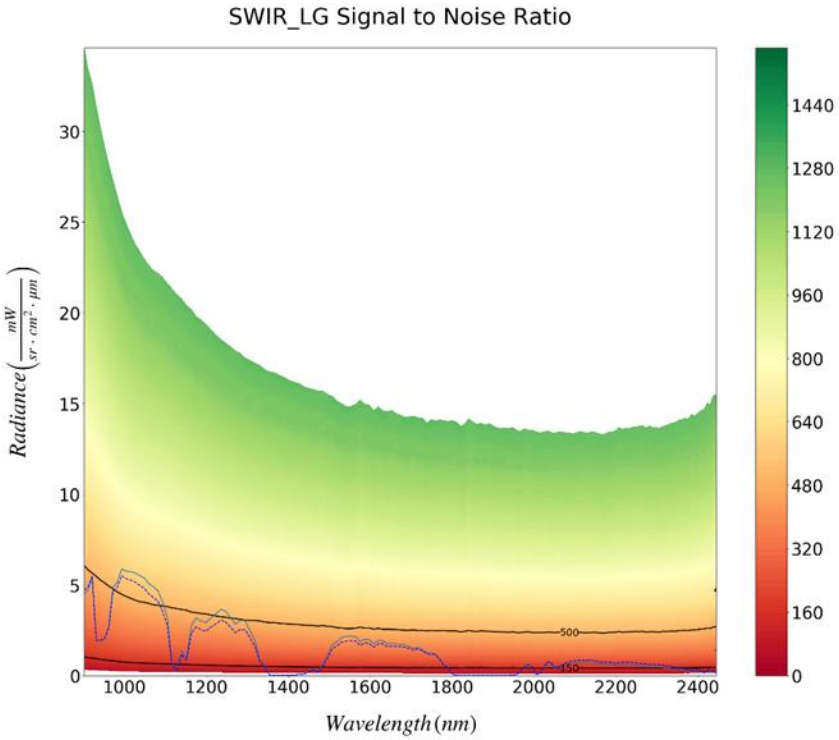


Figure 7-18 SNR contour map for SWIR low gain from the LED linearity observations observed on 14.06.2026. The reference radiance is shown with a blue line and after bandwidth normalization to a 10 nm pixel (dotted). Contour lines with SNR values of 150 and 500 are also shown in black.

The SNR values at the reference radiance spectrum are given in the table below (Table 7-9). The SNR is not determined in absorption regions and when the reference is too low or too high relative to the measured values in the linearity calibration.

Sensor	Wavelength (nm)	Reference Radiance (mW/sr/cm2/µm)	SNR Low gain	SNR High gain
VNIR	418.42	15.62	298.69	310.25
VNIR	424.04	15.32	301.26	312.60
VNIR	429.46	12.09	262.94	279.24
VNIR	434.69	15.07	303.86	314.49
VNIR	439.76	15.69	314.60	341.37
VNIR	444.7	17.29	331.60	343.79
VNIR	449.54	18.44	356.14	368.96
VNIR	454.31	18.18	352.53	366.18
VNIR	459.03	18.29	369.84	374.51
VNIR	463.73	18.2	369.40	375.89
VNIR	468.41	18.62	378.48	375.38
VNIR	473.08	18.2	380.39	381.29
VNIR	477.74	18.8	391.88	
VNIR	482.41	18.42	393.03	
VNIR	487.09	15.98	370.08	373.23
VNIR	491.78	16.46	377.24	400.54
VNIR	496.5	17.36	394.22	
VNIR	501.24	15.97	383.38	467.03
VNIR	506.02	17.31	415.99	
VNIR	510.83	16.57	405.06	
VNIR	515.67	15.92	392.42	
VNIR	520.55	15.48	388.56	
VNIR	525.47	15.6	397.93	
VNIR	530.42	15.98	422.43	
VNIR	535.42	15.84	433.74	
VNIR	540.46	14.72	413.07	
VNIR	545.55	15.36	443.79	
VNIR	550.69	15.03	443.27	
VNIR	555.87	15.02	459.02	
VNIR	561.11	15.03	466.54	
VNIR	566.41	14.13	452.22	
VNIR	571.76	14.36	464.88	
VNIR	577.17	14.47	468.82	
VNIR	582.64	14.61	476.11	
VNIR	588.17	13.5	464.48	
VNIR	593.77	13.32	465.73	
VNIR	599.45	13.48	465.16	
VNIR	605.19	13.77	477.75	
VNIR	611.02	13.33	470.37	

VNIR	616.92	12.67	461.93	
VNIR	622.92	13.07	470.65	
VNIR	628.99	12.85	466.41	
VNIR	635.11	12.9	474.64	
VNIR	641.3	12.76	479.13	
VNIR	647.54	12.04	465.67	
VNIR	653.84	12.4	483.16	
VNIR	660.21	12.43	492.56	
VNIR	666.64	12.48	484.34	
VNIR	673.13	12.41	483.94	
VNIR	679.69	12.21	486.15	
VNIR	686.32	10.69	446.43	
VNIR	693.02	10.52	444.03	
VNIR	699.78	10.76	445.08	
VNIR	706.62	10.96	458.02	
VNIR	713.52	10.96	457.53	
VNIR	720.5	7.95	366.34	377.40
VNIR	727.54	8.29	375.53	367.91
VNIR	734.65	10.03	412.74	
VNIR	741.83	10.13	410.70	
VNIR	749.06	10.45	424.67	
VNIR	756.35	10.32	412.94	
VNIR	763.7	3.91	227.18	275.78
VNIR	771.11	9.86	394.93	
VNIR	778.57	9.87	389.11	
VNIR	786.08	9.53	367.42	413.63
VNIR	793.64	9.01	363.97	380.37
VNIR	801.25	8.78	336.34	359.80
VNIR	808.91	8.66	325.39	343.42
VNIR	816.61	6.28	280.77	311.12
VNIR	824.36	7.09	290.20	310.12
VNIR	832.15	7.15	284.86	312.49
VNIR	839.98	8.18	302.56	328.14
VNIR	847.85	8.25	294.19	309.76
VNIR	855.76	7.74	285.99	303.99
VNIR	863.7	8.09	285.61	305.38
VNIR	871.68	7.88	267.81	294.90
VNIR	879.69	7.66	253.36	278.77
VNIR	887.73	7.41	245.96	269.00
VNIR	895.79	5.56	199.40	245.76
VNIR	903.87	6.03	203.97	240.42
VNIR	911.97	4.85	169.25	219.10
VNIR	920.08	5.54	182.52	224.06
VNIR	928.2	3.8	132.41	160.01

VNIR	936.34	0.89		67.97
VNIR	944.47	1.48		83.23
VNIR	952.61	1.65		87.29
VNIR	960.75	2.58	87.25	102.20
VNIR	968.89	4.74	128.19	130.98
VNIR	977.04	4.53	116.87	141.20
VNIR	985.19	5.41	123.00	144.70
VNIR	993.34	5.87	123.83	143.63
SWIR	901.96	6.12	504.45	
SWIR	911.57	4.75	444.62	
SWIR	921.32	5.38	486.09	
SWIR	931.2	1.91	261.04	
SWIR	941.22	1.95	273.20	
SWIR	951.36	2.03	285.67	
SWIR	961.63	2.7	349.15	
SWIR	972.02	4.85	504.05	
SWIR	982.52	5.13	531.94	
SWIR	993.14	5.87	584.14	
SWIR	1003.88	5.75	587.58	
SWIR	1014.72	5.73	592.08	
SWIR	1025.66	5.66	594.65	
SWIR	1036.7	5.51	592.23	
SWIR	1047.84	5.38	590.60	
SWIR	1059.07	5.07	575.38	
SWIR	1070.39	4.89	569.66	
SWIR	1081.78	4.67	556.76	
SWIR	1093.26	4.06	515.72	
SWIR	1104.81	3.18	451.97	
SWIR	1116.43	0.67	159.05	
SWIR	1128.11	0.35	94.45	
SWIR	1139.84	1.37	276.19	
SWIR	1151.62	0.97	218.42	
SWIR	1163.44	2.76	431.35	
SWIR	1175.3	3.18	475.90	
SWIR	1187.2	2.99	462.44	
SWIR	1199.11	2.91	457.48	
SWIR	1211.05	3.18	485.63	
SWIR	1223	3.39	509.07	
SWIR	1234.97	3.64	534.88	
SWIR	1246.95	3.54	529.12	
SWIR	1258.94	3.18	500.42	
SWIR	1270.93	2.82	470.15	
SWIR	1282.92	3.04	493.86	
SWIR	1294.91	3.02	496.72	

SWIR	1306.89	2.46	442.18	
SWIR	1318.87	1.92	382.27	
SWIR	1330.85	0.89	231.96	
SWIR	1342.82	0.56	165.42	
SWIR	1354.76	0.01		
SWIR	1366.69	0.01		
SWIR	1378.59	0.01		
SWIR	1390.47	0.01		
SWIR	1402.33	0.01		
SWIR	1414.17	0.01		
SWIR	1425.95	0.07		
SWIR	1437.7	0.06		
SWIR	1449.43	0.23	82.95	
SWIR	1461.1	0.38	126.73	
SWIR	1472.74	0.2	75.22	
SWIR	1484.33	0.61	187.05	
SWIR	1495.9	1.11	292.76	
SWIR	1507.41	1.68	377.68	
SWIR	1518.87	1.86	406.51	
SWIR	1530.29	2.09	435.43	
SWIR	1541.67	2.15	449.26	
SWIR	1553.02	2.17	451.86	
SWIR	1564.3	2.14	443.45	
SWIR	1575.55	1.87	404.88	
SWIR	1586.77	2	429.63	
SWIR	1597.91	1.97	422.88	
SWIR	1609.03	1.74	398.13	
SWIR	1620.08	1.92	417.81	
SWIR	1631.1	1.91	422.75	
SWIR	1642.07	1.74	400.05	
SWIR	1653	1.76	401.54	
SWIR	1663.87	1.73	400.35	
SWIR	1674.69	1.71	397.29	
SWIR	1685.46	1.67	391.97	
SWIR	1696.19	1.59	379.84	
SWIR	1706.88	1.49	366.75	
SWIR	1717.5	1.55	377.50	
SWIR	1728.07	1.42	355.57	
SWIR	1738.59	1.25	336.32	
SWIR	1749.08	1.21	324.09	
SWIR	1759.52	1.19	322.72	
SWIR	1769.9	0.91	270.71	
SWIR	1780.21	0.59	197.03	
SWIR	1790.5	0.44	153.35	

SWIR	1800.73	0.07		
SWIR	1810.92	0.01		
SWIR	1821.06	0		
SWIR	1831.16	0		
SWIR	1841.2	0		
SWIR	1851.19	0		
SWIR	1861.16	0		
SWIR	1871.06	0		
SWIR	1880.92	0		
SWIR	1890.73	0		
SWIR	1900.52	0		
SWIR	1910.22	0		
SWIR	1919.91	0		
SWIR	1929.55	0		
SWIR	1939.15	0		
SWIR	1948.69	0.02		
SWIR	1958.19	0.04		30.33
SWIR	1967.66	0.23		120.55
SWIR	1977.07	0.43		187.33
SWIR	1986.45	0.56		222.56
SWIR	1995.79	0.45		194.37
SWIR	2005.08	0.06		41.16
SWIR	2014.33	0.1		58.02
SWIR	2023.54	0.37		173.56
SWIR	2032.7	0.68		253.39
SWIR	2041.83	0.66		247.69
SWIR	2050.92	0.4		183.86
SWIR	2059.96	0.46		197.16
SWIR	2068.96	0.4		183.43
SWIR	2077.93	0.63		241.76
SWIR	2086.85	0.68		253.01
SWIR	2095.74	0.71		263.53
SWIR	2104.59	0.74		270.35
SWIR	2113.41	0.73		263.77
SWIR	2122.17	0.71		262.05
SWIR	2130.91	0.74		269.30
SWIR	2139.6	0.74		266.28
SWIR	2148.27	0.7		258.87
SWIR	2156.89	0.68		254.26
SWIR	2165.46	0.61		240.69
SWIR	2174.03	0.64		245.46
SWIR	2182.54	0.61		236.73
SWIR	2191.02	0.63		243.93
SWIR	2199.45	0.55		221.48

SWIR	2207.86	0.59		232.01
SWIR	2216.24	0.61		235.46
SWIR	2224.58	0.61		235.32
SWIR	2232.89	0.6		234.32
SWIR	2241.16	0.59		229.49
SWIR	2249.41	0.57		224.27
SWIR	2257.61	0.54		216.21
SWIR	2265.8	0.53		213.48
SWIR	2273.93	0.51		212.27
SWIR	2282.05	0.49		205.78
SWIR	2290.13	0.49		204.73
SWIR	2298.17	0.46		196.86
SWIR	2306.18	0.47		201.63
SWIR	2314.17	0.45		194.26
SWIR	2322.14	0.39		174.47
SWIR	2330.06	0.43		187.64
SWIR	2337.94	0.36		167.88
SWIR	2345.81	0.35		160.80
SWIR	2353.64	0.29		139.67
SWIR	2361.43	0.37		169.15
SWIR	2369.2	0.24		123.48
SWIR	2376.94	0.26		127.98
SWIR	2384.66	0.21		111.49
SWIR	2392.34	0.26		126.70
SWIR	2399.99	0.27		134.65
SWIR	2407.61	0.19		101.70
SWIR	2415.21	0.12		69.32
SWIR	2422.79	0.19		100.44
SWIR	2430.32	0.24		115.71
SWIR	2437.83	0.19		94.57
SWIR	2445.31	0.18		90.33

Table 7-9 SNR values per wavelength for VNIR and SWIR low and high gains

Radiometric calibration updates

The following calibration products were generated and delivered:

Product	Type	Date of Generation	Date of Validity Start	Date of Validity End	Delivered to
ENMAP01-CTB_RAD-20260503T000000Z_V040100_20260429T072718Z	CTB_RAD	29.04.2026	03.05.2026	02.07.2026	DIMS
ENMAP01-REF_SUN-20260503T000000Z_V040100_20260429T072718Z	REF_SUN	29.04.2026	03.05.2026	02.07.2026	DIMS
ENMAP01-CTB_RAD-20260703T000000Z_V040100_20260616T092141Z	CTB_RAD	16.06.2026	03.07.2026	-	DIMS
ENMAP01-REF_SUN-20260703T000000Z_V040100_20260616T092141Z	REF_SUN	16.06.2026	03.07.2026	-	DIMS

Table 7-10 Generated radiometric calibration tables

7.5.4 Geometric Calibration

There have been no new geometric calibration tables generated in the reporting period.

Type of Calibration Table	ID of Calibration Table	Date of Generation	Date of Validity Start	Date of Validity End
None				

Table 7-11 Generated new geometric calibration tables

The performance of the geometric calibration table is assessed in chapter 7.6.3.

7.6 Internal Quality Control

7.6.1 Archive

Within the given time period (01.04.2026 to 30.06.2026), 883 datatakes with a total of 14192 tiles were acquired and archived (remark: additional datatakes acquired during this period but for which the archiving is pending might be missing in the statistics).

The overall quality rating statistics are listed in Table 7-12, and in relation to the Solar Zenith Angle (SZA) in Table 7-13. Also these ratings are further detailed for the VNIR and SWIR detector in Table 7-14, showing a nominal performance rating for the given quality thresholds.

In addition, the rating for the atmospheric conditions for the scenes are depicted in Table 7-15. When setting the atmospheric quality rating in relation to the illumination conditions (i.e., large SZA) during data acquisition (Table 7-16), For the reporting period, a slight increase of “reduced quality” scenes can be observed, but the numbers are still very small, 0.3%. One of the reasons is the slight increase in saturated pixels. The rating for the atmospheric conditions for the scenes are depicted below, and the relation to the illumination conditions (i.e., large SZA) during data acquisition, which is a driving factor for the rating. In addition, the “low qualityAtmosphere” rating can be further related to high cloud cover (~46% of the low qualityAtmosphere tiles) and the unavailability of enough DDV pixels (~67%). In comparison to the previous quarter having more low light scenes, the influence of clouds and DDVs on the quality rating is now increased, which is as expected.

Parameter	Value	Number of tiles	Percentage
overallQuality	Nominal	14118	99,48%
	Reduced	43	0.30%
	Low	31	0.22%

Table 7-12 Overall quality rating statistics

Parameter	Sub-Parameter	Number of tiles	Percentage
overallQuality = Low		31	
	Thereof with SZA > 70°	31	100%

Table 7-13 Overall quality rating in relation to Sun Zenith Angle (SZA)

Parameter	Sub-Parameter	Number of tiles	Percentage
overallQuality = Reduced		43	
	Thereof with qualityVNIR nominal	23	53.49%
	Thereof with qualitySWIR nominal	20	46.51%
overallQuality = Low		31	
	Thereof with qualityVNIR nominal or reduced	0	0.00%
	Thereof with qualitySWIR nominal or reduced	24	77.42%

Table 7-14 Reduced and low quality rating statistics

Parameter	Value	Number of tiles	Percentage
QualityAtmosphere	Nominal	7772	54.76%
	Reduced	1599	11.27%
	Low	4821	33.97%

Table 7-15 QualityAtmosphere rating statistics

Parameter	Sub-Parameter	Number of tiles	Percentage
overallAtmosphere = Reduced		1599	
	Thereof with SZA > 65°	0	0%
	Thereof with SZA > 70°	0	0%
	Thereof with SZA > 80°	0	0%
overallAtmosphere = Low		4821	
	Thereof with SZA > 65°	91	1.89%
	Thereof with SZA > 70°	73	1.51%
	Thereof with SZA > 80°	41	0.85%

Table 7-16 QualityAtmosphere rating in realtion to Sun Zenith Angle (SZA)

Parameter	Sub-Parameter	Number of tiles	Percentage
overallAtmosphere = Reduced		1599	
	Thereof with Cloud Cover > 66%	7	0.44%

	Thereof with DDV warnings	825	51.59%
overallAtmosphere = Low		4821	
	Thereof with Cloud Cover > 66%	2219	46.03%
	Thereof with DDV warnings	3220	66.79%

Table 7-17 QualityAtmosphere rating in relation to Cloud Cover and DDV availability

Remark about definition of EnMAP low quality collection

The quality rating of EnMAP products is based on image parameters, such as illumination conditions (i.e., sun elevation angle) and image defects, and on possible anomalies in the image data or instrument telemetry. These parameters are retrieved during the pre-processing and are added to the metadata and quality layers for every archived L0 product. In EOWEB GeoPortal two collections of EnMAP L0 products are available: “EnMAP-HSI (L0)” and “EnMAP-HSI (L0), Low Quality”. An L0 product is assigned to the low-quality collection if the corresponding metadata item qualityFlags.overallQuality is equal to 2 (low quality). This happens for products with a significant number of striping, saturation, artefact or dead pixels, when the screening of data and instrument indicates non-nominal behavior or, in the majority of cases, when the sun elevation angle is less than or equal to 0 (e.g., night scenes). A detailed definition of qualityFlags. overallQuality is given in Sec. 4.4.9 in the L1B ATBD (EN-PCV-TN-4006).

7.6.2 Level 1B

7.6.2.1 Radiometric Performance

Defective / de-calibrated detector elements

Using the Detector Map components, an offline check of possibly defective or de-calibrated detector elements is conducted. In particular, a detector element is identified as “possibly defective” if it is suspicious in at least 75% of the useful tiles. Note that this analysis is based on L1B_RAD data, so no dead / defective pixel interpolation was carried out. Within the given reporting period, the following indications for defective pixels are found for the VNIR and the SWIR camera:

VNIR (total of 14104 tiles, with 14073 suitable for analysis):

Newly found suspicious pixels in green, previously detected in **black**, no longer present ones in ~~red~~.

Band	Cross-track element
~~19~~	~~187~~
77	600
85	14
89	395

Band	Cross-track element
~~19~~	~~187~~
85	14
89	395

Note that the band index starts at 1.

SWIR (total of 14104 tiles, with 13960 suitable for analysis):

Newly found suspicious pixels in green, previously detected in **black**, no longer present ones in ~~red~~.

NOTE: due to the change in SWIR band configuration within the period Q3 2023, the band index from band 45 till 75 did change by +1 (with bands 45, 74 & 75 newly added) w.r.t. the reports before Q3 2023.

Band	Cross-track element	Band	Cross-track element	Band	Cross-track element
1	817	33	560	85	525
2	235, 286, 593, 673	38	241, 919	89	285
3	381	48	511	91	973
4	362, 363, 418	49	218	92	677, 973
5	687	50	311, 344, 395	96	341, 819
7	~~472,~~ 910	~~51~~	~~155~~	100	513
8	801	53	97, ~~98~~	101	318
9	124	54	941	106	107
11	715	56	221, 965	107	265, 764
14	29, 684	58	632, ~~667,~~ 922	108	886
16	535	59	89, 90	111	315
20	84	61	312	118	837
28	104	63	123		
29	~~855,~~ 928	~~66~~	~~93~~		
30	7, 360, ~~855~~	~~69~~	~~864~~		
31	360	72	801, 845		
		~~75~~	~~737~~		

Dead detector elements

Within the given reporting period, the statistics for dead pixels are provided in Table 7-18 and Table 7-19. When comparing these numbers to the estimates in Ch. 7.5.1, one must bear in mind that the latter is based on the full detector readout configuration, while the numbers provided in the following are related to the standard readout configuration as provided in the user product. Because of the smaller readout area, these following dead pixel numbers are lower in comparison.

Parameter	Value (number of pix)	Number of tiles	Percentage
DeadPixelsVNIR	137	14192	100%

Table 7-18 Dead pixel statistics, VNIR

Parameter	Value (number of pix)	Number of tiles	Percentage
DeadPixelsSWIR	1509	14192	100%

Table 7-19 Dead pixel statistics, SWIR

Saturation and radiance levels

Within the given reporting period, no indications for increased saturation defects are found for the VNIR and the SWIR camera (see Table 7-20 and Table 7-21).

Parameter	Value (per mille of scene)	Number of tiles	Percentage of tiles
SaturationCrosstalkVNIR	0	13295	93.68%
	> 0 per mille	897	6.32%
	> 10 per mille	128	0.90%

Table 7-20 Saturation statistics, VNIR

Parameter	Value (per mille of scene)	Number of tiles	Percentage of tiles
SaturationCrosstalkSWIR	0	13426	94.60%
	> 0 per mille	766	5.40%
	> 10 per mille	19	0.13%

Table 7-21 Saturation statistics, SWIR

Other radiometric artifacts

Within the given reporting period, the striping performance is similar to the one encountered during the Commissioning Phase. Within PCV, different de-striping approaches were tested, and the selected one by M. Brell (GFZ) is implemented in processor version V01.02.00 (07.03.2023).

Apart from this, no indications for an increase in general radiometric artifacts are found for the VNIR and the SWIR camera (see following tables).

Parameter	Value (number of pix)	Number of tiles	Percentage
generalArtifactsVNIR	0	0	0%
	> 0	14192	100%
	> 10	643	4.53%
	> 100	192	1.35%
	> 1000	125	0.88%

Table 7-22 Artifacts statistics (without striping), VNIR

Parameter	Value (number of pix)	Number of tiles	Percentage
generalArtifactsSWIR	0	0	0%
	> 0	14192	100%
	> 10	14192	100%
	> 25	378	2.66%
	> 100	108	0.76%
	> 1000	0	0%

Table 7-23 Artifact statistics (without striping), SWIR

7.6.2.2 Spectral Performance

For the analysis of the spectral stability, the Detector Maps of all Earth datatakes acquired in the reporting period were used. Note that no smile correction was applied, so the analysis shows only on the instrument characteristics. At the wavelengths of stable atmospheric features (760 nm Oxygen absorption and CO2 absorption at ~2050 nm), simulations of spectral shifts were carried out by resampling the absorption in the interval of +/- 3.0 nm with steps of 0.05 nm. Then the signal of the Detector Maps and the simulated shifted absorptions were normalized, and a least-square fit was used where the sensed absorption matches the simulations. Also an additional polynomial fitting was applied, as especially the CO2 absorption band region has low signal an is thus significantly influenced by noise.

For the VNIR, when aggregating the shifts (Figure 7-19) the mean derivation is almost constant in across-track direction and -as before- around 0.55 nm towards shorter wavelengths, underpinning the consistency with the in-orbit spectral calibration and especially regarding the shape of the spectral smile. Note that of course these results are consistent within the limitations of this vicarious approach. Additionally, the variability of the vicariously estimated spectral calibration can be expressed as the standard deviation at 1 sigma and is ~0.31 nm, which includes the spectral stability of EnMAP and as well the variations of the used Earth datatakes and the limitations of the method.

In summary, for the VNIR the estimated differences to the CTB_SPC consistent with the results of previous reporting periods, confirming the validity of the spectral calibration and the spectral stability of the instrument taking into accounts the limitations of the vicarious approach.

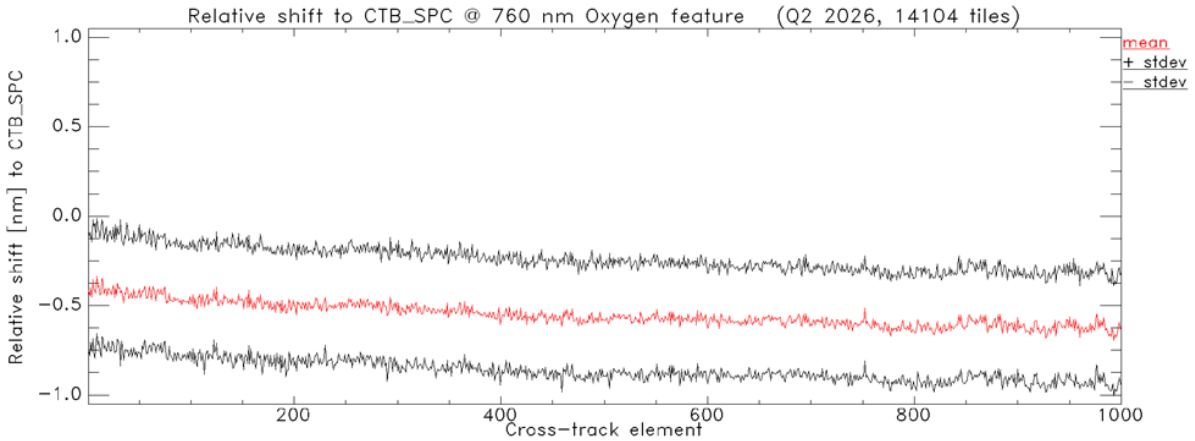


Figure 7-19 VNIR estimated spectral shift at 760 nm w.r.t the valid spectral calibration table (CTB_SPC), and relative spectral stability expressed at 1 sigma (Q2 2026, 14104 tiles)

For this analysis, the reference is thus not the nominal center wavelengths (i.e., a single number per band), but the CW per cross-track pixel, thus explicitly including the spectral smile (see Figure 7-20).

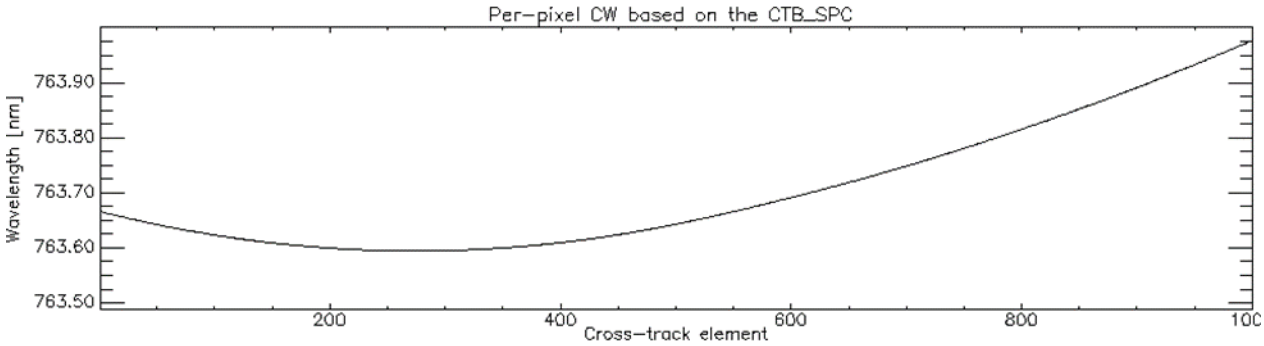


Figure 7-20 Center wavelengths per cross-track pixel based on the spectral calibration table (VNIR band 62) in the calibration table (CTB_SPC).

For the SWIR having less pronounced atmospheric absorption features, more influence of the background and a much lower signal level, the fitting also results in more clutter, as shown in Figure 7-21.

In order to demonstrate that the mean derivation to the CTB_SPC is within the spread of the data, the mean and standard deviation are calculated using the relative values, as shown in Figure 7-21. For Q2 2026, a small shift of ~0.14 nm towards longer wavelengths is visible when comparing to CTB_SPC (Figure 7-22) , and having a standard deviation of ~0.48 nm. This shift is equal for all cross-track elements, so the shape of the spectral smile did not change and is well represented in the CTB_SPC. When comparing this small spectral shift to the results in the past quarter, the mean shift to the CTB_SPC is slightly reduced by ~0.21 nm. As before, the spectral shift is the same for all cross-track elements, so the shape of the spectral smile did not change and is well represented in the CTB_SPC. In addition, the spread around the estimated mean with a standard deviation of ~ 0.5 nm (1 sigma) indicates no significant change of the good overall stability of the instrument.

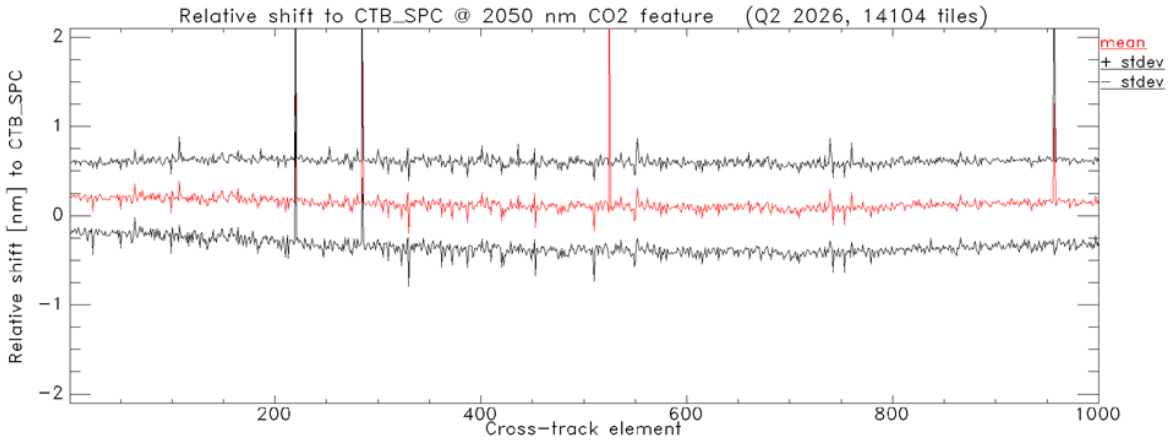


Figure 7-21 SWIR estimated spectral shift at 2050 nm w.r.t the valid spectral calibration table (CTB_SPC, shown below), and relative spectral stability expressed at 1 sigma (Q2 2026, 14104 tiles)

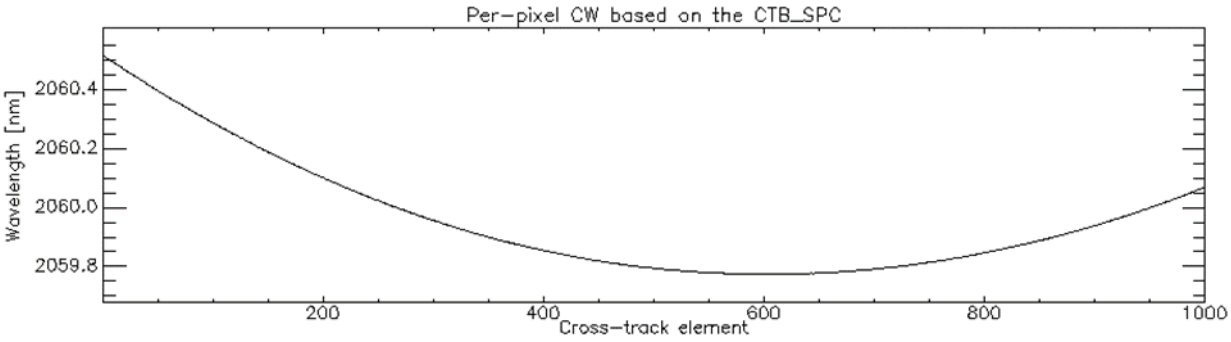


Figure 7-22 Center wavelengths per cross-track pixel based on the spectral calibration table (SWIR band 86).

7.6.3 Level 1C

This report covers the timeframe from 01.04.2026 to 30.06.2026. No geometric calibration was performed during this period.

In the timeframe of this report, 1566 datatakes have been acquired. In 1092 of those datatakes (~70 %), enough ground control points (GCP) and independent check points (ICP) were found to perform a geometric accuracy assessment. The datatakes without enough GCPs were not assessed quantitatively, but a random subset of them was inspected visually. The vast majority of those datatakes was either almost fully covered with clouds or showing only water, desert or rain forest. The behavior is thus as expected.

The assessment of the RMSE values in the metadata is shown below in Figure 7-23.

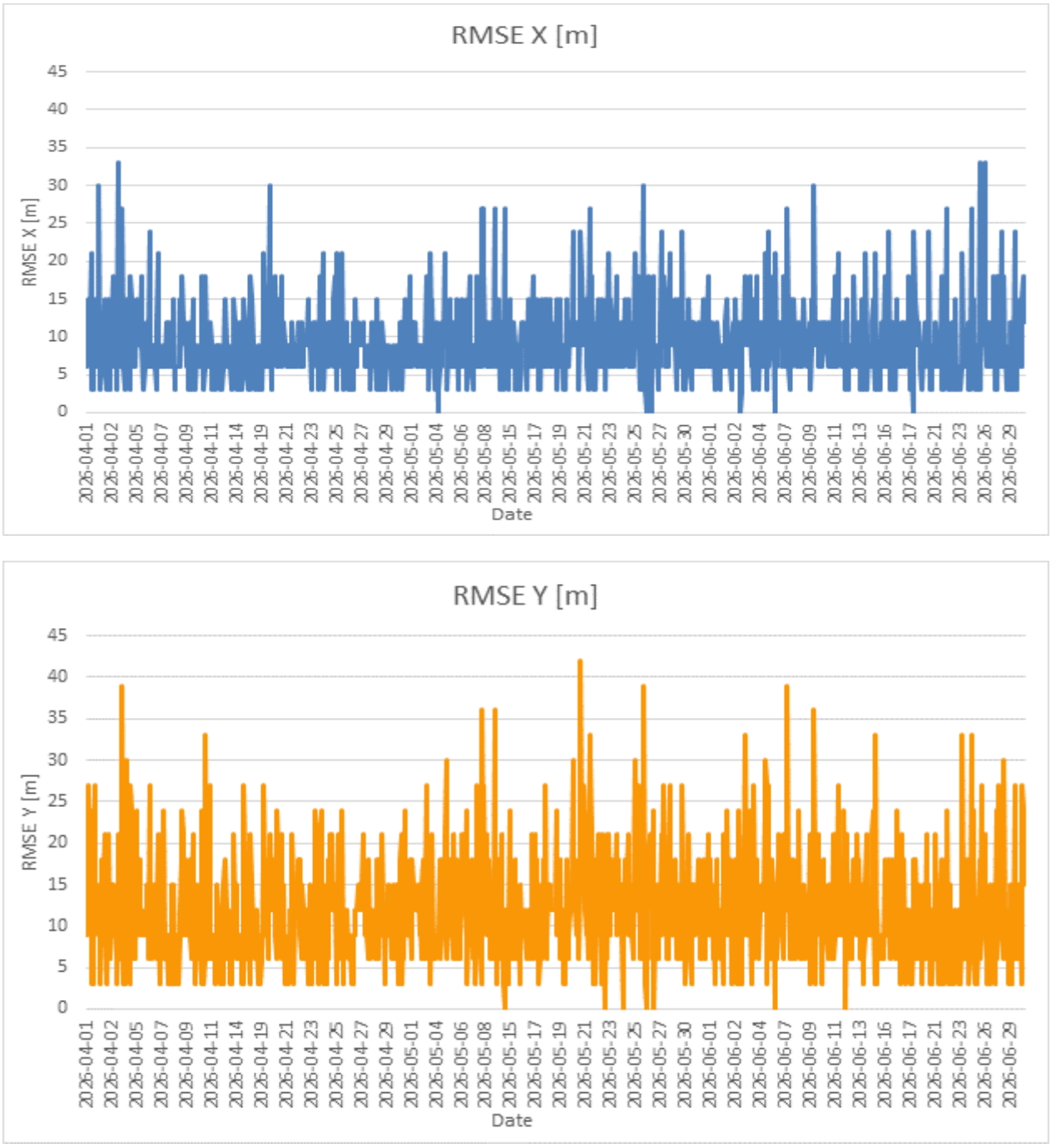


Figure 7-23 Assessment of RMSE X values (top) and RMSE Y values (bottom), calculated based on found ICPs, for all datatakes where ICP could be found

In x-direction, 3 datatakes (~0.3%) had an RMSE value above 30 m (1 GSD), whereas in y-direction, 13 datatakes (~1.2%) are above this threshold. For most of those datatakes, only very few GCP and ICP could be found during processing, making the results less reliable. The mean values are 9.27 m in x-direction and 11.85 m in y direction. This shows a very high geolocation accuracy for the datatakes where matching was possible. The requirement GRD-PCV-0155 (1 GSD) is thus fulfilled.

The average boresight angles, which can be interpreted as the correction and thus the error of the scene if no GCPs could have been found, correspond to approximately -3 m in x direction with a standard deviation of approximately 21 m and -44 m in y direction with a standard deviation of approximately 19 m on ground. It is reasonable to assume that the scenes where no GCPs could be found are in the same accuracy range

and thus well within the requirement of 100 m (GRD-PCV-0150). Note that the x and y direction mentioned in this report are not in the image coordinate system but in UTM, as the evaluation is done on L1C products.

7.6.3.1 Geometric accuracy

EnMAP L1C products are matched against a reference image (Sentinel-2 data, if not stated otherwise) by using image matching techniques to assess the geometric accuracy. At the obtained checkpoints (CP), statistics are calculated to provide mean and RMSE values (Figure 7-24) for each scene. Note that the obtained accuracy in the analysis is always w.r.t. the reference image. This report covers EnMAP data from 01.04.2026 to 30.06.2026. A random sample of 459 L1C tiles was selected based on visual inspection of the catalogue quicklooks (e.g. to avoid cloudy images).

The requirement GRD-PCV-0155 shall be fulfilled:

The geolocation accuracy at nadir look direction of level 1C and 2A products shall be better than 1 GSD (1 sigma) in each direction with respect to reference images provided that reference images are available and sufficient similarity.

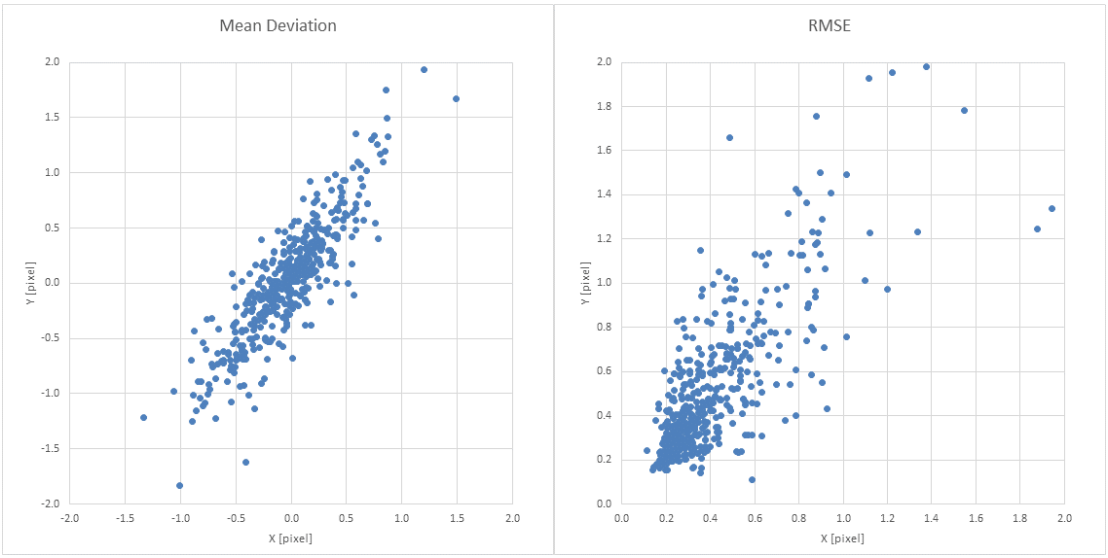


Figure 7-24 Mean deviation of EnMAP L1C products in pixel (left). RMSE value for EnMAP L1C products in pixel (right)

Note, that during processing the boresight angles and the geometric accuracy related quality flags are calculated on datatake level while in the figures and tables above, the accuracy is assessed per tile. The mean values over all 459 L1C tiles are -0.03 and 0.02 pixel in mean deviation with a standard deviation of 0.38 and 0.52 pixel while the mean RMSE values are 0.42 and 0.53 pixel, all in x and y direction respectively. The data show that for the vast majority of scenes the accuracy wrt. reference image is better than one pixel and thus the requirements are fulfilled. Compared to the last geometric QC report, the values are very stable (see Figure 7-26).

7.6.3.2 Co-registration accuracy

In this section, the co-registration accuracy is checked against the Space Segment requirement SRDS-PIM-0050 (EN-KT-RFW-003 is also to be considered here):

*The HS-Imager shall be designed such, that the geometric co-registration is ≤ 20 % of the nominal Ground Sampling Distance (0.2 * GSD linear displacement in both directions).*

For the assessment of co-registration accuracy, the SWIR data of EnMAP L1C products are matched against the corresponding VNIR data and the mean deviation values shown in this section (Figure 7-25).

This report covers EnMAP data from 01.04.2026 to 30.06.2026. A random sample of 568 L1C tiles was selected based on visual inspection of the catalogue quicklooks (e.g. to avoid cloudy images).

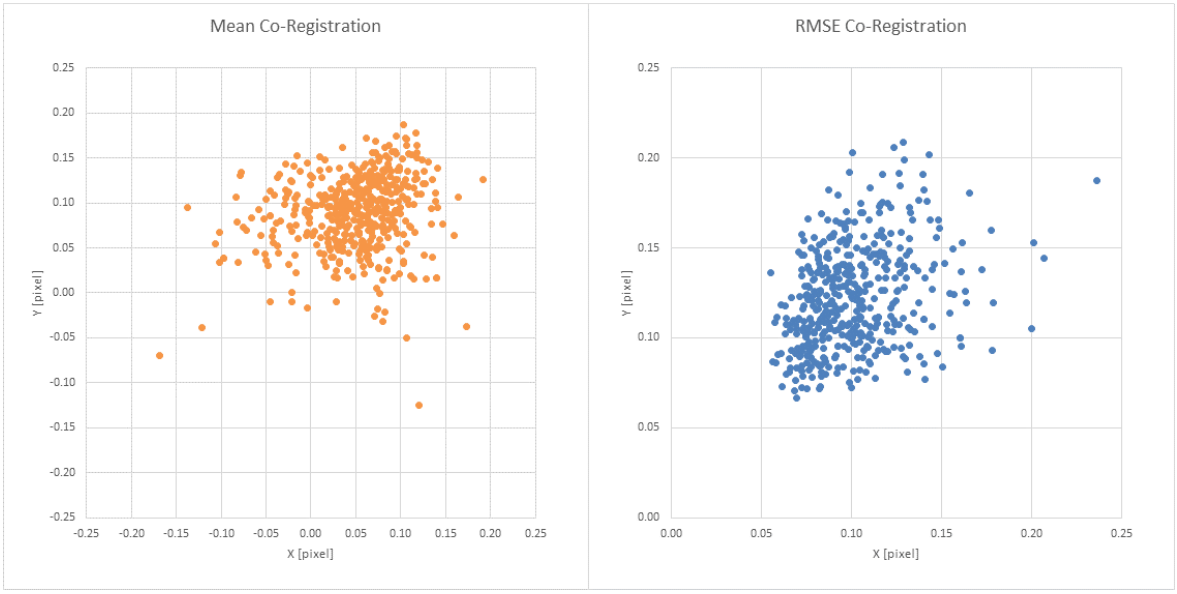


Figure 7-25 Mean deviation in pixel between VNIR and SWIR data of EnMAP L1C products (left). RMSE in pixel between VNIR and SWIR data of EnMAP L1C Products (right)

The data show, that the mean co-registration is well within the requirement. Note that the theoretical accuracy of the used matching algorithm is 0.1 pixel, and as can be seen in the RMSE values, still some mismatches were not removed by the blunder detection techniques that were applied. The mean deviation over all analyzed tiles are 0.05 pixel in x-direction with a standard deviation of 0.05 pixel and 0.09 pixel in y direction with a standard deviation of 0.04 pixel. Compared to the results in the previous geometric QC report, the values are very stable as can be seen in Figure 7-26.

7.6.3.3 **Development of geometric performance**

Since the launch of EnMAP on April 1st 2022, the geometric performance has been improved significantly. This was achieved by different geometric calibrations and processor updates. Table 7-24 shows the measures performed, their date and their effect.

Date	Measure	Effect
01.08.2022	Fix of attitude processing	Improvement of absolute geolocation (w/o matching)
20.09.2022	Boresight Calibration	Improvement of absolute geolocation (w/o matching)
03.11.2022	1st Geometric Calibration	Improvement of absolute geolocation (w/o matching) Improvement of VNIR/SWIR co-registration (~0.8 pix -> ~0.4 pix)
11.02.2023	2nd Geometric Calibration	Improvement of VNIR/SWIR co-registration (~0.4 pix -> ~0.15 pix)
29.03.2023	Processor update (v01.02.00)	Improvement of VNIR/SWIR co-registration (~0.15 pix -> ~0.06 pix)
05.05.2023	Processor update (v01.03.01)	Improvement of geolocation accuracy

Table 7-24 Improvement of geometric performance

Figure 7-26 shows the development of the co-registration accuracy, measured as described in previous section. Again, after a significant improvement since commissioning phase, over the last report periods the accuracy has been very stable.

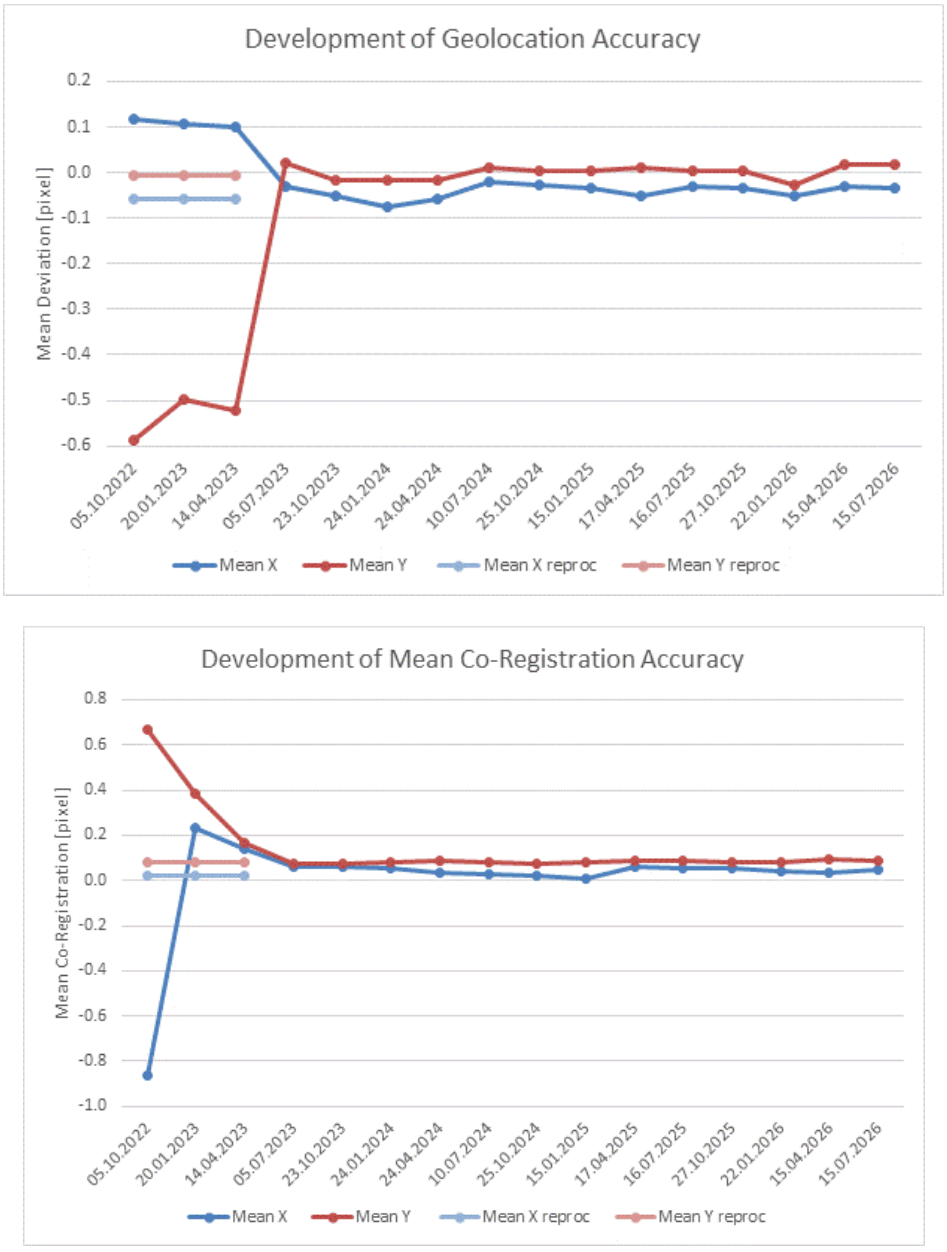


Figure 7-26 Development of co-registration accuracy based on the previous geometric QC reports. The values with re-processed L0 data and archived version ≥V01.03.00 are also shown

As most of the geometric processing – especially the matching against a reference image – is done on datatake level during L0 processing, the geometric accuracy and co-registration of data acquired earlier during the mission is not automatically improved when higher level products (L1B, L1C, L2A) are processed with the current processor version. However, after completing the L0 reprocessing of the whole archive, the geometric processing is executed with the latest processor version and geometric calibration table to make sure that the best geometric quality and co-registration is reached also for the reprocessed data. Today, the geometric performance of the products available in the Mission Archive with date earlier than 29.03.2023 is the same as for the products acquired after that date. Users can recognize reprocessed data by checking the metadata tag **archivedVersion**: if the version is 01.03.00 or higher, then the geometric performance should be as analyzed in this report, regardless of the acquisition date of the product.

7.6.4 Level 2A

7.6.4.1 **Validity of generated L2A "water" data**

7.6.4.1.1 Analyzed scenes

The following scenes were taken into consideration:

DataTake - ID	Tile - ID	Date	Location	L2A Option	Cirrus / Haze Removal	Overall Quality
201073	03	2023-06-27	ITA, Venice	Water mode, water type "clear"	Cirrus	Nominal
200080	14	2026-06-22	AUS, Middle Island	Water mode, water type "clear"	Cirrus	Nominal
196468	13	2026-05-27	TUR, Atatürk Dam	Water mode, water type "clear"	Cirrus	Nominal
197357	04	2026-06-09	IDN, Pulau Rak	Water mode, water type "clear"	Cirrus	Nominal
200437	02	2026-06-24	MDG, Mayotte	Water mode, water type "clear"	Cirrus	Nominal

Table 7-25 Datatake IDs of analyzed water products

The below listed parameters were checked for above mentioned scenes by EOMAP:

Parameter	Check
Masking (Land, Water, Clouds, etc.)	No issues found.
Adjacency correction	No issues found.
Retrieval of atmospheric properties	No issues found.
Cirrus – correction	No issues found.
Retrieval of water leaving reflectance	No issues found.
Quality Mask	No issues found.

*Details to the updates are presented below.

7.6.4.1.2 Data Checks

For the checks described in the following, multiple scenes were used. The corresponding scene - IDs and locations can be found in Table 7-25.

Every scene was processed using the EnMAP Processor 01.05.06 and MIP version 1.4.2.

- Masking

First, the geo mask is checked. The different parts of the scene shown masked (see Figure 7-27and Figure 7-28) are classified as expected.



Figure 7-27 Scene-ID 200437; RGB-Quicklook with Bands 611.02nm – 550.69nm – 463.73nm

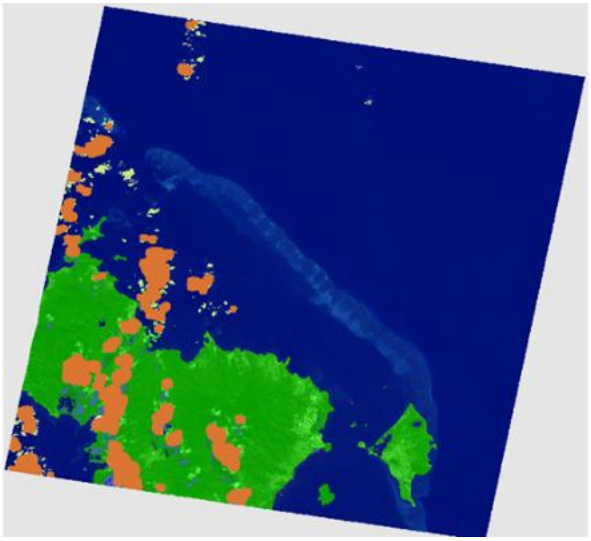


Figure 7-28 Scene-ID 200437; Geo Mask with Blue – Water, Green – Land, Light Blue - Shadows, Orange – Clouds, White – NA

- Cirrus and Adjacency Correction

Next, we check for the adjacency correction using the two sites ‘AC1’ and ‘AC2’ shown in .

The coordinates of the sample locations are as follows:

AC 1: LAT -12.72271647 | LON 45.19355044

AC 2: LAT -12.61395740| LON 45.31223644

For sampling, we choose two locations, one located over shallow water, the other over deep water (see for the sample locations).

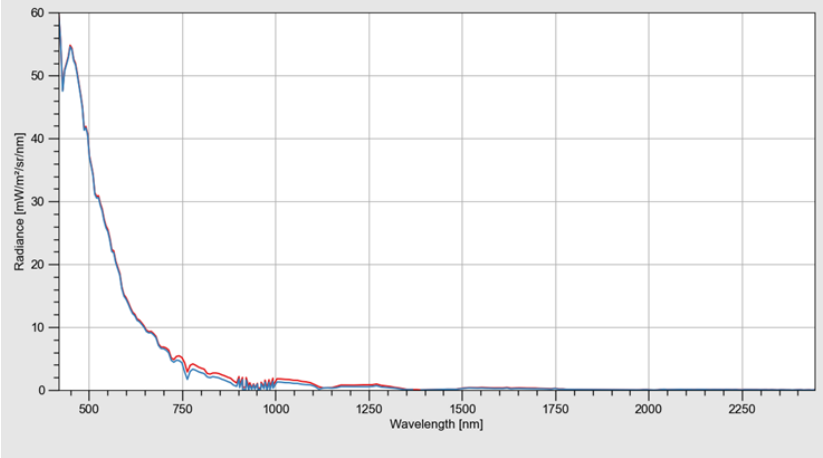


Figure 7-29 Scene-ID 200437; At-sensor-radiance sampled at location AC 1; red: measured, blue: adjacency corrected

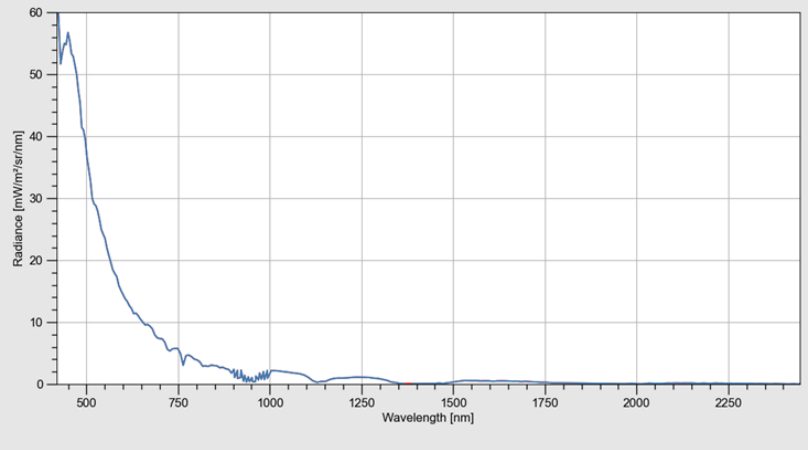


Figure 7-30 ID 200437; At-sensor-radiance sampled at location AC 2; red: measured, blue: adjacency corrected

Figure 7-29 and Figure 7-30 depict the sampled at-sensor-radiance - signal for location AC 1 and AC 2, respectively. The effect of the adjacency correction is clearly depicted in Figure 7-29. This is what we expect, since the sample location was placed near high reflective terrestrial objects. In contrast, a differentiation between the two plotted signals in Figure 7-30 is not possible, since the effect here is near zero. Due the sample – placement in an offshore region, this is as well the behavior we expect.

Thus, overall, the adjacency correction works as intended.

- Reflectance Product

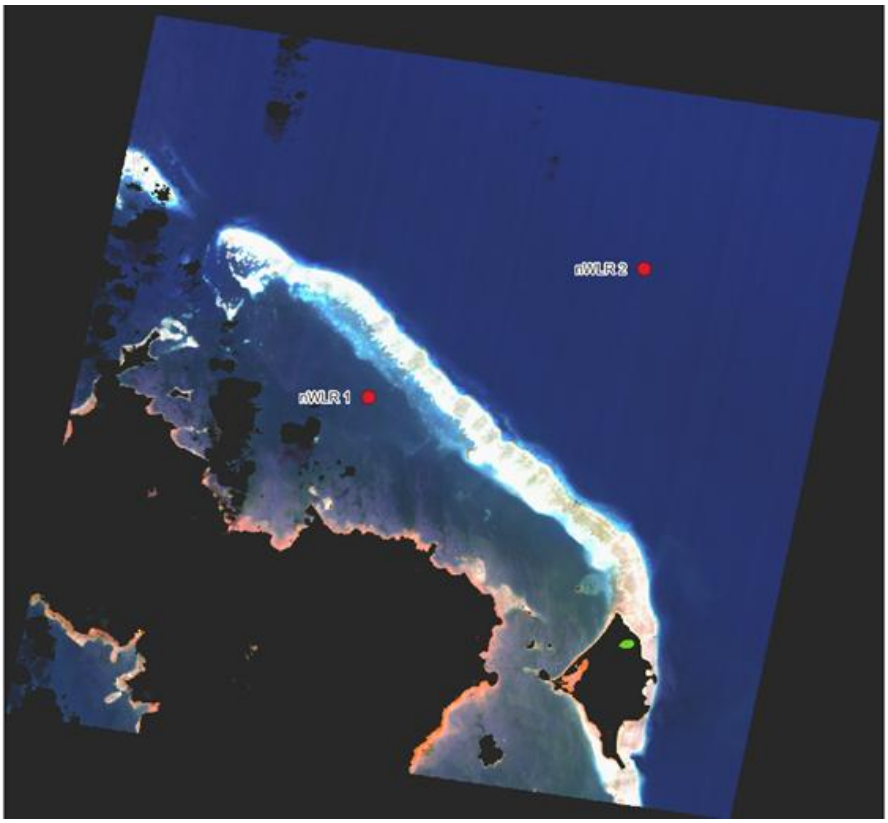


Figure 7-31 Normalized Water Leaving Reflectance of scene-ID 200437; Wavelengths for RGB: 611.02nm – 550.69nm – 463.73nm

For the labeled locations in Figure 7-31, the sampling coordinates are as follows:

nWLR 1: LAT -12.67632764 | LON 45.18755547

nWLR 2: LAT -12.62730462 | LON 45.29437399

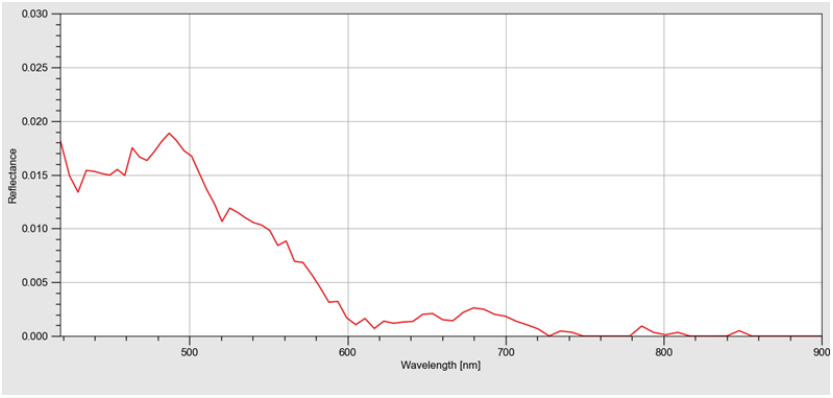


Figure 7-32 Scene-ID 200437; nWLR sampled at location nWLR 1

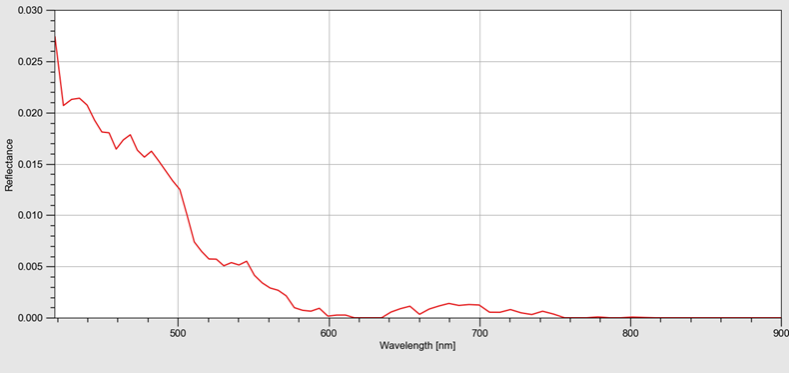


Figure 7-33 Scene-ID 200437; nWLR sampled at location nWLR 2

Figure 7-32 and Figure 7-33 depict the normalized water leaving reflectance sampled at location nWLR1 and nWLR 2, respectively. We picked the signal for nWLR 1 in the optically shallow part of the water body. Thus, we can see the spectral influence of the bottom in the signal, especially when compared to nWLR 2. This location was placed in an optically deep area, where the signal comes solely from the water body being not affected by the bottom.

Summing up, the atmospheric correction workflow works as we expect it to.

7.6.4.2 **Validity of generated L2A "land" data**

7.6.4.2.1 Analyzed scenes

Within the time interval between 01.04.2026 to 30.06.2026, an interactive in-depth analysis has been conducted for the following scenes:

Datatake-ID	Tile-ID	date	location	L2A option	cirrus and haze removal	Archived Version	processor version	Overall Quality	Quality Atm
187507	007	2026-04-10	Macedonia	land	no	01.05.06	V010506	Reduced	Nominal
191634	003	2026-05-03	Porto Velho, Brazil	land	no	01.05.06	V010506	Reduced	Reduced WV 4.123 g/cm², AOT 0.076 + haze & cirrus
191634	004	2026-05-03	Porto Velho, Brazil	land	no	01.05.06	V010506	Reduced	Reduced WV 4.175 g/cm², AOT 0.072 + haze & cirrus
202075	010	2026-06-20	Kogelberg, South Africa	land	no	01.05.06	V010506	Reduced	Reduced

Table 7-26 Datatake IDs of analyzed land products

For the selection of L2A data, several data takes acquired within the reporting period and covering different landscapes at different conditions were analyzed.

7.6.4.2.2 Data Checks

In the following, the different tiles were checked for the shape and magnitude of the BOA_ref spectra, and also the quality of the generated masks is evaluated when meaningful.

For all tiles the visual image impression is fine. For the masking, there are known issues of mis-classifications which are currently being investigated. The BOA_ref spectra all show the typical shape and magnitude, indicating the correct L2A correction.

- **Macedonia (DT187507, T07, 2026-04-10)**

For this mountainous region (Figure 7-34), the lakes were masked correctly, and some dark areas with terrain shadow were incorrectly included in the water mask. Next, regarding further masking (Figure 7-35, Figure 7-36), the snow-covered areas are very well represented in the snow mask, and sometimes additionally masked as clouds; additionally cloudy areas are correctly included in the cloud mask, and the adjacent areas are also correctly masked as haze. The masked CloudShadow is related to an area with topographic shadow and a cloud nearby, and is thus plausible from a spectral point of view (see especially Figure 7-36). In summary, while some of the masked clouds are likely snow, the overall masking is correct.

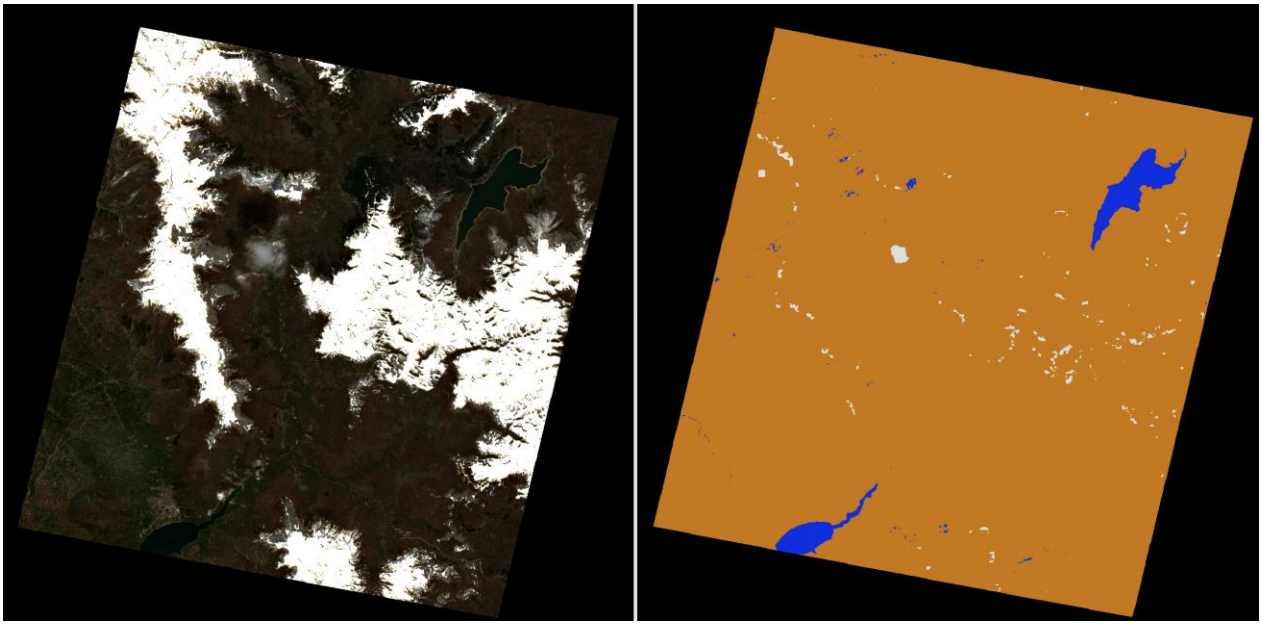


Figure 7-34 DT187507, TrueColorComposite (left) and QualityClasses (right; blue: water, brown: land, white: other).

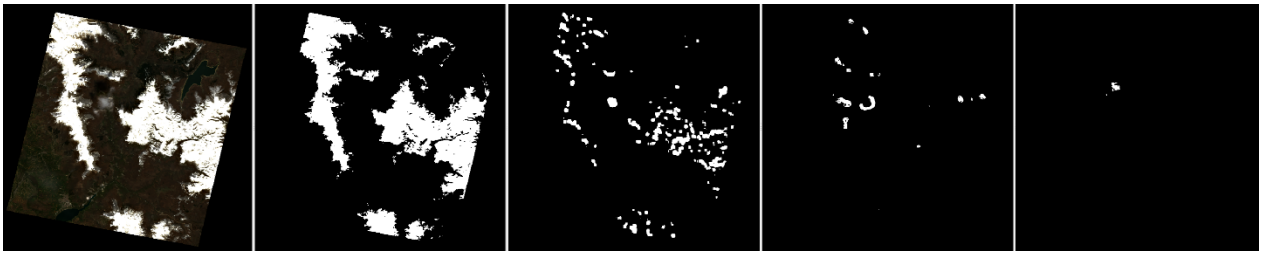


Figure 7-35 DT187507, from left to right: TrueColorComposite; Snow Mask, Cloud Mask, Haze Mask, Cloud Shadow Mask; all other masks are correctly empty.

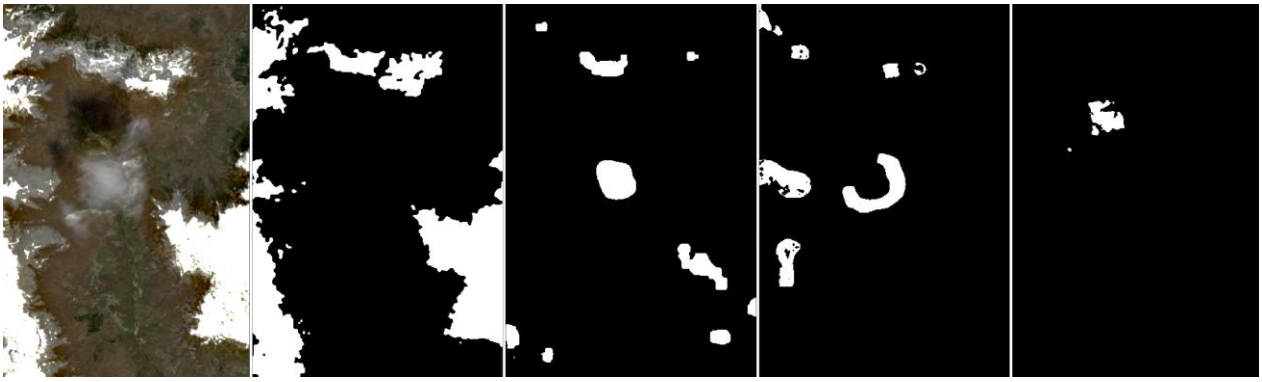


Figure 7-36 DT187507, as before now zoomed in.

The overall image impression of the atmospherically corrected dataset is characterized by the high dynamic range band stark contrast between dark vegetation and water areas, and bright snow/ice surfaces (Figure 7-37). When adjusting the image stretch, no artefacts from terrain correction are visible, indicating a good correction of these effects despite the high mountainous scene content. And only in first bands (see truecolor), slightly too low reflectance artefacts close to snow boarders show up, but these are non-existing in longer wavelengths, as seen already in the CIR composite.

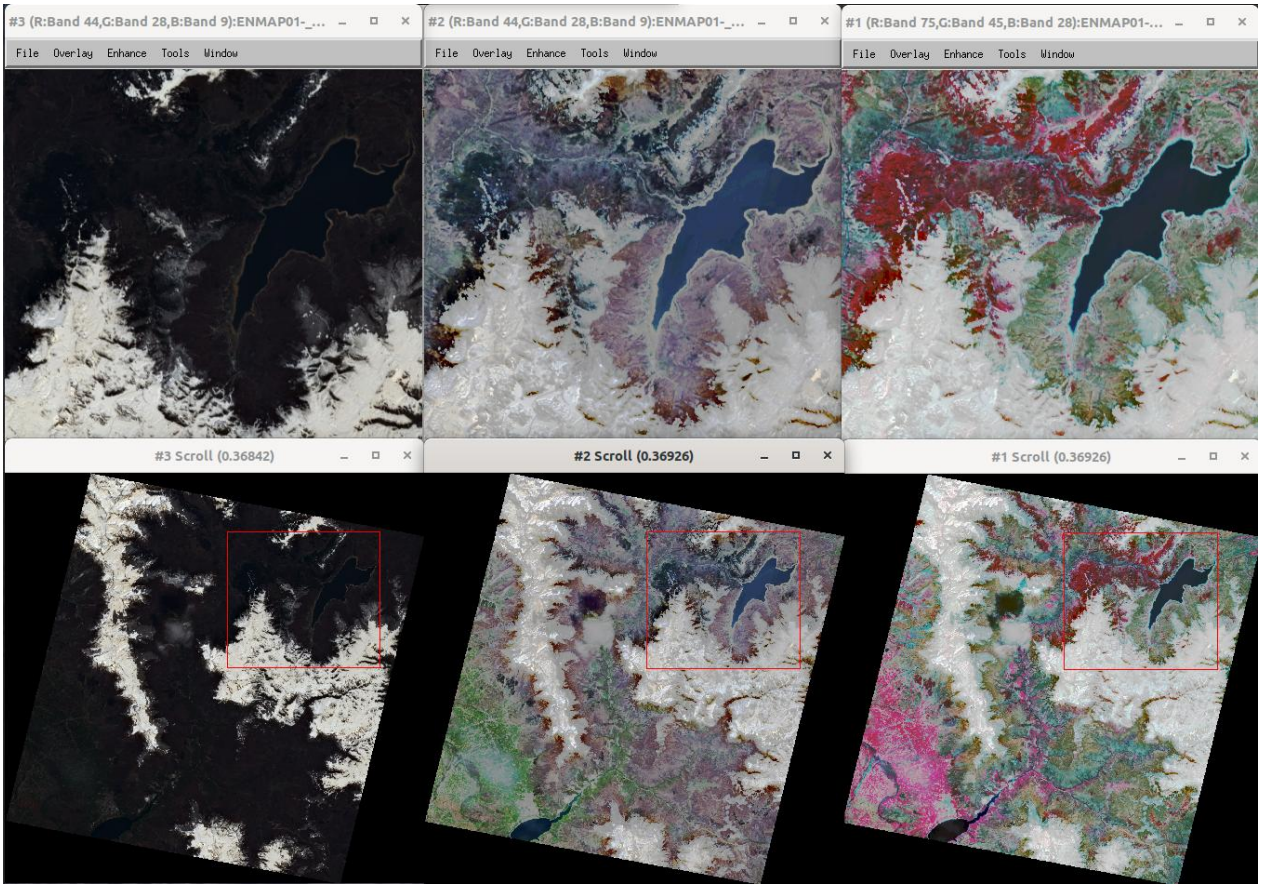


Figure 7-37 DT187507, left to right: TrueColor, linear stretch; TrueColor, nonlinear stretch; CIR nonlinear stretch

Regarding the shape and magnitude of the retrieved BOA_ref spectral signatures, both land surfaces (Figure 7-38) and the critical snow& ice surfaces (Figure 7-39) are as expected, indicating a correct atmospheric correction.

To conclude, for the vast majority of this scene, both the retrieved surface reflectance values and the generated masks are as expected. And while the snow mask is accurate, the additional inclusion of snowy areas in the cloud mask is not a severe problem.

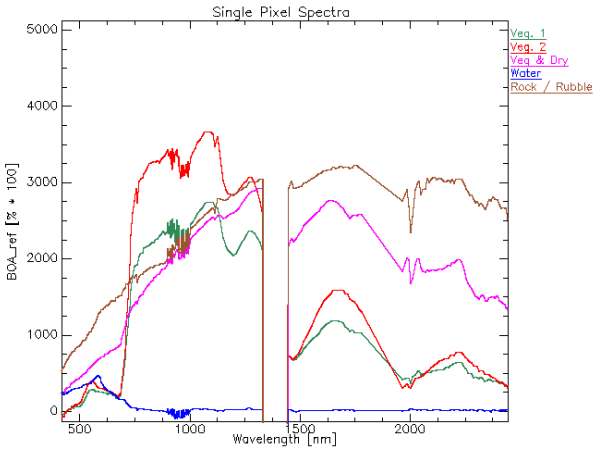


Figure 7-38 DT187507, single pixel spectra of various surfaces

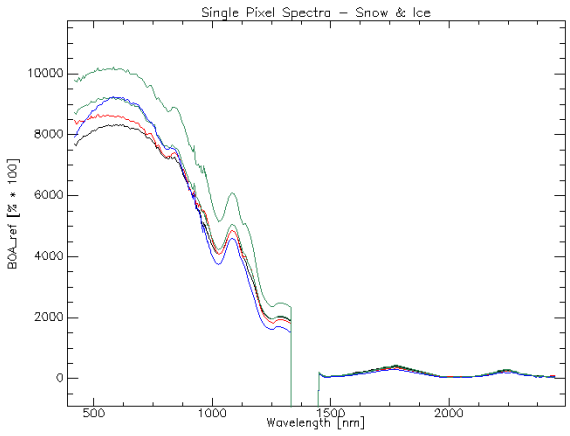


Figure 7-39 DT187507, single pixel spectra of snow & ice areas surfaces

- **Porto Velho (DT180304191634, T03, 2026-05-03)**

This EnMAP scene is taken over the Brazilian rainforest, with challenging atmospheric conditions: as depicted in Figure 7-40 and Figure 7-41, few dense clouds exist in the scene and in the cloud mask, and additionally cirrus at different densities and haze is masked. When zooming in (Figure 7-42), the transit from clear conditions to thin and thick haze, and finally to clouds at the center can be seen, which is correctly represented in the generated masks. Additionally, haze is flagged in the surrounding areas.

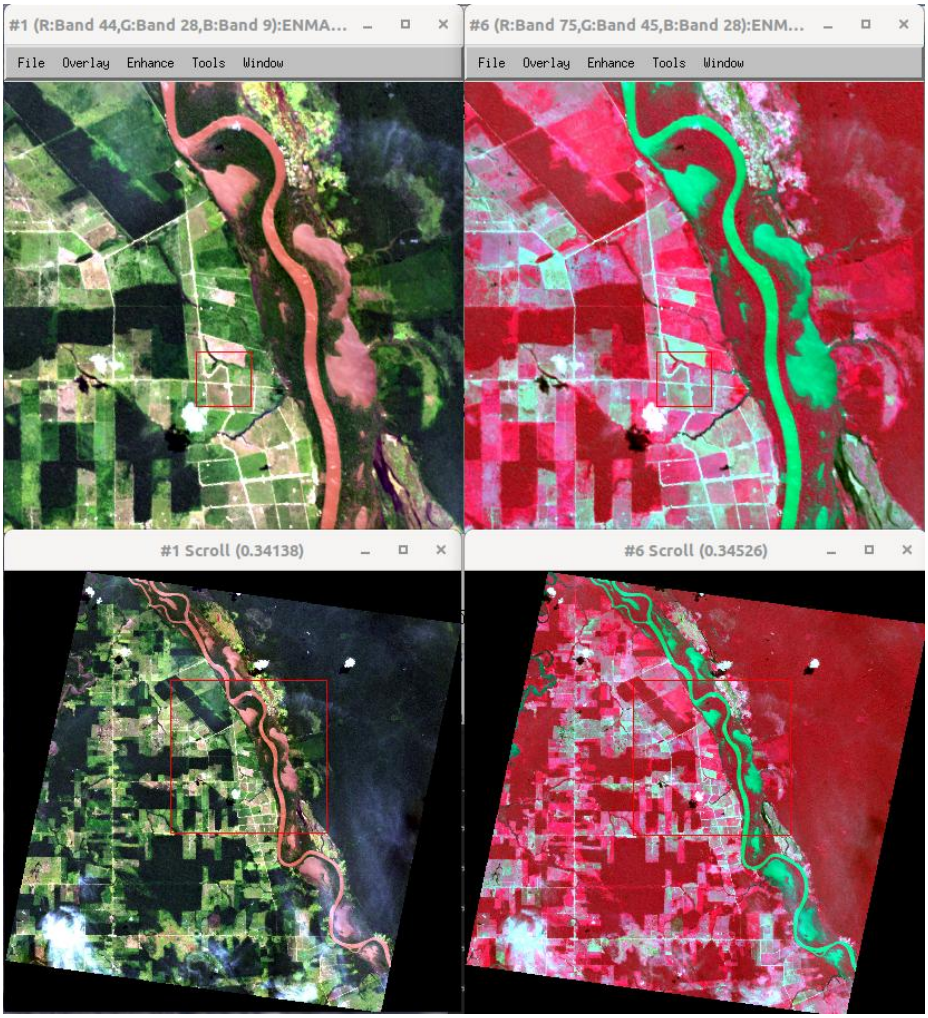


Figure 7-40 DT191634, T03, TrueColorComposite (left) and CIR (right)

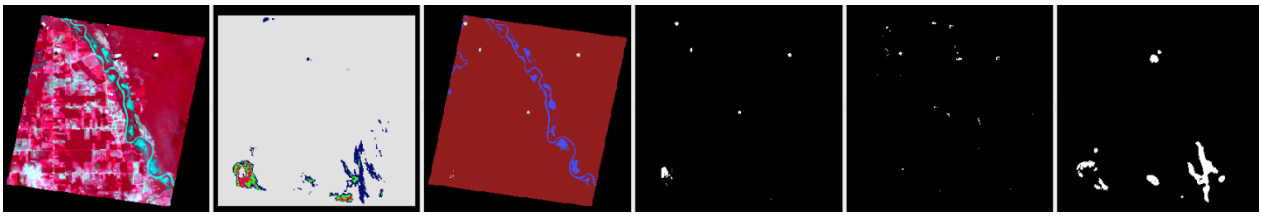


Figure 7-41 DT191634, T03, from left to right: CIR; Cirrus Classes (grey: clear; blue: thin cirrus; green: medium cirrus; red: thick cirrus); QualityClasses (blue: water, brown: land, white: other); Cloud Mask; Cloud Shadow Mask; Haze Mask; all other masks are correctly empty.

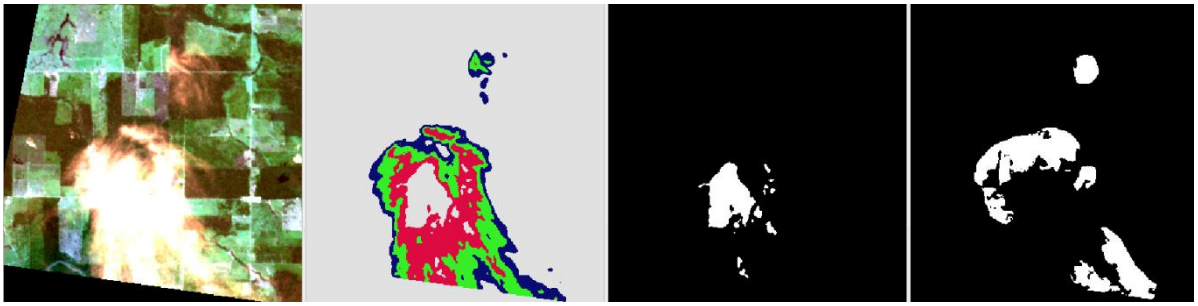


Figure 7-42 DT191634, T03, zoom in. From left to right: TrueColorComposite; Cirrus Classes (grey: clear; blue: thin cirrus; green: medium cirrus; red: thick cirrus); Cloud Mask; Haze Mask.

Also, when checking the BOA_ref spectra of different land and water surfaces (Figure 7-43), all is as expected. It is worth pointing out that the river as well as the adjacent lakes have a high sedimental load and a reddish colon, resulting in a higher reflectance in the VIS, and are still correctly included in the land-water mask (Figure 7-41). To conclude, this challenging scene is correctly processed.

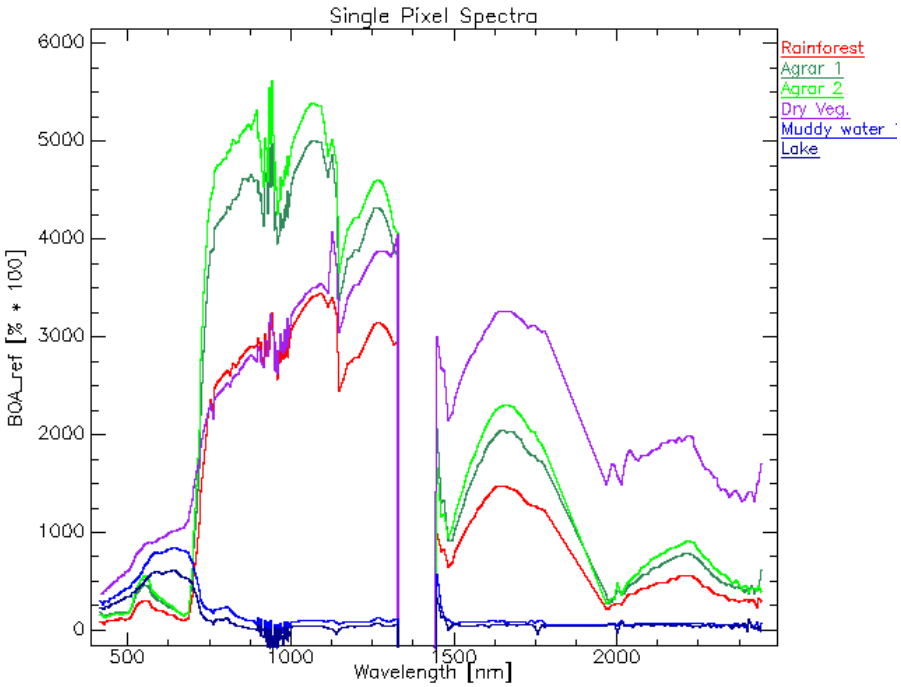


Figure 7-43 DT191634, T03, single pixel spectra of various surfaces.

- **Porto Velho (DT180304191634, T04, 2026-05-03)**

Also for the adjacent tile depicted in Figure 7-44, the masking (Figure 7-45) including cirrus and haze, as well as the visual image impression are as expected. Only some of the smaller clouds are not included as clouds, but as haze

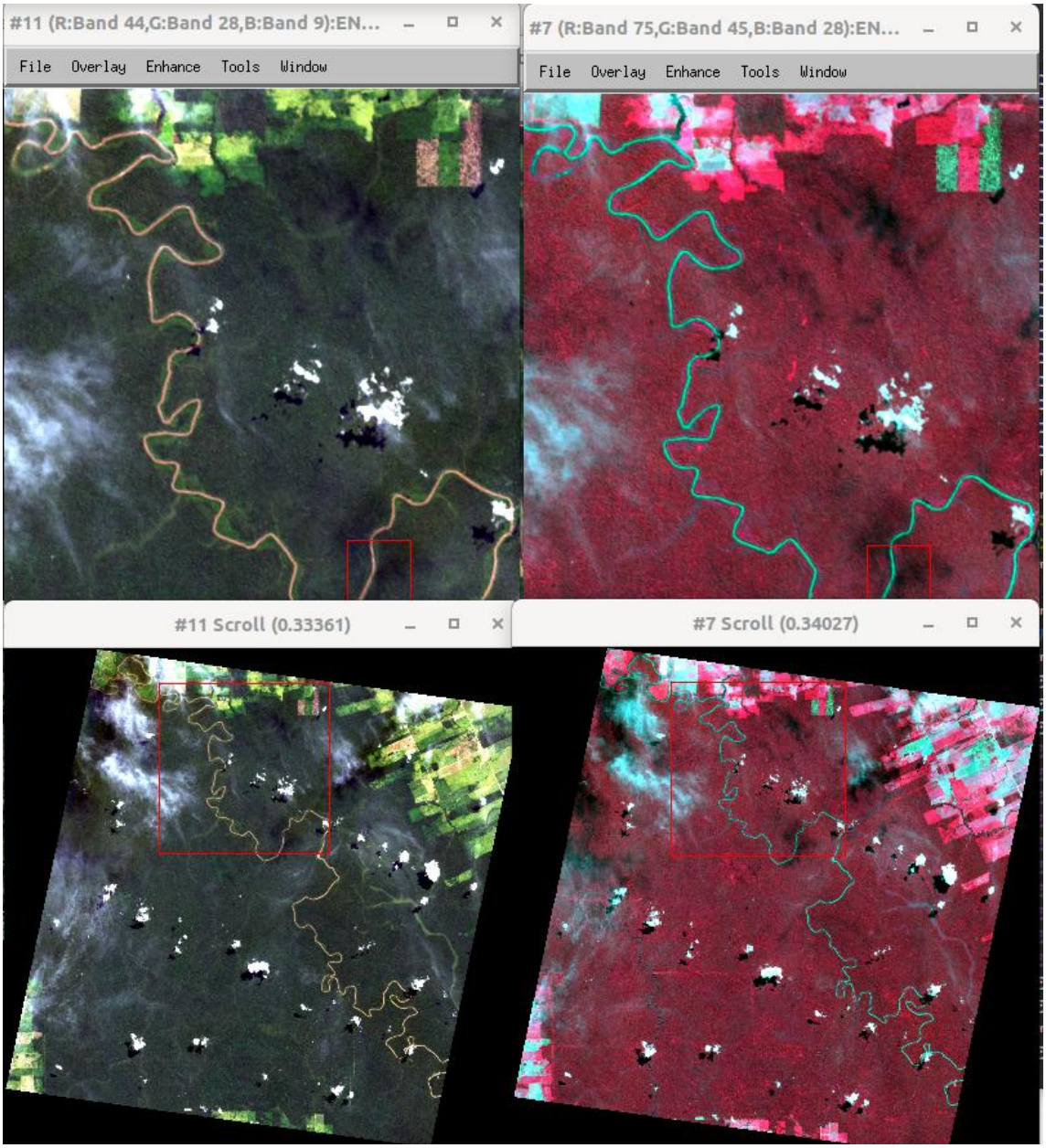


Figure 7-44 DT191634, T04, TrueColorComposite (left) and CIR (right)

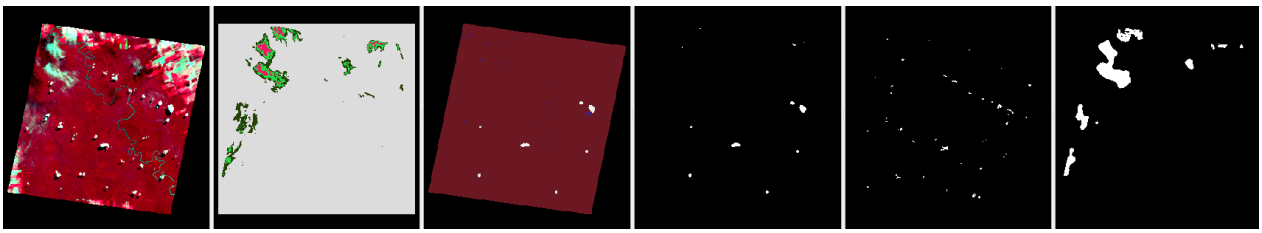


Figure 7-45 DT191634, T04, from left to right: CIR; Cirrus Classes (grey: clear; blue: thin cirrus; green: medium cirrus; red: thick cirrus); QualityClasses (blue: water, brown: land, white: other); Cloud Mask; Cloud Shadow Mask; Haze Mask; all other masks are correctly empty.

It is worth pointing out that as depicted, some of the river has extremely muddy water, resulting in reflectance values of ~3-4% in the NIR and 1-2% in the SWIR. Still, this water is correctly included in the masks (Figure 7-46). Note that the clouds not flagged in this subset are included in the haze mask.

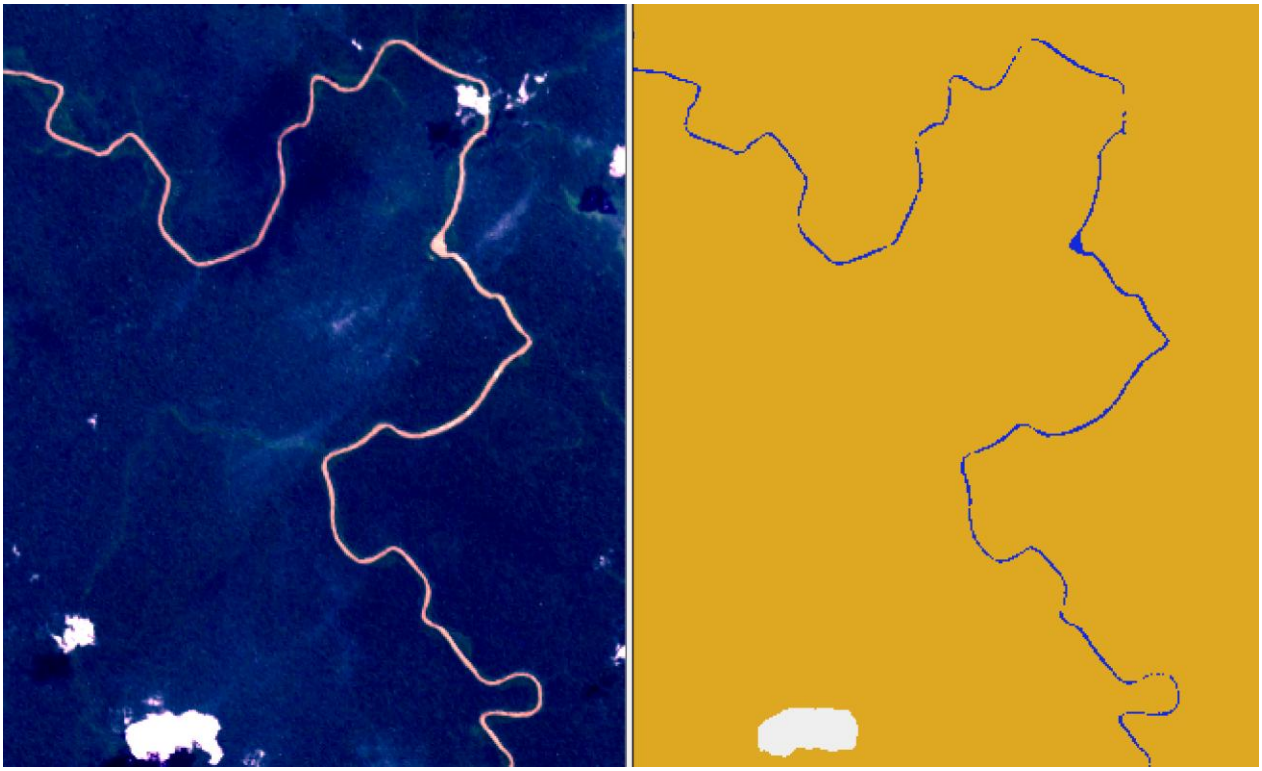


Figure 7-46 DT191634, T04, zoom in: CIR image (left) and QualityClasses (blue: water, brown: land, white: other)

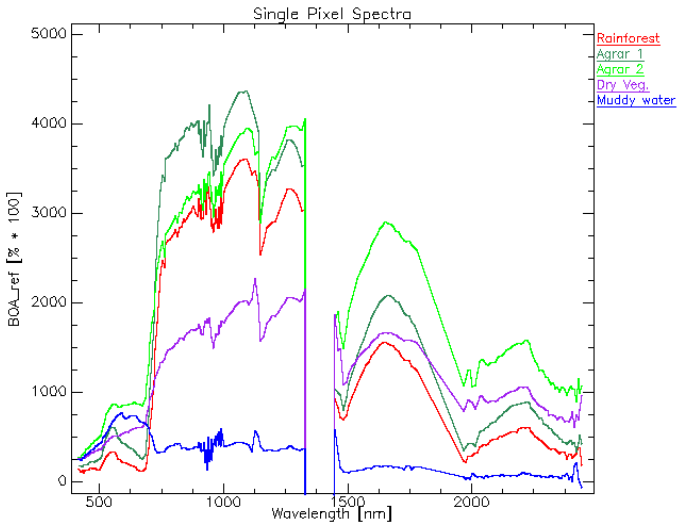


Figure 7-47 DT191634, T04, single pixel spectra of various surfaces.

- **Porto Velho, mosaicked dataset (DT180304191634, T03 & 04, 2026-05-03)**

As described before, this datatake over the Brazilian rainforest has challenging atmospheric conditions. Therefore, also the seamless processing was investigated by mosaicking both tiles and checking the quality. As depicted in Figure 7-48, the border between the two tiles is not visible both in the shorter wavelengths

as well as in the infrared, indicating that the retrieval of AOT and WaterVapour between tiles is consistent, and that the corresponding atmospheric correction is accurate, providing a visually seamless dataset across tiles.

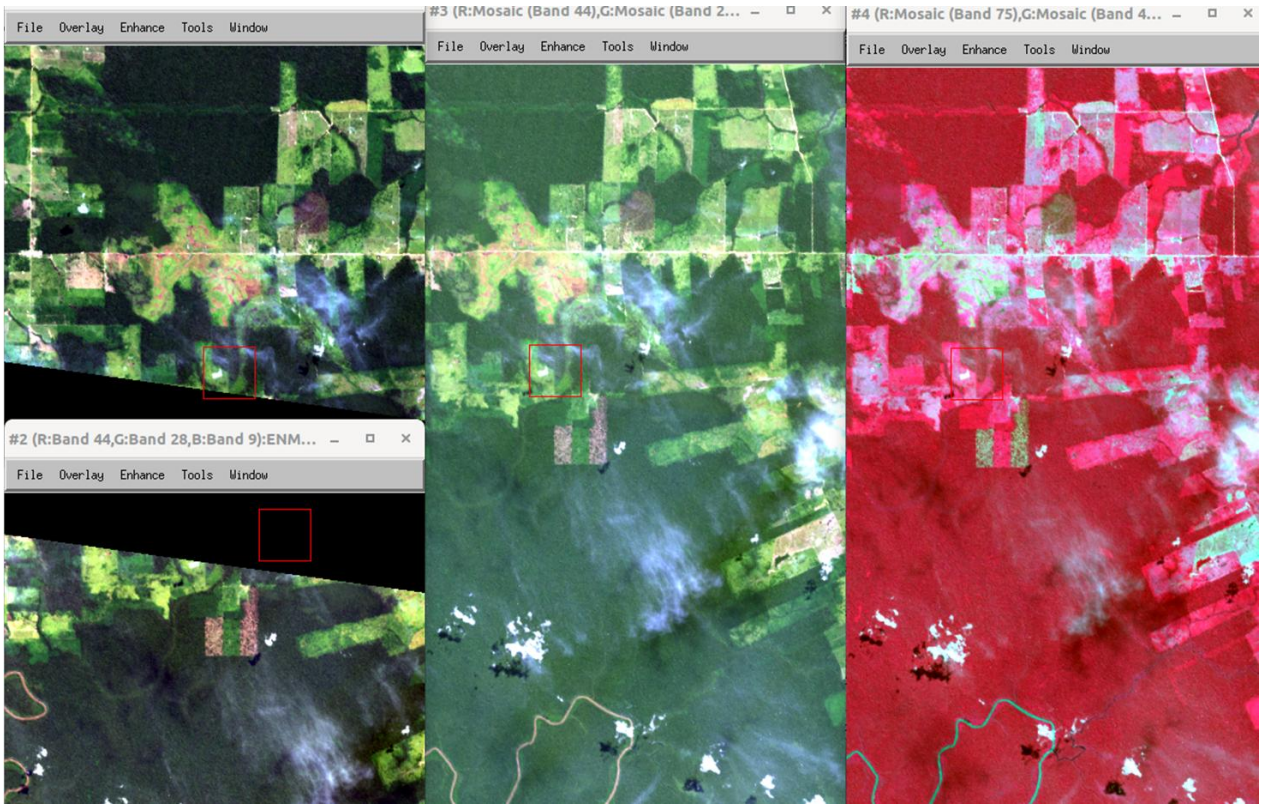


Figure 7-48 DT191634; top-left: T03 in TrueColourComposite; bottom-left: T04 in TrueColorComposite; center: mosaicked TrueColorComposite; right: mosaicked CIR.

- **Kogelberg (DT202075, T010, 2026-06-20)**

The datatake over the Kogelsberg area in South Africa is characterized by open ocean and a steep mountain plateau with rough terrain and consequently areas shaded by the terrain, and also many small inland water bodies (Figure 7-49). When checking the produced masks (Figure 7-50), some haze areas close to the coast are flagged, as well as a large number of smaller and larger inland waterbodies. Checking if these inland lakes on the rough plateau are not confused with terrain shadows due to similar spectral behavior, this classification is most often correct as depicted in Figure 7-51, showing the large number of smaller lakes. Additionally, no artefacts from the terrain correction are visible.



Figure 7-49 DT202075, T010, TrueColorComposite

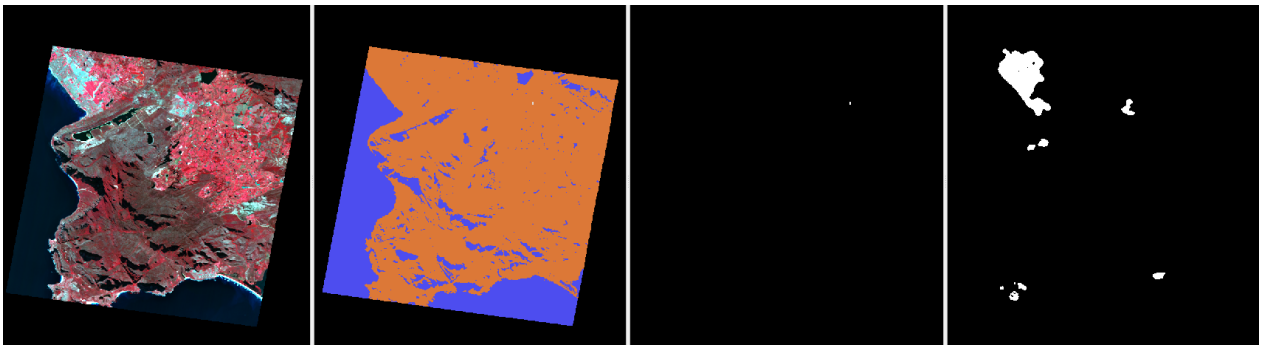


Figure 7-50 DT202075, T010, from left to right: CIR; QualityClasses (blue: water, brown: land, white: other); cloud mask; haze mask; all other masks are correctly empty.

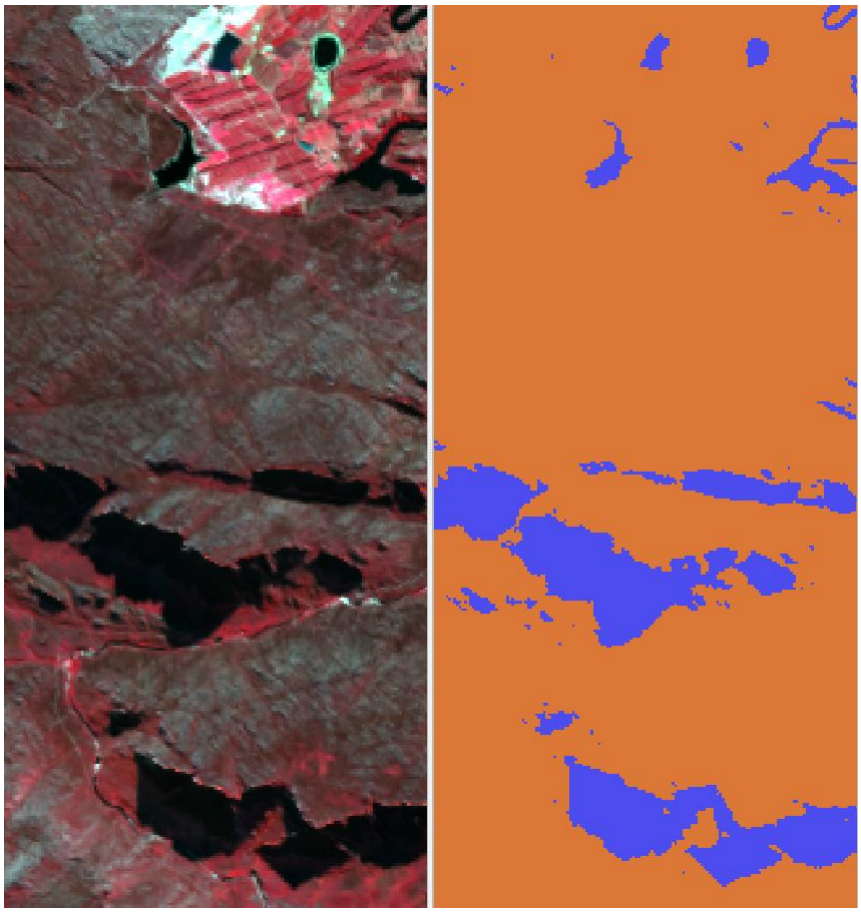


Figure 7-51 DT202075, T010, zoom in area on plateau: CIR (left); QualityClasses (right; blue: water, brown: land, white: other).

Also, when checking the BOA reflectance spectra (Figure 7-52), all land surfaces as well as the different water surfaces show the expected spectral shape and overall intensities, indicating a correct processing.

To conclude, also for this scene the atmospheric correction including terrain correction works as expected, and the produced masks are correct, especially in case of the correct flagging of land and water in challenging terrain.

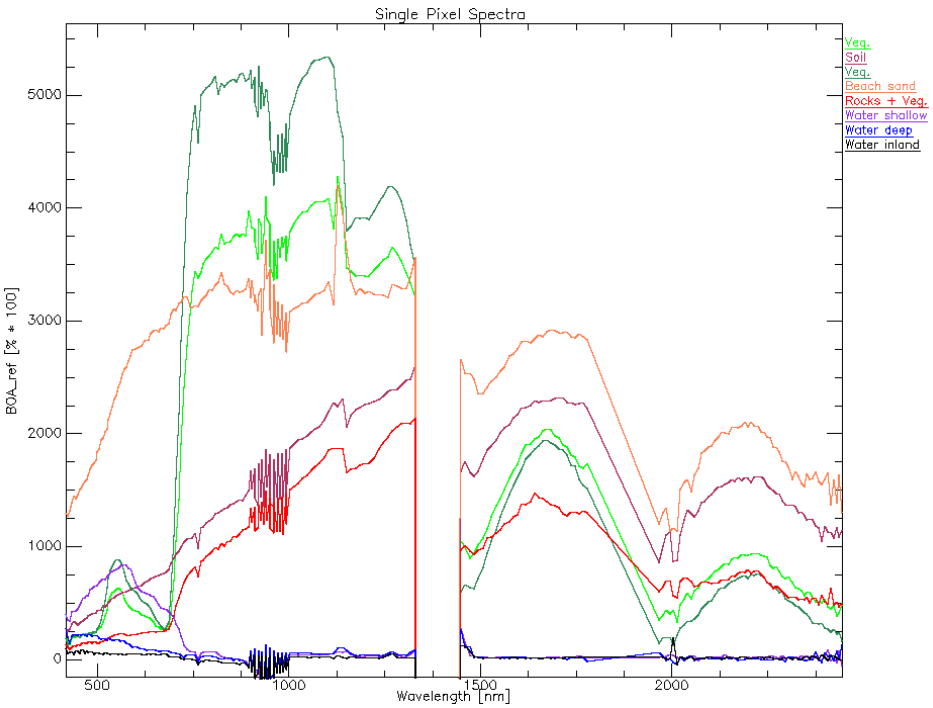


Figure 7-52 DT202075, T010, single pixel spectra of various surfaces.

8 External Product Validation

The standard quality parameters were validated in the external product validation process for the reporting period. The validation included 84 Level 1B, 108 Level 1C and 66 Level 2A products. All EnMAP products used for the validation have the latest product version V01.05.06.

8.1 Level 1B

The following validation scenarios were performed to validate Level 1B products:

- TOA Radiance
- Signal-to-Noise Ratio (SNR)

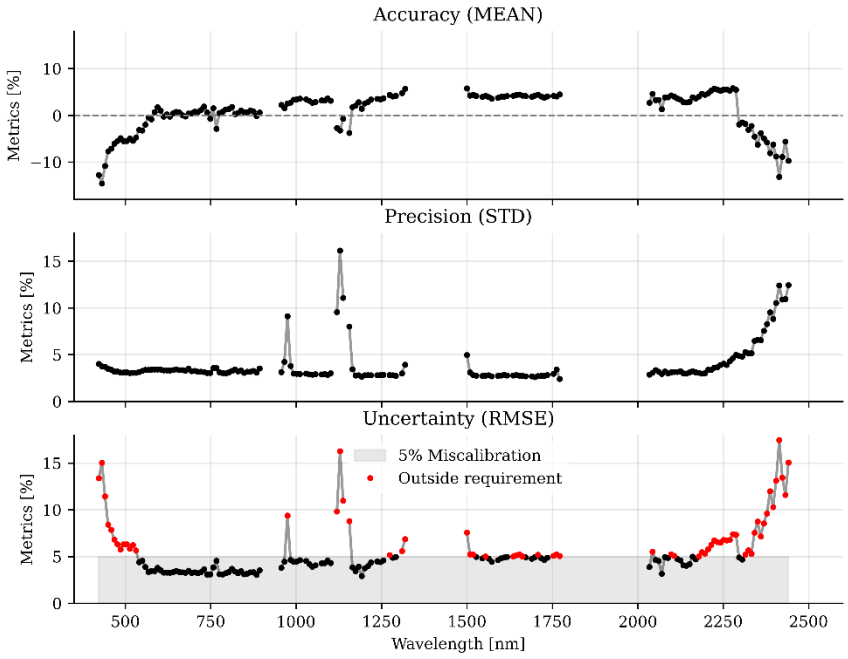


Figure 8-1: Errors between EnMAP TOA radiance and propagated TOA radiance from in situ measurements against wavelength for all arid validation sites based on 47 match-up

Three new match-ups have been added to the Level-1B TOA radiance validation, including one from the RadCalNet station Gobabeb (GONA) and two from the HYPERNETS station Gobabeb (GHNA). This increased the number of available match-ups from 44 to 47. Despite the larger sample size, the results remain consistent with those reported in the previous Mission Quarterly Report (MQR15) (see Figure 8-1 and Figure 8-2).

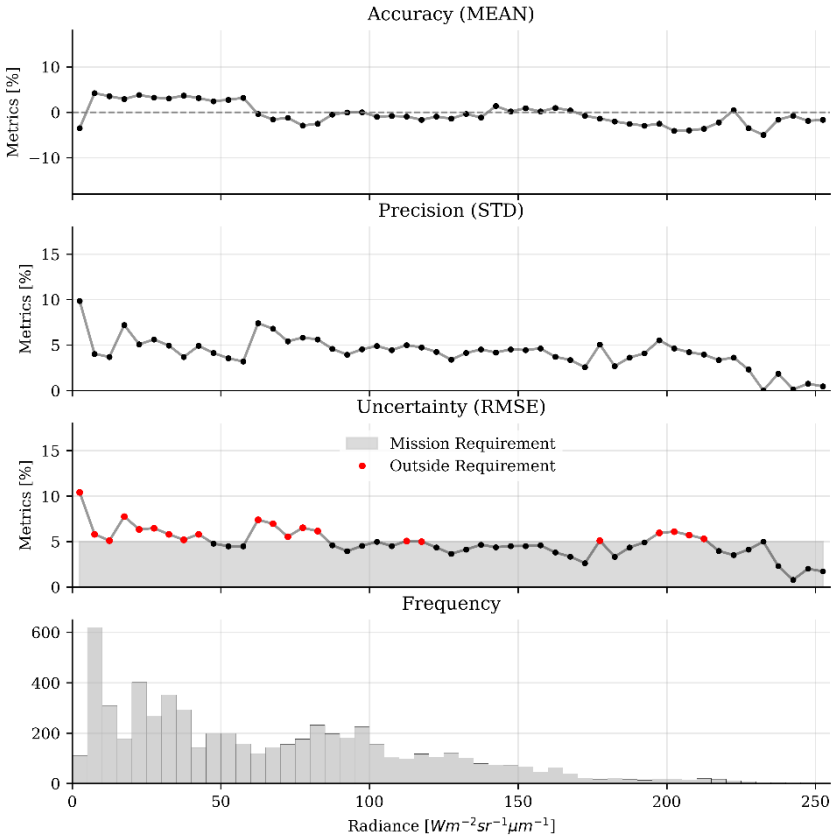


Figure 8-2 Errors between EnMAP TOA radiance and propagated TOA radiance from in situ measurements against radiance level for all arid validation sites based on 47 match-ups.

The mission requirements are defined for a reference radiance corresponding to a 30 % reflective target and a standard full width at half maximum (FWHM). For this report, the reference radiance has been updated to be fully consistent with the one used by the DLR ground segment during the radiometric calibration process.

Figure 8-3 compares the reference radiance used in previous reports with the updated version. The updated reference radiance is lower at the wavelengths relevant for the mission requirements (496 nm in the VNIR and 2200 nm in the SWIR). As the signal-to-noise ratio (SNR) is evaluated at these reference radiance levels, the reported SNR values are correspondingly lower than those presented in previous reports.

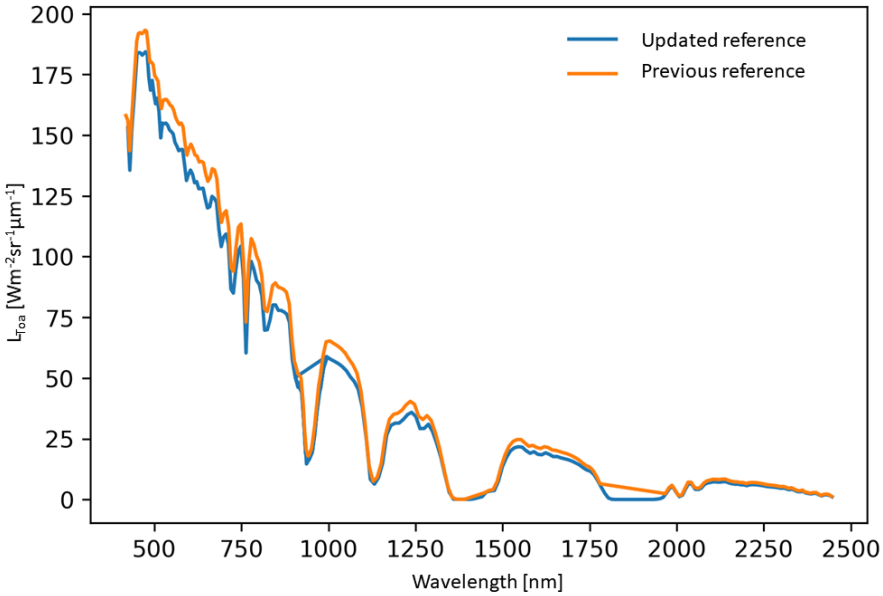


Figure 8-3 Previously used reference radiance curve (orange) and updated reference radiance curve (blue) as a function of wavelength.

The SNR assessment is based on 84 tiles (VNIR: 42; SWIR: 42) from product version 01.05.06. At 496 nm the SNR corresponding to the reference radiance (SNR_{ref}) reaches 354:1, while the value normalized to a spectral sample interval of 10 nm reaches 577:1, well within the mission requirements (>343:1). At 2200 nm (Fig. 7b), SNR_{ref} reaches 240:1 and the normalized value 263:1, thus also fulfilling the SWIR requirement.

8.2 Level 1C

The following Level 1C validation scenarios have been performed:

- VNIR-to-SWIR spatial co-registration
- Absolute spatial accuracy

The VNIR-to-SWIR spatial co-registration was assessed using 108 products processed with product version V01.05.06. Compared to the previous report, the RMSE in the X direction increased slightly to 5.6 m, while the RMSE in the Y direction remained stable at 6.4 m. Overall, the spatial co-registration performance remains stable and well within the mission requirement of less than 30% of a pixel.

The absolute spatial accuracy was assessed using 106 products processed with product version V01.05.06. Compared to the previous report, the RMSE increased slightly to 9.9 m in the X direction and 12.4 m in the Y direction. These values remain well within the mission requirements of <30 m for scenes with GCPs and <100 m for scenes without GCPs.

8.3 Level 2A

Land

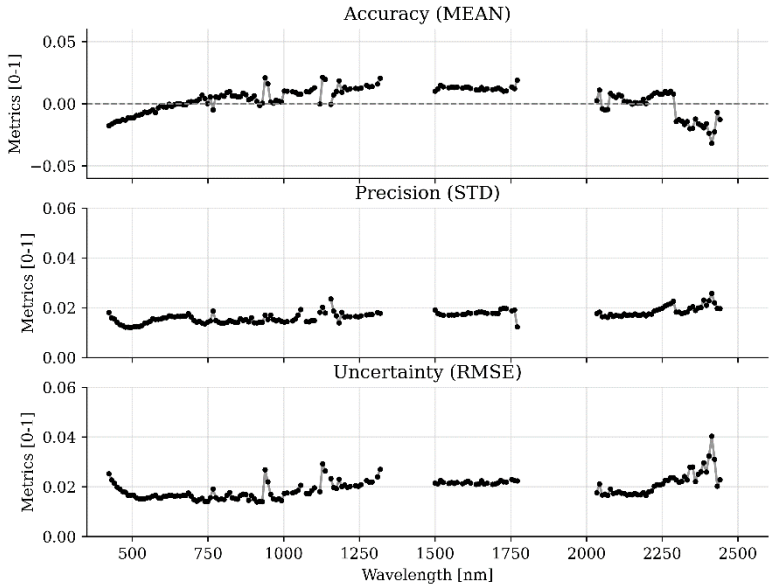


Figure 8-4 Errors between EnMAP and in situ BOA reflectance against wavelength for all validation sites based on 66 match-ups.

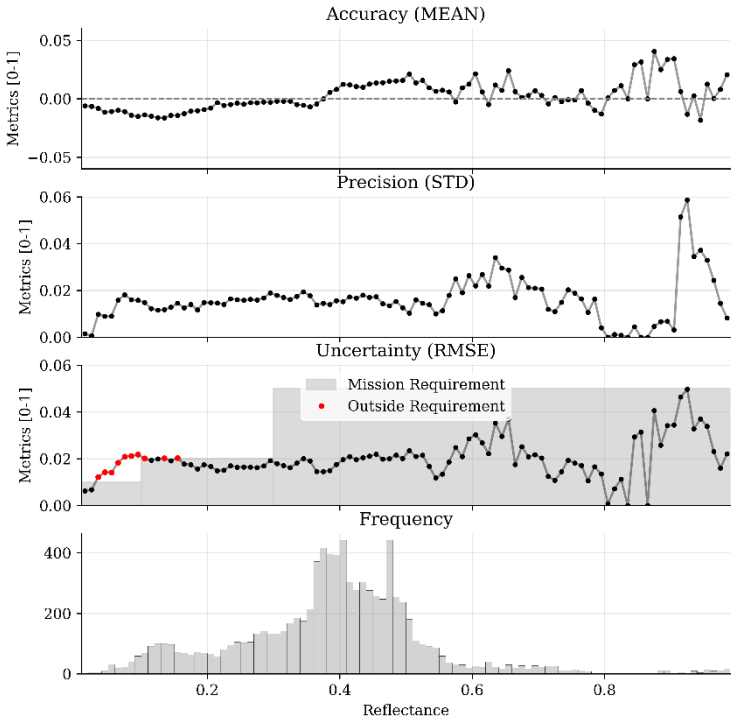


Figure 8-5 Errors between EnMAP and in situ BOA reflectance against reflectance level for all validation sites based on 66 match-ups.

Four new match-ups have been added to the Level-2A BOA reflectance validation dataset, including two from GONA and two from GHNA. This increased the total number of validation match-ups to 66. The Level-2A BOA reflectance validation results remain consistent with those reported in previous reports (see Figure 8-4 and Figure 8-5).

Water

Since the previous report, no new water match-up has been added to the validation dataset. Therefore, no new result is reported for the water reflectance validation, and the previous results, presented in MQR15 remain unchanged.

8.4 Summary of External Product Monitoring

The standard quality parameters were validated for Level-1B, Level-1C, and Level-2A products processed with the latest EnMAP processor version, V01.05.06. The validation results confirm a stable and overall high radiometric, spectral, and geometric data quality, consistent with previous reporting periods. The updated reference radiance used for the SNR assessment results in slightly lower reported SNR values than in previous reports. However, all reported SNR values remain within the mission requirements.

9 Others

EnMAP Mission Operations and Status Publications:

- Brell, M., Reiners, P., Guanter, L., Segl, K., Chabrillat, S., Scheffler, D., Soppa, M., Bohn, N., Gorrono, J., Kokhanovsky, A., Bracher, A., Bachmann, M., Pato, M., Schneider, M., de los Reyes, R., Langheinrich, M., Holzwarth, S., Carmona, E., Storch, T., Pinnel, N., Kokaly, R., Ong, C., Green, R.O., Moreno, J.F., Gascon, F., Hank, T., Ben-Dor, E., Di Mauro, B., Colombo, R., Milewski, R., Brede, B., Schmid, T., Anderson, C., Schickling, A., Krieger, V., Bock, M., La Porta, L., Fischer, S. (2026). Assessment of EnMAP data quality through global product validation activities, Remote Sens. Environment, 342, 115459. https://doi.org/10.1016/j.rse.2026.115459

EnMAP Mission Operations and Status Presentations:

- **EARSeL 2026 (Helsinki, 02-04 June 2026)**
  - “EnMAP mission status overview”, Presentation by L. La Porta
  - “EnMAP mission science highlights”, Poster by S. Chabrillat
  - “EnMAP mission operations status and future plans”. Poster by E. Carmona
  - “EnMAP Moon Observations for Instrument Monitoring and Radiometric Validation”. Presentation by M. Pato
  - “Operational Lessons from the EnMAP Foreground Mission during the ESA CARMA 2025 Campaign”. Presentation by N. Pinnel
  - “Radiometric and Spectral Calibration and Validation Activities for EnMAP”. Presentation by P. Reiners and D. Marshall
  - “Atmospheric Correction for Hyperspectral Missions: Lessons Learned from Present Narrow – like EnMAP - to Future Wide Swath Instruments”. Presentation by T. Eckert
  - “Data Quality Control for EnMAP - Verifying the Spectral Performance over 4 Years in Orbit”. Poster by M. Bachmann
  - “EnMAP tutorial #1” Data access training by N. Pinnel